

Petroleum coke slags: characterization and dissolution

by

Jun Lu

Dissertation submitted to the Faculty of

Virginia Polytechnic Institute and State University

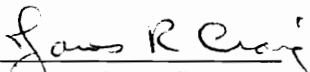
in partial fulfillment of the requirements of the degree of


DOCTOR OF PHILOSOPHY

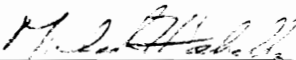
IN


GEOLOGY


APPROVED:


James R. Craig, Chairman


J. Donald Rimstidt, Co-chairman


Michael F. Hochella


Robert J. Bodnar


David A. Hewitt

May, 1997

Blacksburg, Virginia

Key words: Lu, petroleum coke slags, characterization, dissolution

.2

LD
5655
V856
1997
L8
c.2

Petroleum coke slags: characterization and dissolution

by

Jun Lu

Committee Chairman: James R. Craig

Geological Sciences

(ABSTRACT)

Slags are crystalline to vitreous by-product materials generated in many high temperature industrial processes. This study presents a general technique for the identification of the phases present in petroleum coke gasification slags, documents the phase assemblages and textures, and finally determines the dissolution of vanadium from these slags as part of the considerations of potential resource reclamation. The general identification procedure utilizes (1) recognition of separate phases using optical microscopy and scanning electron microscopy; (2) electron probe microanalysis (EPM) of chemical compositions of individual phases; (3) statistical analysis of the EPM data to eliminate spurious data; (4) estimation of valence states of transition metals using thermodynamic and computational methods; (5) derivation of chemical formulae for the phases using computational methods and chemistry of ionic substitutions; (6) verification of phase identity using X-ray diffraction analysis.

More than twenty phases were determined in petroleum coke slags including oxides, silicates, vanadates, sulfate, sulfides and alloys. The reduced slags are rich in V_2O_3 with silicates and minor amounts of sulfides and native metals whereas the oxidized slags are composed of V_2O_4 , nickel aluminum spinels, various vanadates and glass. Textural analysis provided information on the crystallization process, reaction with gasifier refractory lining materials, sulfide exsolution processes, glass devitrification, and the

development of chemical zonation in some spinels. This information offers some perspectives on the potential of resource reclamation.

Resource reclamation for petroleum coke slags is best assessed with a knowledge of phases, phase assemblages, textures and dissolution behavior of the material. The dissolution of vanadium, the most significant element, was examined using long term dissolution experiments. These demonstrate that vanadium concentrations are pH dependent ranging from 1500 ppm to 5000 ppm with a minimum concentration near pH 6. Vanadium dissolution rates range from $1.28 \times 10^{-4} \text{ mol m}^{-2} \text{ sec}^{-1}$ to $3.08 \times 10^{-5} \text{ mol m}^{-2} \text{ sec}^{-1}$. In view of the strategic nature of vanadium and the fact that the concentration of vanadium in slags is almost two orders of magnitude higher than the current mining grades, petroleum coke slags offer significant potential to serve as resources for vanadium.

ACKNOWLEDGEMENTS

I would like to express my greatest appreciation to my parents, especially my father who has been so dedicated to my education. Throughout my schooling, they pushed me to excel and offered financial support in time of need. Of course, I want to offer my apologies to my wife and my son, with whom I have shared so little time during my doctoral research. Without their patience and support, my dissertation would not have been possible.

Many thanks to my advisor, Dr. James R. Craig, my gratitude for his assistance is beyond words. His enthusiasm and encouragement always made me feel as though I was doing a great thing. I greatly appreciate his reviewing my dissertation again and again with unbelievable patience and for his help in providing financial support. I would like to thank Dr. J. Donald Rimstidt for his accessibility and willingness to discuss questions and problems almost at a moment's notice. His close association with students and dedication to teaching provided an atmosphere where learning becomes interesting and efficient. Dr. Mike Hochella is thanked for his help in X-ray photon spectroscopic study of petroleum coke slags, his patience in listening to and discussing with me session after session and for his very valuable input for my dissertation. Dr. Robert Bodnar is thanked for his valuable academic advice whenever I turned to him. I have especially appreciated his enthusiasm in advising the Society of Economic Geology from which I learned a great deal about ore deposits in the United States and had a lot of fun. I am thankful to Dr. John Groen and Texaco who provided the samples for my studies and conducted some geochemical analyses for me. Whenever he came to Virginia Tech, he always spent a lot of time with me discussing the project and answering my questions. I also would like to extend my thanks to Dr. Robert Tracy, who was always more than willing to discuss crystal chemistry, Dr. David Hewitt, who generally shared his knowledge of thermodynamics, and Dr. Gerald Gibbs for his suggestions on my dissertation. This research would not have been possible without the generous support of Texaco.

I would also like to thank all my fellow graduate students for their help in almost every aspect of my everyday life and graduate studies. I especially benefited from discussions about my dissertation research with John Mavrogenes, Jim Student, Jing Gu, Zhuang Sun, and Peter Welch.

The office staff here is undoubtedly the finest. Karen Hunt has the warmest heart toward students; Mary McMurray always goes beyond her duties to help; Linda Bland never runs out smiles; and Carolyn Williams' courtesy is an excellent model to follow. Dean Hefner's, Belinda Pauley's and Kathy Shelor's excellent services will all be embedded in my memory.

My thanks are also extended to those who helped me in the course of my studies including Todd Solberg, who assisted me in the probe analysis, Sharon Chiang for her advice on drafting, Dan Smith for his excellent service, Mark Fortney for his assistance in photo development, Brenda Kutz, Hal Pentrik, and Frank Harrison for their friendly help in time of need.

To those I may have missed, I extend my thanks. I believe that the Department of Geological Sciences at Virginia Tech is one of the finest and I have greatly enjoyed my stay in Blacksburg, Virginia.

TABLE OF CONTENTS

Title Page	i
Abstract	ii
Acknowledgments	iv
Table of Contents	vi
List of Figures	ix
List of Tables	xi
List of Appendices	xii
Chapter 1. Introduction	1
Chapter 2. Petroleum coke slags: determination of inorganic phases	
Introduction	4
Methods	7
Samples and Instrumental analysis	7
Sample acquisition and preparation	7
Microscopic observations	10
Bulk chemical analysis	10
Scanning electron microscopy	11
Electron probe microanalysis	11
X-ray diffraction	12
Data analysis	12
Data filtering-Chauvenet's criterion	12
Optimization of total oxide weight percentages	14
Estimation of valence states of transition metals: thermodynamic constraints	16
Optimization of total oxide weight percentages: a numeric approach	21

Derivation of chemical formulae	24
Stoichiometry and integer criteria	24
Ionic substitutions and the screening process	27
X-ray diffraction confirmation	35
Results	38
Summary	38
References	41
Chapter 3. Petroleum coke slags: phase assemblages and textures	
Introduction	44
Methods	44
Phase assemblages, textures and their formation mechanisms	45
Phase assemblages	45
Slags formed under reduced conditions	45
Slags formed under oxidized conditions	52
Formation mechanisms	57
Textures	65
Refractory - slag reaction	65
Cavity filling	69
Eutectic or eutectoid textures	69
Sulfides, metals and textures	71
Fractional crystallization	71
Spinel zonation	74
Summary	77
References	78

Chapter 4. Petroleum coke slags: potential resource reclamation

Introduction	79
Methods	79
Characterization of petroleum coke slags	79
Dissolution experiments	79
Long term dissolution experiments	79
Kinetics experiments	80
Results	81
Elements of significance	81
Dissolution behavior	81
Long term dissolution	81
Dissolution kinetics	84
Discussion	84
Conclusions	90
References	91
Vita	150

LIST OF FIGURES

Chapter 2

1. Schematic of the Texaco Gasification Process	5
2. Procedures for the determination of the phases in petroleum coke slags	8
3. Oxygen pressure - temperature diagram for vanadium and its oxides	18
4. Constraints for oxygen pressures in reduced petroleum coke slags	19
5. Oxygen pressure - temperature diagram for Cr, Ti and Mn and their oxides	20
6. X-ray diffractogram of Type 1 oxidized petroleum coke slags	37

Chapter 3

1. Four zones in reduced petroleum coke slags and their textures	48
2. Various phases in Zone 1 of reduced petroleum coke slags	49
3. Various phases in Zone 2 of reduced petroleum coke slags	51
4. Various phases and their physical mode of occurrence in Zone 4 of reduced petroleum coke slags	53
5. Textures resulting from oxidation	54
6. Oxidized petroleum coke slags, their phase assemblages and textures	55
7. Various phases in Type 1 oxidized petroleum coke slags	56
8. Various textures in Type 2 oxidized petroleum coke slags	58
9. Diagram showing chemical behavior of elements and phase formation under reduced and oxidized conditions	64
10. Electron probe X-ray mapping of altered refractory brick ($MgCr_2O_4$)	66
11. An electron probe traverse analysis of altered spinel brick	67
12. Various cavity filling textures in reduced petroleum coke slags	68
13. The occurrence of V_2O_3 phase in the cavities in reduced petroleum coke slags	70
14. Hypereutectoid steel	72

15. Various forms of sulfides in reduced petroleum coke slags	73
16. Back-scattered image of one of spinel crystals	75
17. An electron probe traverse analysis of a chemically zoned spinel	76

Chapter 4

1. Log-log diagram for concentrations of elements in petroleum coke slags vs elemental abundance in the earth's crust	83
2. Comparison between phase assemblages in Type 1 oxidized petroleum coke slags before dissolution and after dissolution	85
3. Concentration of vanadium in solutions that remained in contact with oxidized petroleum coke slags for 8 months at various pH values	87
4. Concentration of vanadium versus time at 25°C	89

LIST OF TABLES

Chapter 2

1. Electron microprobe chemical analyses of a sodium aluminum silicate	15
2. Optimization of the total oxide weight percentages for a calcium nickel vanadate	23
3. Optimization of the total oxide weight percentages for a sodium vanadate	25
4. Possible chemical formulae based on stoichiometry and integer criteria for a calcium nickel vanadate	28
5. Ionic substitution priority table	33
6. A short list of calcium nickel vanadate chemical formulae which passed ionic substitution test	36
7. Phases present in petroleum coke slags	39

Chapter 3

1. Phases present in petroleum coke slags	46
2. Glass compositions in oxidized petroleum coke slags	61
3. Bulk chemical analyses of reduced petroleum coke slags	63

Chapter 4

1. Bulk chemical analyses of reduced petroleum coke slags	82
2. Results of long term dissolution experiments using oxidized petroleum coke slags	86
3. Vanadium concentrations versus time for reduced and oxidized petroleum coke slags	88

LIST OF APPENDICES

Chapter 2

1. Bulk chemical analyses of reduced petroleum coke slags	98
2. Excel macro for data rejection	101
3. Excel macro for transition element valence state calculation	108
4. Excel macro for chemical formula calculation	118
5. Excel macro for creation of ionic substitution priority table	135
6. Excel macro for a short list of chemical formulae	143

CHAPTER 1. INTRODUCTION

Slags are crystalline to vitreous materials generated in many high temperature industrial processes, such as gasification, refining, energy production, and combustion used to reduce the volume of municipal solid wastes. The nature and properties of slags have been studied for well over half a century with widely differing objectives. In the early days of research on these materials, attention tended to focus on the properties of glasses and phase equilibrium among the silicate phases. From the mid-1920's through the 1930's, much of the research was centered upon slag-metal reactions, which were closely associated with the development of open-hearth steel making. Since the 1940's, greater emphasis was given to the application of physicochemical and thermodynamic principles to pursue a better understanding of the properties of polymeric melts, and their reactions with gases, metals and refractory materials; in relation to ore smelting, metal refining, melting and forming of glass, and studies of the geological formations associated with the generation and emplacement of magmas.

In the past several decades, there has been growing interest in the compositions and properties of the slags which are produced during the combustion of municipal solid wastes and from new energy production technologies. Much of this interest during the 1980's was fueled by concerns about adequate landfill capacity and the realization that the combustion of municipal solid wastes could accomplish the dual goals of volume reduction and energy production. Since 1985, the amount of municipal solid wastes treated in this manner has increased from 11.7 million tons (7.1% of the total) to 31.9 million tons (16.3% of the total) in 1990. In countries which have limited land space such as Japan, solid waste disposal is an especially severe problem; consequently, the Japanese now combust most of their municipal solid wastes and almost 60% of dry sludge solids. To

further reduce the volume of the residue (ash), high temperature melting and solidifying technologies are under development.

Petroleum coke, a solid, tar-like hydrocarbon residue left after refining of petroleum, has been generated in large quantities for many years but generally had little value. In the past 15 years, however, several companies have worked on coal gasification techniques to generate usable gases from petroleum coke. During gasification, hydrocarbon constituents react with steam under low oxygen activities to produce a gaseous mixture rich in CO and H₂, with lesser amounts of CO₂ and H₂O, and minor amounts of H₂S, CH₄, etc. This gaseous mixture is collectively known as "synthesis gas". During gasification, the non-combustible inorganic constituents are left as fused residues, or slags. The continuing increase in the quantities of regular crude oils being refined and the increasing interest in heavy oils and tar sands undoubtedly will lead to ever increasing generation of petroleum coke, and thus greater use of petroleum coke gasification processes. These in turn will generate increasing quantities of petroleum coke slags.

An obvious feature of gasification is that as the total volume of feedstock is reduced, constituent metals are substantially concentrated in the inorganic residue. For example, bulk chemical analyses of petroleum coke slags reveal concentrations of vanadium as high as 38% whereas the original oils from which they were produced generally contained 0.1-1,000 ppm vanadium.

The nature of petroleum coke gasification slags is important because their physical and chemical behavior may have direct effects on the operation of the gasifiers. Furthermore, the generation of large quantities of slags may warrant the research on the later use of these materials. The assessment of the nature of inorganic by-products is commonly based on their bulk chemical compositions. However, the knowledge of bulk chemistry alone is far from sufficient to provide an understanding of slags and ashes. Indeed, to thoroughly understand the chemical properties of slags and ashes, knowledge of

chemical phases, phase assemblages, textures and their genesis are indispensable. Knowledge of the phases is basic for almost any application. Knowledge of phase assemblages and textures are equally important because they help in understanding the sequence of phase formation, the nature of elemental partitioning, and the interpretation and prediction of dissolution kinetics. Knowledge of formation mechanisms may permit subtle alteration of operational parameters such as temperature, pressure, or additives to suppress the formation of undesirable phases or enhance formation of desirable phases.

This dissertation study was conducted with the aim of increasing our understanding of the inorganic by-products of industrial processes. Previous works have demonstrated that petroleum coke slags are extremely complicated because of the unusual combinations of chemical elements and varying operating conditions under which these slags were generated. Petroleum coke slags were selected as research media for the present study in the belief that the development of techniques applicable to petroleum coke slags, which are very complex, would provide methods applicable to the inorganic by-products generated by other high temperature industrial processes, which are generally less complex. The study is presented in three subsequent chapters. The first is focused on development of a general technique for determination of inorganic phases in petroleum coke slags. The second is a detailed investigations of the phase assemblages and textures of petroleum coke slags and discussions of their genesis. The third is an assessment of petroleum coke slags from the perspectives of resource reclamation.

CHAPTER 2. PETROLEUM COKE SLAGS: DETERMINATION OF INORGANIC PHASES

INTRODUCTION

Petroleum coke, a solid tar-like hydrocarbon residue left after refining of petroleum, has been generated in large quantities for many years but generally had little value. In the past 15 years, however, several companies actively applied coal gasification techniques to generate usable gases from petroleum coke (Schlinger 1978; Conoco, Inc. and Foster Wheeler Energy Corp. 1981; Galloway et al. 1983; Spencer and Gluckman 1983; Lacey et al. 1984; Evans et al. 1985; Thimsen et al. 1985; Matsunaga 1987; Revankar et al. 1987; Sueyama and Katagiri 1989; Curran 1990; Timpe et al. 1990; Siegart 1992; and Philips et al. 1992). Petroleum coke is generated at many refineries from many different crudes, but the quantity increases with heavier crudes because there are fewer lighter fractions distilled off as gaseous or liquid products. Furthermore, the cokes generated from heavier crudes tend to contain greater quantities of non-hydrocarbon, inorganic constituents. The continuing increase in the quantities of regular crude oils being refined and the increasing interest in heavy oils and tar sands will no doubt produce ever increasing amounts of petroleum coke that can be converted by gasification into valuable resources.

The Texaco Gasification Process (Figure 1) is the leading petroleum coke gasification system. In this process, the hydrocarbon constituents react with steam and controlled quantities of oxygen to produce primarily CO and H₂. As the hydrocarbons are converted to gaseous species, the inorganic constituents are left as a fused residue known as petroleum coke slag. Such slags contain metals in concentrations of tens of percents compared to concentrations of parts per million in the original oils because the total volume of the petroleum has been reduced by approximately ten thousand in producing the slag

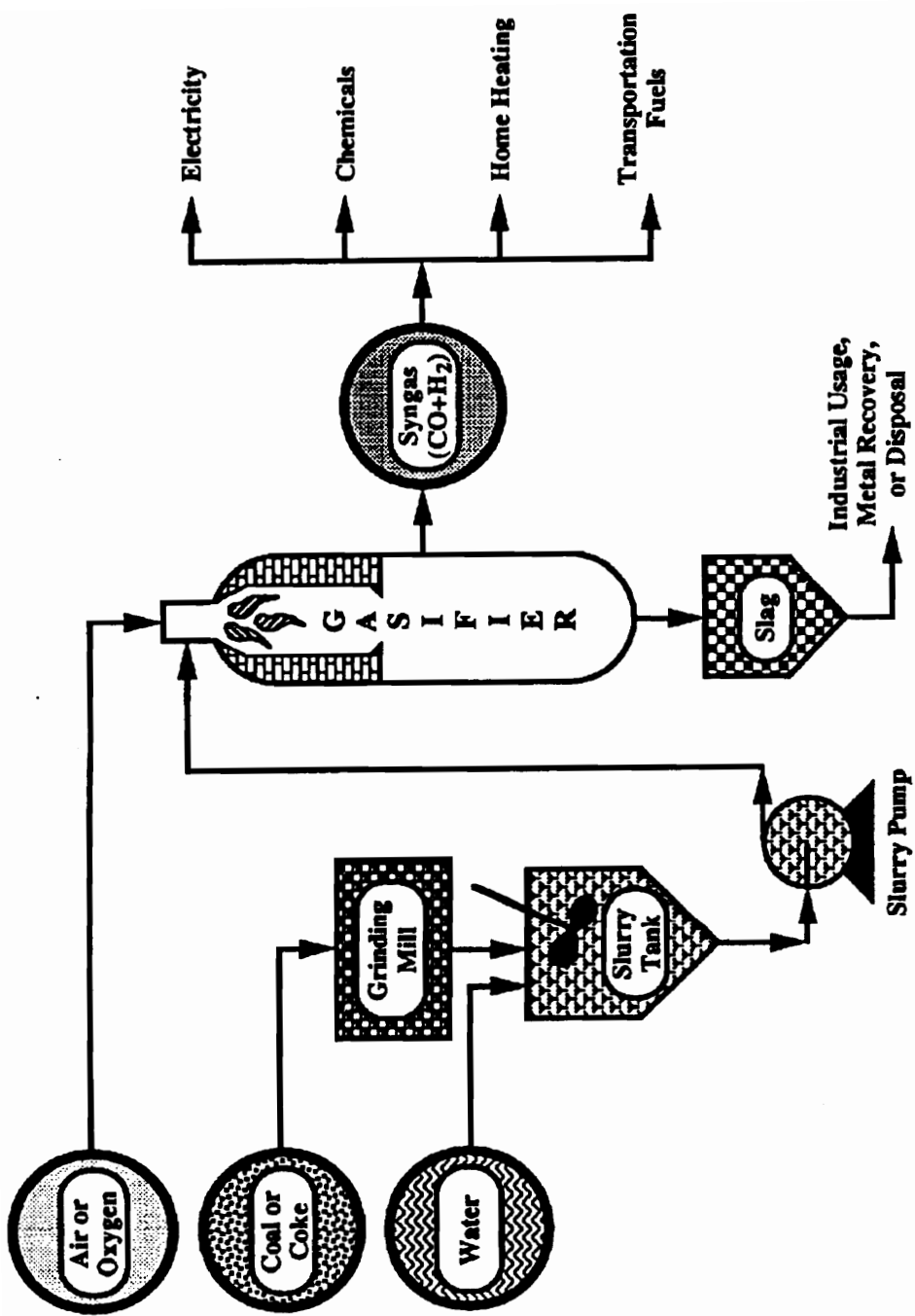


Figure 1. Schematic of the Texaco Gasification Process which operates in an entrained flow, slagging mode at 1200°C to 1500°C (after Groen 1992).

(Groen and Craig 1994). For example, oils typically contain 0.1-1000 ppm vanadium (Groen 1992) but bulk chemical analyses of petroleum coke slags show concentrations of vanadium as high as 38 weight percent (Lu et al. 1994).

Petroleum coke gasification slags are of interest from at least three perspectives: (1) their physical and chemical behavior in the gasifier; (2) their resource recovery potential; and (3) environmental concerns regarding disposal. The first step in the assessment of the nature of solid wastes is a simple bulk chemical analysis. However, the mere knowledge of bulk chemistry is far from sufficient. To thoroughly understand the chemical properties of petroleum coke slags or any other material with similar complexity, knowledge of phase chemistry, phase assemblages, textures, and formation mechanisms are indispensable. Knowing what phases are present is basic for almost any application, and thus the determination of phases is the most vital step in characterizing the petroleum coke slags.

X-ray diffraction (XRD) has been one of the most widely used techniques to identify the phases in heterogeneous materials. However, the use of XRD has been of limited use in previous studies of petroleum coke slags because of the difficulty of separating phases (Groen 1992). The situation is further complicated by extensive elemental substitutions among components in the phases of petroleum coke slags and by the occasional presence of previously unknown phases. Elemental substitution can cause substantial shifting of peak positions, which complicates the problem of resolving and assigning overlapping peaks to specific phases. In this study, great efforts have been made to derive reliable chemical formulae for individual phases, so that the phase verification by XRD is guided by a minimal number of candidate formulae. The positive identification of a phase is based on comparison of the observed peak patterns of the unknown with the peak patterns of known phases.

The method for deriving chemical formulae of unknown phases is discussed in most general chemistry books (e.g. Whitten et al. 1988) as well as mineralogy books (e.g. Klein

and Hurlbut 1993). The complexity of this process, and its subsequent success, varies depending on the degree to which chemical compositions and crystal chemistries are known. If the compounds do not contain transition elements and there are no extensive substitutions among the components, the calculation of chemical formulae is relatively straightforward. However, if compounds contain transition elements, and have significant solid solution as occurs in some petroleum coke slag phases, the derivation of chemical formulae is more complicated. This paper presents a procedure for identifying phases in petroleum coke slags specifically and more broadly for identifying the inorganic phases in any complex material.

A flowchart for the overall process is shown in Figure 2. Microscopic observations, bulk chemical analyses, and scanning electron microscopic examination all aided in obtaining high quality electron microprobe compositional data of individual phases. The compositional data were subjected to rigorous statistical evaluation to eliminate incompatible data. The valence states of transition elements were estimated using a thermodynamic approach, and subsequently used to obtain total oxide weight percentages. Calculation of cation proportions were carried out using a spread sheet program and the chemical formulae were derived on the basis of stoichiometric and integer criteria. A small number of highly probable chemical formulae were obtained by considering possible ionic substitutions, and then these formulae were used as candidates to facilitate the final XRD identification of the phases.

METHODS

Samples and Instrumental analysis

Sample acquisition and preparation

Gasifiers are operated at about 1400°C. As the hydrocarbons in the petroleum coke feedstock react with steam and oxygen to form synthesis gas (principally CO and H₂), the noncombustible inorganic constituents accumulate on the surface of the refractory material

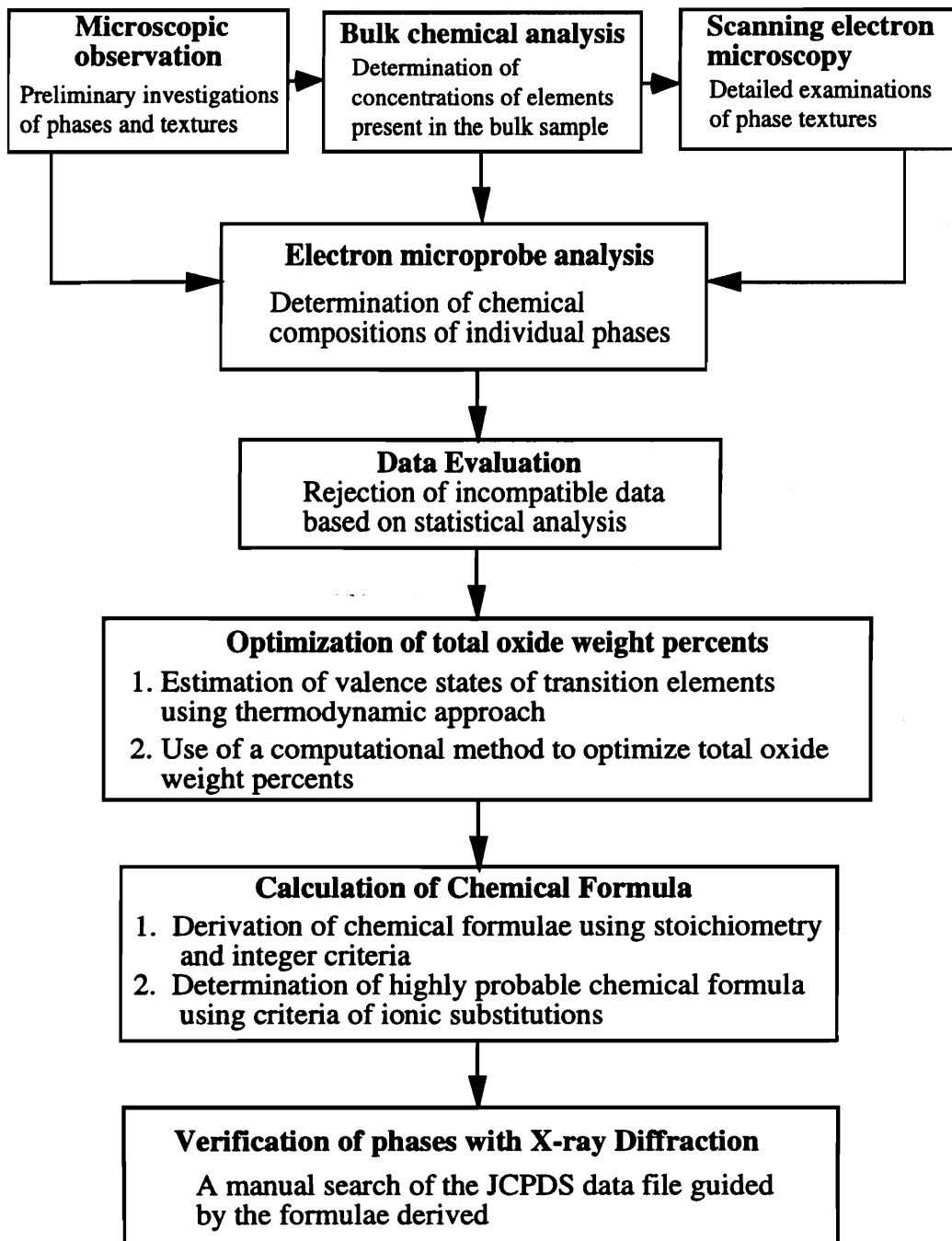


Figure. 2. Procedures for the determination of the phases in petroleum coke slags

that lines the gasifier. The exact processes by which the constituents accumulate are not known with certainty, but there is likely the combined effects of the physical entrapment of tiny particles in the violent non-laminar flow of gases, the transport of metals as sulfide and organometallic species, and some vaporization and condensation of metals. The net result is the buildup of complex, porous masses of crystalline and liquid phases on the surface of the refractory. Under normal operating conditions, the slags are reduced and contain native metals and sulfides that only exist under very low oxygen activities. These samples are preserved as formed by flooding the gasifier with an inert gas during cooling (over several days) to prevent reaction with atmospheric oxygen. The first set of samples studied (the reduced samples) were collected from the surface of the refractory material. A second set of samples consisting of oxidized slag, was produced when the gasifier was vented and the hot slag was allowed to react with oxygen. Under these conditions, oxygen rapidly reacts with the metal- and sulfur-bearing phases, converting many metals into oxides and the sulfur either into sulfate or volatile SO_x gases. Although the bulk chemistry of the slag changes very little except for sulfur loss and oxygen gain, the phase assemblages undergo significant changes during oxidation.

The reduced slag samples were 7 to 10 cm thick and were removed from the gasifier such that their orientation was known. The samples were cut using a diamond saw into a series of slabs oriented perpendicular to the wall of the gasifier so that the cross section from gasifier wall inward was visible. The slabs were subsequently cut into smaller sections on the basis of visible macroscopic zonations. In order to reduce the possibility of water/slag reaction, cut slabs were immediately dried in an oven at temperatures of 50°-80°C for a short period of time. Microscopic examination revealed no obvious evidence of reaction with the water or any changes resulting from drying.

Oxidized slag samples are more or less random in size, shape and orientation, because during the oxidation process the slag melts and flows down the walls of the

gasifier, eventually falling into a quench chamber below the gasifier. This material is periodically discharged into a collection bin. The reaction of oxygen with the slag and subsequent mixing through slag flow more or less homogenizes the samples so that little could be learned from oriented samples, even if they were available. Standard polished sections and doubly polished thin sections were made from reduced and oxidized slags to facilitate examination by both reflected and transmitted light microscopy, and by scanning electron microscopic techniques. The procedures used are well documented in Craig and Vaughan (1994).

Microscopic observations

Reflected and transmitted light optical microscopic examination was carried out using a Leitz Ortholux Plan microscope. This examination provided initial information on: 1) the number of phases present in the slags and the proportion of crystalline phases to glassy materials, 2) the general textures of the phase assemblages, and 3) the homogeneity of the phase distributions (zoning).

Bulk chemical analysis

In order to obtain information on the bulk chemistry of the slags, three samples were taken from the reduced slag in a sequential manner based on the zones observed through preliminary microscopic examinations: one from the side in contact with the refractory material, one from the middle of the slag mass, and one from the outermost side toward the center of the gasifier. They represent, by volume, approximately 10, 85, and 5 percent of the reduced slag, respectively. Chemical analyses were conducted at TSL/ASSAYERS Laboratories using ICP (inductively coupled plasma) and wet chemical techniques. The samples were ground to approximately 100 mesh. ICP was conducted for most elements. Lithium metaborate fusion was used to analyze oxides of Si, Al, Fe, Ca, Mg, Na, K, Ti,

Mn, and P, and elemental Ba, Sr, Zr, Y, Sc, Nb, Be, Ni, Cr, and V. Aqua-regia digestion was used for Ag, As, B, Bi, Cd, Co, Cu, Mo, Ni, Pb, Sb, Sn, W, and Zn. A 0.5 gram sample was digested with 2 mL of 3:1 HCl/HNO₃ at 95°C for 90 minutes and diluted to 10 mL with deionized water. Due to the extremely high concentration of vanadium and the difficulty of sulfur analysis with ICP, these two elements were analyzed by wet chemical methods. More than 30 elements were determined in the analyses and the results are presented in Appendix I. In this study, bulk chemical data were primarily used to facilitate interpretations for qualitative determination of elements present using scanning electron microscopy (EDS) and to determine which elements should be analyzed using electron probe microanalysis (WDS).

Scanning electron microscopy

A Cam Scan II scanning electron microscope was employed for the purpose of: 1) distinguishing phases and their textures on scales which are too fine to be resolved using light microscopy; and 2) obtaining qualitative and semi-quantitative estimates of phase compositions using an hnu energy dispersive spectrometer (EDS).

Electron probe microanalysis (EPMA)

In-situ nondestructive quantitative chemical analysis of phases down to 1 micrometer (micron) in size were carried out using a Cameca SX-50 electron microprobe automated by a Sun workstation. The microprobe was operated in both wavelength-dispersive (WDS) and energy-dispersive (EDS) modes. A previous study (Mavrogenes, 1994, per. comm.) revealed that the valence of vanadium in compounds is very sensitive to the energy of incident electron and laser beams. In view of this fact, the beam current was set to a low value (10 nA) and the accelerating voltage was set at 15kV. This appears to have successfully avoided sample oxidation because repeated analyses on a single grain or spot

did not reveal any alteration of the original phases or systematic drift of the analytical result. In order to obtain representative chemical compositions for the phases present, each phase was analyzed between five and thirty times on different crystals. Standards consisted of NaAlSi₃O₈, MgO, KAlSi₃O₈, CaSiO₃, TiO₂, V₂O₃, Cr₂O₃, MnO₂, Fe₂O₃, Fe₃O₄, NiO, ZrSiO₄, and BaSO₄.

X-ray diffraction

A Scintag X-ray powder diffractometer automated by the Scintag Diffraction Management System was used for all XRD work. The slag samples were ground in alcohol until grains were about 10 μm in size. In order to minimize problems of crystal orientation, and obtain good counting statistics, each sample was split into two, and spread onto glass supports. Each split was scanned twice with a rotation of the samples after each scan. The averaged data from these four scans was used for further identification efforts. Cu K-alpha radiation was used with a Ni filter at an accelerating voltage of 45 kV, and a current of 35 mA.

Data analysis

Data filtering using Chauvenet's criterion

The compositional data obtained during electron microprobe analysis of the petroleum coke gasification slag phases display some variability. Such variation may result from: 1) real compositional variability; 2) contamination resulting from impurities (inclusions) or artificial surface defects (cracks, pits); 3) drift of the electronics of the electron microprobe during analysis; 4) random error. During the analysis, great care was taken in selecting grains which appeared homogeneous (not zoned), and analysis areas which were well polished and free from charging problems. The chemical compositions of the phases

analyzed were corrected against the standards; therefore the variations are not likely caused by systematic instrumental errors such as electronic drift. Thus it is believed that the anomalies merely represent random errors. For example, the analytical volume of the electron beam (0.5-2 microns) may be large enough to allow for contamination from a phase lying one micron beneath the phase being analyzed.

A variety of statistical methods can be used to give reliable estimates of the random errors and provide a well-defined procedure for reducing them. In the present study, a procedure known as Chauvenet's criterion was adopted for aid in recognizing and rejecting outlier data because it is simple to apply and merely relies on the assumption that there is a normal or Gaussian distribution of data (Taylor 1982). The evaluation is done by performing the following calculations: 1) the mean (\bar{X}) and standard deviation (σ); 2) the difference between an individual data point (x) and the mean (\bar{X}); 3) the deviation factor f ($(x-\bar{X})/\sigma$); 4) the probability that a measurement will differ from \bar{X} by f or more; and 5) the product of the probability times the total number of analyses. The decision to retain or discard a datum is based on the critical number (0.5 by Chauvenet's criterion). If the product is less than 0.5, the datum will be discarded.

It can be seen that in Chauvenet's analysis, the amount of calculation depends on the way that individual data values are selected for evaluation. If only a few values were selected, the calculation can be done manually. However, this could introduce subjectiveness into data evaluation. In order to evaluate the large number of data on a completely objective basis, all the data were processed in a rigorous manner. This vastly increased the number of calculations, but these were readily handled using a computer programming technique. In the present study, the more sophisticated procedures were chosen to obtain a good set of data to represent the best possible composition for each individual phase. The computer program for the evaluation process can be found in Appendix II.

Table 1 lists 25 electron microprobe analyses of 15 elements for a sodium aluminum silicate phase in the reduced slags. The sodium aluminum silicate has been chosen to illustrate the application of Chauvenet's criterion. Note that the data for each element possesses some variability (i.e. Na from 14.24 to 21.94 weight percent and Si from 40.47 to 47.14 weight percent). The evaluation proceeds according to the procedures defined. For a data set of 25 analyses with each having 15 elements, the procedure will be carried out up to 375 (25 X 15) times. The program checks one element after another and for each element, one analysis after another. When an outlier was found, the whole data set containing that outlier (numbers 1, 18, 24 and 25) was eliminated because an error in one major element may have affected the analytical totals of other elements. Elements present in concentrations lower than 5 weight percent were not included in the evaluation process because low values tend to have large standard deviations . If they were included, it is possible that all the data would be eliminated. After data evaluation, four data sets (with light margins) were eliminated. The elimination of outlier data from the analyses does not change averages significantly, but it improves standard deviation dramatically. In this example, the standard deviations for Si, Na, and Al were reduced 8 percent, 26 percent, and 50 percent respectively.

Optimization of total oxide weight percentages

The next step in phase identification is to obtain the relative weight percentages of the oxides. However, the relative weight percentages can be calculated only when the valence states of the ions are known. For phases with elements possessing only one possible valence state, the oxide weight percentages are readily calculated. However, for phases containing transition elements whose valence states are variable, specific valence states of the elements must be determined in order to calculate the actual weight percentages.

Table 1. Electron microprobe chemical analyses of a sodium aluminum silicate (wt.%)

Spot No.	Na	Mg	Al	Si	Zr	K	Ca	Fe	Mn	Ni	Ti	S	V	Cr	Ba
1	18.31	0.31	36.83	47.14	0.01	0.14	0.25	0.21	0.02	0.06	0.09	0.05	0.93	0.00	0.09
2	17.18	0.06	36.82	43.22	0.00	0.18	3.68	0.11	0.00	0.00	0.05	0.00	0.11	0.64	0.03
3	17.46	0.14	36.74	44.15	0.00	0.29	2.88	0.20	0.06	0.00	0.04	0.03	0.30	0.00	0.19
4	18.27	0.09	35.96	42.92	0.01	0.23	3.18	0.17	0.00	0.07	0.03	0.04	0.02	0.00	0.05
5	18.50	0.29	35.83	45.31	0.00	0.10	0.25	0.27	0.02	0.07	0.09	0.04	0.89	0.00	0.13
6	20.22	0.13	35.80	43.63	0.00	0.07	0.06	0.08	0.00	0.05	0.03	0.18	0.79	0.00	0.00
7	17.84	0.10	35.75	42.21	0.03	0.20	3.17	0.04	0.00	0.03	0.01	0.05	0.05	0.00	0.16
8	17.89	0.12	35.70	42.49	0.09	0.21	3.01	0.21	0.00	0.00	0.02	0.01	0.31	0.00	0.17
9	17.47	0.11	35.48	41.65	0.00	0.19	3.24	0.16	0.04	0.02	0.06	0.05	0.17	0.00	0.17
10	20.75	0.33	35.43	42.55	0.00	0.16	0.65	0.09	0.00	0.00	0.04	0.06	0.97	0.00	0.00
11	17.93	0.16	35.29	43.01	0.00	0.18	2.41	0.11	0.03	0.01	0.02	0.02	0.12	0.13	0.09
12	19.14	0.27	34.90	42.74	0.00	0.17	0.49	0.14	0.01	0.10	0.03	0.03	0.78	0.00	0.16
13	20.70	0.28	34.89	42.89	0.00	0.15	0.60	0.17	0.00	0.03	0.01	0.02	0.90	0.00	0.11
14	18.56	0.10	34.82	43.90	0.00	0.17	1.72	0.25	0.03	0.00	0.08	0.00	0.11	0.08	0.13
15	20.96	0.20	34.63	42.53	0.00	0.10	0.20	0.17	0.01	0.00	0.03	0.08	0.95	0.00	0.05
16	19.36	0.06	34.62	44.64	0.09	0.17	1.10	0.19	0.06	0.11	0.05	0.04	0.02	0.00	0.03
17	18.72	0.04	34.50	43.62	0.03	0.17	1.58	0.18	0.02	0.00	0.07	0.02	0.03	0.00	0.17
18	21.94	0.11	34.20	40.47	0.00	0.18	0.38	0.24	0.00	0.00	0.00	0.04	0.02	0.00	0.11
19	18.93	0.07	34.01	44.21	0.00	0.14	1.17	0.18	0.02	0.05	0.06	0.03	0.04	0.11	0.00
20	21.03	0.09	33.75	41.16	0.06	0.12	0.15	0.50	0.00	0.10	0.04	0.16	0.30	0.00	0.05
21	17.07	0.46	32.95	44.35	0.07	0.13	4.33	0.11	0.00	0.00	0.00	0.03	0.39	0.00	0.28
22	16.34	0.32	32.48	44.43	0.08	0.11	3.50	0.28	0.06	0.13	0.25	0.05	3.68	0.00	0.21
23	18.75	0.16	31.25	41.92	0.01	0.05	4.25	0.15	0.00	0.06	0.35	0.16	2.58	0.16	0.00
24	14.67	1.51	27.73	43.23	0.06	0.10	11.86	0.35	0.07	0.06	0.05	0.02	0.64	0.00	0.19
25	14.24	3.15	24.37	44.73	0.00	0.07	13.22	0.31	0.02	0.11	0.00	0.06	0.45	0.00	0.27
Initial Aver.	18.49	0.35	34.19	43.32	0.02	0.15	2.69	0.20	0.02	0.04	0.06	0.05	0.62	0.04	0.11
Initial Stdev.	1.86	0.65	2.77	1.17	0.03	0.05	3.25	0.10	0.02	0.04	0.08	0.05	0.84	0.13	0.08
Aver.	18.72	0.17	34.84	43.22	0.02	0.15	1.98	0.18	0.02	0.04	0.07	0.05	0.64	0.05	0.10
Stdev.	1.37	0.11	1.37	1.08	0.03	0.05	1.47	0.10	0.02	0.04	0.08	0.05	0.91	0.14	0.08

* Analyses #1, 18, 24 and 25 were eliminated from subsequent calculations using Chauvenet's criterion. The outlier values are enclosed in the bold boxes.

Estimation of valence states of transition elements: thermodynamic constraints

Various spectroscopic methods have been used to determine the valence states of ions directly; these include Mossbauer, X-ray photon spectroscopy (XPS) and Synchrotron X-ray absorption spectroscopy. However, in most cases it is not practical to use these instruments due to accessibility, cost, the small size and intergrown nature of phases, and interpretational complications. For the present study, a thermodynamic method has been employed to estimate the valence states of various transition ions in the phases of both reduced and oxidized slags.

In order to make such determinations, it is necessary to assume that equilibrium conditions were achieved between co-existing phases. This assumption is not valid for oxidized slags as the occurrence of zoned spinel crystals and abundant glass provide evidence of incomplete equilibration on cooling. However, the assumption is believed valid for the reduced slags because of the high operating temperatures of the gasifier. The actual gasification temperatures are on the order of 1300-1500°C. It is also known that the gasifier walls are essentially at the same temperature as the process itself from heat flow calculations (Groen 1996, pers. comm.). Furthermore, individual grains have been found to be uniform in composition and there is no evidence of post-crystallization reaction rims between phases.

In reduced slags, two pieces of information are critical for determining the valence states of transition elements: 1) the occurrence of V_2O_3 , one of the dominant phases, and 2) the coexistence of iron-bearing alloys and iron-bearing sulfides. The valence of vanadium is concluded to be +3, because of the abundance of V_2O_3 , which was determined with confidence on the basis of the elemental weight percentage of vanadium obtained in numerous electron probe analyses. The coexistence of iron-bearing alloys and iron-bearing sulfides constrains the valence states of iron to be +2 or lower. With these constraints, valence states of other transition elements were derived.

The stability fields of various valence states of transition elements were plotted in P_{O_2} - T space by considering oxidation/reduction reactions. Figure 3 is an example for vanadium. There are 10 oxidation/reduction reactions, but only four of them (bold) are equilibrium reactions and these were used to delimit the stability fields of various valence states. Analogous plots for other transition elements were constructed in the same way but are not shown here. The free energy data for vanadium oxides, iron oxides, titanium oxides and manganese oxides were obtained from Robie et al. (1978) and that for chromium oxides from Samsonov (1982).

The range of oxygen pressures under which the reduced slags formed is illustrated in Figure 4. Based on Figure 4a, the possible oxygen pressures are in the V^{+3} field (light shaded). This range can be further constrained by incorporating $Fe^{+2} / Fe^{+2}-Fe^{+3}$ bounding line in P_{O_2} - T space in Figure 4b. The temperatures can not be easily constrained, but even with only oxygen pressure constraints, the valence states of other transition elements can be narrowed down substantially.

Figure 5 shows the oxygen pressure-temperature diagrams for chromium, titanium, and manganese. The shaded box on each diagram indicates the probable oxygen pressure range during the slag crystallization. Cr^{+4} can be ruled out because it is far above the shaded area. The valence states possible are Cr^0 and Cr^{+3} , but Cr^0 can be ruled out because there is no pure chromium metal or chromium alloy found in any of the phase assemblages. The valence state is clearly +4 for titanium and +2 for manganese.

The valence states of transition elements occurring in the oxidized slags can not be determined using a thermodynamic approach because the phase assemblages indicate disequilibrium. However, the valence states of the transition elements still can be constrained using those in reduced slag phases. Ti will be +4 because +4 is the highest possible valence state; Cr is probably still +3 because Cr^{+4} can only occur at temperature below approximately 100°C which is not likely; iron and manganese both can occur as +2 and +3

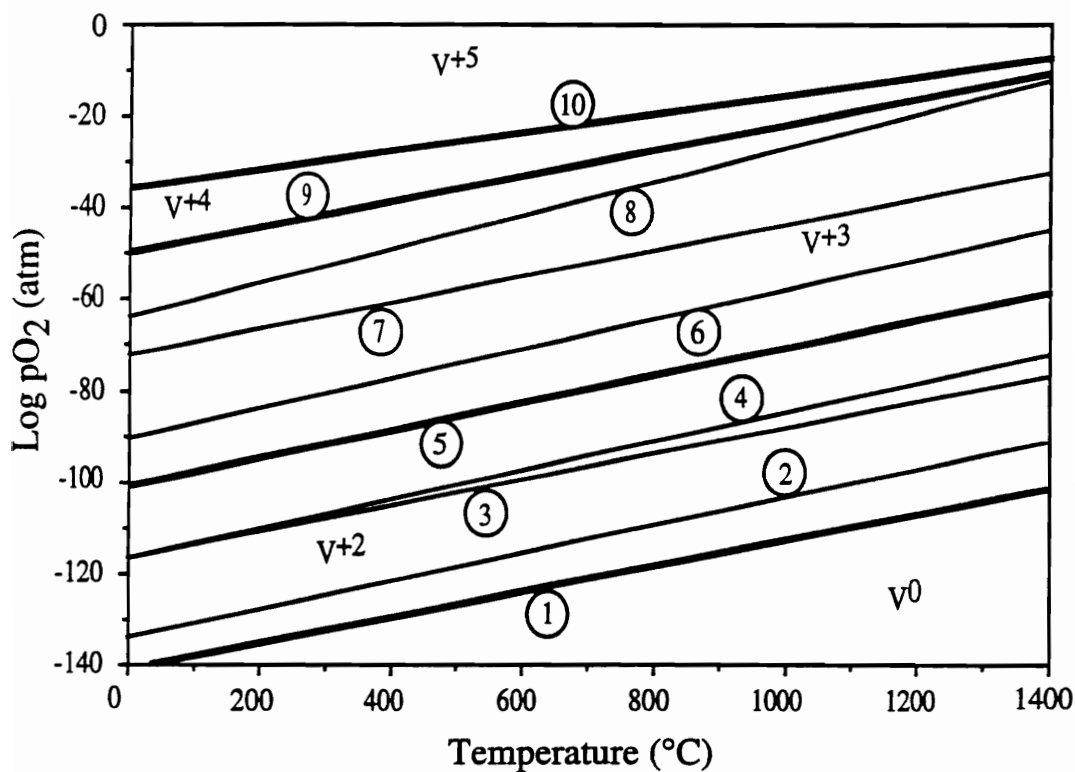


Fig. 3. Oxygen pressure - temperature diagram for vanadium and its oxides. Each line represents a reaction equation as follows. The heavy lines represent the equilibrium reactions (bold). The area between every two adjacent heavy lines indicates the stable field for a certain valence state. For example, V⁺² is stable between heavy lines labeled 1 and 5.

- | | |
|--|--|
| 1. $2\text{V} + \text{O}_2 = 2\text{VO}$ | 6. $4\text{VO} + \text{O}_2 = 2\text{V}_2\text{O}_3$ |
| 2. $4\text{V} + 3\text{O}_2 = 2\text{V}_2\text{O}_3$ | 7. $2\text{VO} + \text{O}_2 = 2\text{VO}_2$ |
| 3. $\text{V} + \text{O}_2 = \text{VO}_2$ | 8. $\text{VO} + \text{O}_2 = \text{V}_2\text{O}_5$ |
| 4. $4\text{V} + 5\text{O}_2 = 2\text{V}_2\text{O}_5$ | 9. $\text{V}_2\text{O}_3 + \text{O}_2 = \text{VO}_2$ |
| 5. $4\text{VO} + \text{O}_2 = 2\text{V}_2\text{O}_3$ | 10. $\text{VO}_2 + \text{O}_2 = \text{V}_2\text{O}_5$ |

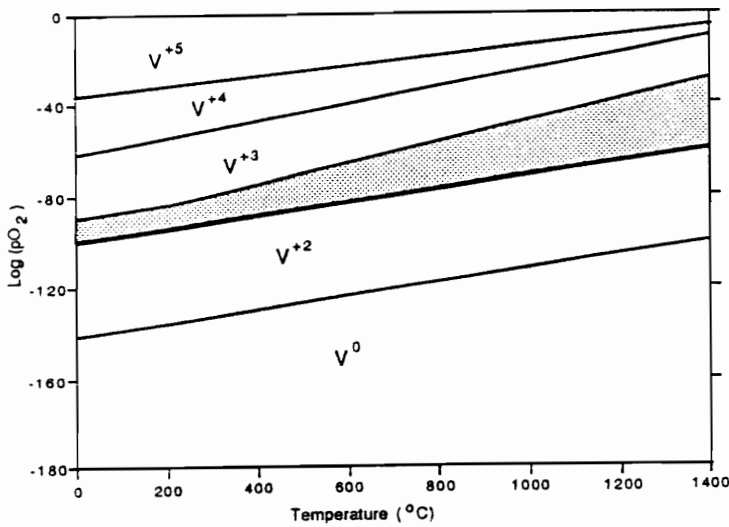
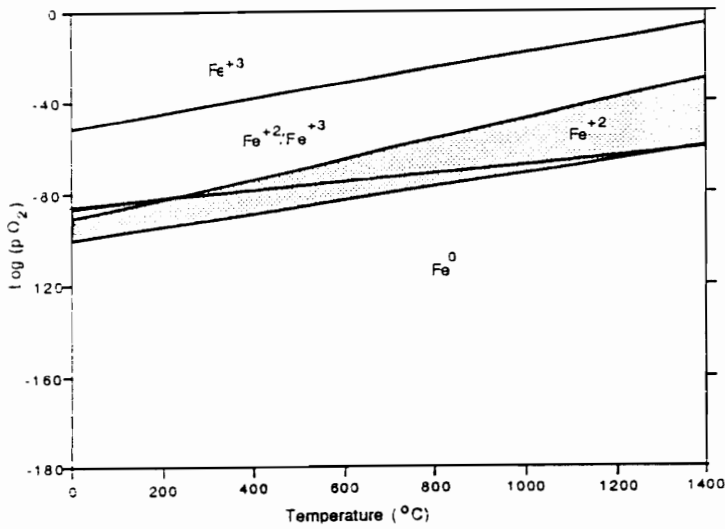


Figure 4. Constraints for oxygen pressures in reduced petroleum coke slags for Fe and V. The shaded areas on this and the next diagram represent the conditions expected while the reduced slag was forming as indicated by the oxidation states of the iron and vanadium phases.

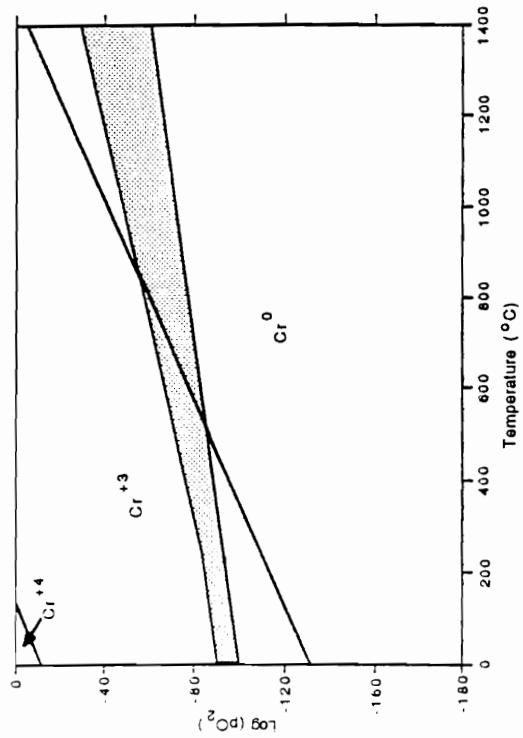
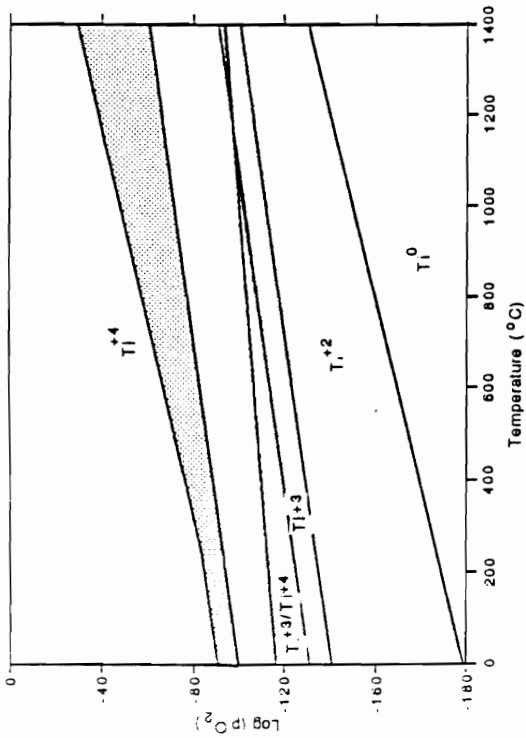
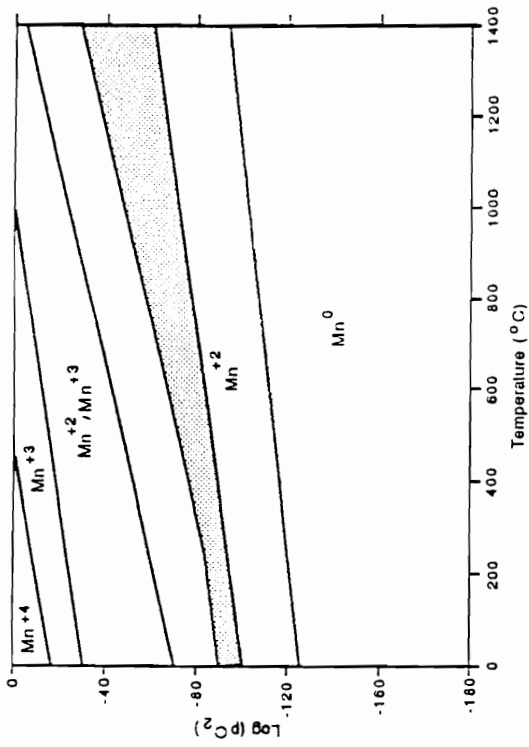


Figure 5. Oxygen pressure-temperature diagrams for Cr, Ti, and Mn and their oxides. The shaded areas represent the conditions expected while the reduced slag was forming as indicated by the oxidation states of iron and vanadium phases.

and can not be further constrained. Vanadium occurs both as +4 and as +5 because V^{+4} and V^{+5} occur in the two most abundant phases V_2O_4 and CaV_2O_6 which were determined with confidence on the basis of the elemental weight percentage of vanadium obtained in electron probe analyses. The occurrence of V^{+3} , although not likely, can not be ruled out.

Optimization of total oxide weight percentages: a numeric approach

If all the valence states of the elements present in a phase are known, the total oxide weight percentage can be simply calculated by summing up all individual oxides. Since the valence states of iron, manganese, and in some phases vanadium are not known with certainty, all possible valence states should be considered. Numerically, we can calculate all the possibilities on the basis of all possible combinations of valence states. The number of the possibilities can be narrowed down substantially by discarding those numerically impossible combinations. Theoretically, all correct assignment of valence states for the elements involved should total 100 percent, but it is recognized that all analyses have some random analytical errors. Accordingly, calculations were considered acceptable if the summation ranged between 97 and 103 percent.

A 100 ± 3 percent of the total oxide weight percentage can be obtained either by changing the valence state(s) and/or by splitting the element(s) into two valence states. Splitting into more than two states is not likely unless the phase was formed under non-equilibrium conditions. For a phase which contains only one transition element, this process is reasonably straightforward. First, all the valence states of the element can be tested to see if a reasonable total oxide weight percentage can be found for any single specific valence state. If not, calculations are performed by variably splitting the element between two adjacent valence states. For a phase which contains two or more transition elements of unknown valence states, a unique solution is not possible because mathematically, we are faced with a system of equations that is unresolvable. If no valence

splitting appears necessary in such a phase, all combinations of the reasonable valence states of transition elements can be tried; if valence splitting is necessary, then a decision must be made to split the most likely element and keep the valence states of the other elements constant. This is due to the fact that if the valences of all the elements are split, there will be an unlimited number of solutions.

Table 2 is an example of the procedure for optimizing the total oxide weight percentages for a calcium nickel vanadate occurring in the oxidized slag. The table consists of 10 columns. As discussed already, the valence states of titanium and chromium are constrained thermodynamically to be +4 and +3, respectively, and are marked with a light border in columns 3 and 4. The valence states of vanadium, manganese, and iron are unknown (heavy border) and all possible combinations will be tried to obtain corresponding total oxide weight percentages as shown in columns 9 and 10. It can be seen that there are four possibilities that meet the criterion of 100 ± 3 total oxide weight percent (bold). The selection among these possibilities is rather arbitrary, but a reasonable decision still can be made. As discussed already, the valence states of iron and manganese both can be +2 and +3 in the gasification conditions. In a relative sense, they can be expected to have a higher average valence under the oxidizing condition (oxidized slag) and a lower average valence under the reducing condition (reduced slag). The example phase in Table 2 occurs in the oxidized slag and therefore the valence states of manganese and iron are most likely to be +3. Using the valence states of vanadium (+5), manganese (+3), and iron (+3), the total oxide weight percent for this phase is 98.47 percent.

It should be pointed out that during the process, it is possible that no combination of valence states will produce an oxide sum of 100 ± 3 weight percent. In such cases, water or other components should be considered. Table 3 is an example for a sodium vanadate occurring in the oxidized slag. It can be seen that the major components in the phase are sodium and vanadium. The total oxide weight percentage can be adjusted to only 83.3

Table 2. Optimization of the total weight percent oxide for a calcium nickel vanadate

1*	2	3	4	5	6	7	8	9	10
Na	23.0	2	1	62	5.80	4.30	5.80	V+5Mn+3Fe+3	98.47
Mg	24.3	1	1	40.3	4.63	2.79	4.63	V+5Mn+2Fe+3	98.46
Al	27.0	2	3	102	0.17	0.09	0.17	V+5Mn+3Fe+2	98.17
Si	28.1	1	2	60.1	0.21	0.10	0.21	V+5Mn+2Fe+2	98.16
Zr	91.2	1	2	123.2	0.01	0.01	0.01	V+4Mn+3Fe+3	94.22
K	39.1	2	1	94.2	0.01	0.00	0.01	V+4Mn+2Fe+3	94.21
Ca	40.1	1	1	56.1	20.62	14.74	20.62	V+4Mn+3Fe+2	93.92
Fe	55.8	2	3	159.6	2.70	2.10	3.00	V+4Mn+2Fe+2	93.91
Mn	55.0	2	3	158	0.10	0.08	0.12	V+3Mn+3Fe+3	89.97
Ni	58.7	1	1	74.7	15.28	12.01	15.28	V+3Mn+2Fe+3	89.96
Ti	47.9	1	2	79.9	0.15	0.09	0.15	V+3Mn+3Fe+2	89.67
S	32.1	1	3	80.1	0.03	0.01	0.03	V+3Mn+2Fe+2	89.66
V	50.9	2	5	181.8	39.79	27.04	48.29		
Cr	52.0	2	3	152	0.13	0.09	0.13		
Ba	137.3	1	1	153.3	0.03	0.03	0.03		
Total				89.66	63.48	98.47			

- * 1: Titles of elements; 2: Atomic weight;
3: Number of cations; 4: Number of oxygen;
5: Molecular weight; 6: Original weight percentage of oxides;
7: Elemental concentrations; 8: Recalculated weight percentage of oxides;
9: Combinations of various valence states; 10: Total oxide weight percents

percent (marked by dashed border), even when all the vanadium is assumed to be in the highest valence state (+5). In this case, it seems reasonable to infer that water is responsible for the discrepancy of the total oxide weight percentage of the phase. The presence of water in this phase is possible considering the nearby proximity of the quench chamber. The program which performs the preceding calculations can be found in Appendix III.

Derivation of chemical formulae

After the total oxide weight percentages are determined, cation proportions can be calculated easily using a spreadsheet program. This begins by grouping the cations to fit to an assumed formula. For the present study, a numeric method using stoichiometry and integer criteria was used to derive chemical formulae. This is followed by using knowledge of substitutional chemistry to obtain a short list of highly probable chemical formulae.

Stoichiometry and integer criteria

The numeric method is based on two assumptions: compound stoichiometry and integer criteria. Statistically, inorganic phases are dominated by those which possess one, two or three major cations. For an unknown phase, the stoichiometry can be worked out on a trial and error basis. For phases containing one dominant cation, the chemical formula can be derived easily because all other minor cations should only substitute for the major cation. For phases in which dominance of cations is not obvious, the judgement of whether the compound has two or three major cations is not obvious. In this case, it is necessary to consider both possibilities. In petroleum coke slags, the only significant anion found, other than sulfide, is oxygen. For any specific phase, the number of oxygens is derived from proportions of cations in the phase because oxygen is not determined during analysis.

Table 3. Optimization of the total oxide weight percent for a sodium vanadate

1*	2	3	4	5	6	7	8	9	10
Na	23.0	2	1	62.0	11.6	8.6	11.6	V+5Mn+3Fe+3	92.8
Mg	24.3	1	1	40.3	0.1	0.0	0.1	V+5Mn+2Fe+3	92.8
Al	27.0	2	3	102.0	0.9	0.5	0.9	V+5Mn+3Fe+2	92.7
Si	28.1	1	2	60.1	0.8	0.4	0.8	V+5Mn+2Fe+2	92.7
Zr	91.2	1	2	123.2	0.1	0.1	0.1	V+4Mn+3Fe+3	86.1
K	39.1	2	1	94.2	0.2	0.1	0.2	V+4Mn+2Fe+3	86.1
Ca	40.1	1	1	56.1	1.2	0.9	1.2	V+4Mn+3Fe+2	86.0
Fe	55.8	2	3	159.6	0.8	0.6	0.8	V+4Mn+2Fe+2	86.0
Mn	55.0	1	2	87.0	0.0	0.0	0.0	V+3Mn+3Fe+3	79.4
Ni	58.7	1	1	74.7	0.1	0.1	0.1	V+3Mn+2Fe+3	79.4
Ti	47.9	1	2	79.9	0.5	0.3	0.5	V+3Mn+3Fe+2	79.3
S	32.1	1	3	80.1	0.1	0.0	0.1	V+3Mn+2Fe+2	79.3
V	50.9	2	5	181.8	62.6	42.5	76.0		
Cr	52.0	2	3	152.0	0.1	0.1	0.1		
Ba	137.3	1	1	153.3	0.3	0.2	0.3		
H	1.0	2	1	18.0	4.0	0.4	4.0		
Total					83.3	54.9	96.8		

- * 1: Titles of elements; 2: Atomic weight;
 3: Number of cations; 4: Number of oxygen;
 5: Molecular weight; 6: Original weight percentage of oxides;
 7: Elemental concentrations; 8: Recalculated weight percentage of oxides;
 9: Combinations of various valence states 10: Total oxide weight percents

The integer criteria employed here assumes that the trace elements substitute for major atoms at regular lattice positions. Chemical stoichiometry requires that each structural site as a whole have an integral number of atoms per site. The Ni-Al spinel phase (NiAl_2O_4) provides an example. If there are substitutions of Mg for Ni, and Cr for Al, the formula will be $(\text{Ni, Mg})(\text{Al, Cr})_2\text{O}_4$. It should be pointed out that although the assumption is generally valid, there are exceptions whereby trace elements in phases are controlled by mechanisms such as adsorption, kinetics of crystal growth, and disequilibrium processes (Ahrens 1953; De Vore 1955a, b, 1957).

On the basis of the assumptions made above, chemical formulae were calculated. If a phase contains two major cations (denoted as A and B) and several minor cations, there are four possibilities for the locations of the minor cations in the crystal structure: 1) all of them go to A; 2) all of them go to B; 3) some cations go to A and all the remaining cations go to B; and 4) some of each cation goes to A and the remainder of that cation goes to B. For the present study, only the first three cases were considered. The fourth case was not considered because although element partitioning among different sites is not uncommon, the element is, in general, dominantly distributed in one site and the amount in other sites is insignificant. Furthermore, if partitioning for all the minor cations over all possible sites are considered, too many formulae would be derived to be meaningful.

The calculations for the first two cases are straightforward. For the third case, the calculation requires a computer model to consider all the possibilities. The flow chart and the source code for the program to accomplish this task are in Appendix IV. The general procedures are briefly described below.

The model considers formulae with up to two different formula types: $\text{M1}_{x1}\text{M2}_{x2}\text{O}_{x3}$ (two cation sites M1 and M2) and $\text{M1}_{x1}\text{M2}_{x2}\text{M3}_{x3}\text{O}_{x4}$ (three cation sites M1, M2 and M3) and an unlimited range of the number of oxygen. The decision of whether only one of the two formula types or both of them are tested and on the range in the number of oxygen is

dependent upon knowledge of the phase of interest. When these parameters are determined, the program will calculate all possible formulae based on the formula type(s) and the range of the oxygen numbers.

Consider calculations for an unknown calcium nickel vanadate phase for example. Both formula types were assumed and the oxygen number ranges were set from 3 to 24. The program began with the formula type as $M1_{x1}M2_{x2}O_{x3}$ and set the number of oxygens at 3. The program then calculated all possible combinations of the minor cations and their summed values. This was followed by combining minor cations with the major cations to see if integer criteria were obtained. If so, the combination was retained as a possible substitution; if not, the combination was discarded. When the calculation for three oxygens was done, the program proceeded to four oxygens and so on, until the upper limit of 24 oxygens was reached. Then the program proceeded to the next formula type which is $M1_{x1}M2_{x2}M3_{x3}O_{x4}$. The procedures began all over again as described above. The result of these calculations is shown in Table 4.

Ionic substitutions and the screening process

As stated previously, the formulae derived above are based on stoichiometry and integer criteria. Examinations of the formulae demonstrate that some of the formulae are highly unlikely, if not impossible. Take formula No. 2, $(Ca,Ni,Mg,Fe)(V,Na)O_3$ for example. In this formula, substitution of vanadium by sodium is not likely because of the large radius difference (>80%), large bond character difference (~80%) and large charge difference (Na^{+1} vs. V^{+5}). To eliminate these formulae on a reasonably objective basis, knowledge of ionic substitution chemistry has to be utilized.

Theories of ion substitutions are briefly reviewed here. Goldschmidt (1937), in the first attempt to outline the laws of distribution of the chemical elements, proposed a series of rules governing the mutual replacement of ions in magmatic minerals based on the assumption that the bonding in those minerals was purely ionic. Ringwood (1955)

Table 4. Possible chemical formulae derived based on stoichiometry and integer criteria for a calcium nickel vanadate

I. Two cation sites

No.	Site 1	Site 2	No.	Site 1	Site 2
1	VNi	1 CaNaMgFe	1 0	3 VNa	3 CaNiMgFe
2	VNa	1 CaNiMgFe	1 0	3 VNiNa	4 CaMgFe
3	VNiFe	1 CaNaMg	1 0	3 VNiFe	3 CaNaMg
4	VNaFe	1 CaNiMg	1 0	3 VNaFe	3 CaNiMg
5	VMgFe	1 CaNiNa	1 0	3 VMgFe	3 CaNiNa
6	VNiNaFe	2 CaMg	1 0	5 VNiNaFe	4 CaMg
7	VNi	2 CaNaMgFe	2 0	6 V	2 CaNiNaMgFe
8	VNa	2 CaNiMgFe	2 0	6 VNi	3 CaNaMgFe
9	VNiFe	2 CaNaMg	2 0	6 VNa	3 CaNiMgFe
10	VNaFe	2 CaNiMg	2 0	6 VMg	3 CaNiNaFe
11	VMgFe	2 CaNiNa	2 0	6 VNiMg	4 CaNaFe
12	VNiNaMg	3 CaFe	1 0	6 VNaMg	4 CaNiFe
13	VNiNaMgFe	3 Ca	1 0	6 VNiNaMg	5 CaFe
14	VFe	2 CaNiNaMg	3 0	7 VNiNaFe	4 CaMg
15	VNiMg	3 CaNaFe	2 0	7 VNa	4 CaNiMgFe
16	VNaMgFe	3 CaNi	2 0	7 VMg	3 CaNiNaFe
17	VFe	2 CaNiNaMg	3 0	8 VFe	3 CaNiNaMg
18	VNiMg	3 CaNaFe	2 0	8 VNiMg	4 CaNaFe
19	VNaMg	3 CaNiFe	2 0	8 VNiFe	4 CaNaMg
20	VNiMgFe	3 CaNa	2 0	8 VNaMg	4 CaNiFe
21	VNaMgFe	3 CaNi	2 0	8 VNiNaMg	5 CaFe
22	V	2 CaNiNaMgFe	3 0	8 VNiMgFe	4 CaNa
23	VNi	3 CaNaMgFe	3 0	9 VNaMgFe	4 CaNi

(to be continued)

No.	Site 1	Site 2	No.	Site 1	Site 2
47	VNiNaMgFe	5 Ca	11	VNa	5 CaNiMgFe
48	VNi	4 CaNaMgFe	12	VMg	4 CaNiNaFe
49	VNa	4 CaNiMgFe	12	VFe	4 CaNiNaMg
50	VFe	3 CaNiNaMg	12	VNiNa	6 CaMgFe
51	VNiNa	5 CaMgFe	12	VNiMg	5 CaNaFe
52	VNiMg	5 CaNaFe	12	VNiFe	5 CaNaMg
53	VNiFe	4 CaNaMg	12	VNaMg	5 CaNiFe
54	VNaMg	5 CaNiFe	12	VNaFe	5 CaNiMg
55	VNaFe	4 CaNiMg	12	VMgFe	4 CaNiNa
56	VMgFe	4 CaNiNa	12	VNiNaFe	6 CaMg
57	VNiNaMg	6 CaFe	12	VNaMgFe	6 CaNi
58	VNiMgFe	5 CaNa	12	VNi	5 CaNaMgFe
59	VNaMgFe	5 CaNi	12	VNa	5 CaNiMgFe
60	VNiNaMgFe	6 Ca	12	VMg	4 CaNiNaFe
61	V	3 CaNiNaMgFe	12	VFe	4 CaNiNaMg
62	VNi	4 CaNaMgFe	13	VNiMg	6 CaNaFe
63	VNa	4 CaNiMgFe	13	VNiFe	5 CaNaMg
64	VMg	4 CaNiNaFe	13	VNaMg	6 CaNiFe
65	VNiNa	5 CaMgFe	13	VNaFe	5 CaNiMg
66	VNiFe	5 CaNaMg	13	VMgFe	5 CaNiNa
67	VNaMg	5 CaNiFe	13	VNiNaMg	7 CaFe
68	VNaFe	4 CaNiMg	13	VNiNaFe	7 CaMg
69	VMgFe	4 CaNiNa	13	VNiMgFe	6 CaNa
70	VNiNaFe	6 CaMg	13	VNaMgFe	6 CaNi
71	VNiMgFe	5 CaNa	13	V	4 CaNiNaMgFe
72	VNiNaMgFe	6 Ca	13	VNi	5 CaNaMgFe
73	V	3 CaNiNaMgFe	13	VNa	5 CaNiMgFe
74	VNi	5 CaNaMgFe	14		

(to be continued)

II. Three cation sites

No.	Site 1	Site 2	Site 3		No.	Site 1	Site 2	Site 3	
102	VNa	2 Ca	1 NiMgFe	1 0	6	128	VFe	4 NiMg	2 0
103	VMgFe	2 Ca	1 NiNa	1 0	6	129	V	3 NiNaFe	3 0
104	VNa	3 CaMg	2 NiFe	1 0	9	130	V	4 NiMg	2 0
105	V	2 CaNaMg	3 NiFe	1 0	9	131	VMg	3 NiNa	3 0
106	VNa	3 CaMg	2 NiFe	1 0	10	132	V	3 NiNaMg	4 0
107	VMg	3 CaNaFe	3 Ni	1 0	10	133	V	4 NiNa	3 0
108	VNaMg	4 CaFe	2 Ni	1 0	10	134	VNa	4 NiFe	2 0
109	VMg	3 CaFe	2 NiNa	2 0	11	135	VNa	3 NiMgFe	3 0
110	VMg	3 CaNaFe	3 Ni	1 0	11	136	VMg	4 NiFe	2 0
111	VMg	3 Ca	2 NiNaFe	2 0	11	137	VMg	3 NiNa	3 0
112	VFe	3 CaNaMg	3 Ni	1 0	11	138	VMg	3 NiNaFe	3 0
113	VNaMg	4 CaFe	2 Ni	1 0	11	139	VFe	4 NiNa	3 0
114	VNa	4 CaMgFe	3 Ni	1 0	12	140	VFe	3 NiNaMg	4 0
115	VNa	4 Ca	2 NiMgFe	2 0	12	141	VNaMg	3 NiFe	2 0
116	VFe	3 CaNaMg	4 Ni	1 0	12	142	VMgFe	3 NiNa	3 0
117	VFe	3 Ca	2 NiNaMg	3 0	12	143	V	4 NiMgFe	3 0
118	VNaMg	5 CaFe	2 Ni	1 0	12	144	V	4 NiNaFe	3 0
119	VMgFe	4 CaNa	3 Ni	1 0	12	145	V	3 NiNaMg	4 0
120	VMgFe	4 Ca	2 NiNa	2 0	12	146	V	5 NiFe	2 0
121	V	3 CaNa	3 NiMgFe	2 0	12	147	V	4 NiNa	3 0
122	V	3 CaFe	2 NiNaMg	3 0	12	148	VNa	4 NiFe	2 0
123	V	3 CaMgFe	3 NiNa	2 0	12	149	VNa	3 NiMgFe	3 0
124	VNa	4 Ca	2 NiMgFe	2 0	13	150	VMg	5 NiFe	2 0
125	VNaFe	4 Ca	2 NiMg	2 0	13	151	VMg	3 NiNa	3 0
126	V	3 CaNa	3 NiMgFe	2 0	13	152	VFe	4 NiNa	3 0
127	VNa	5 CaFe	3 NiMg	2 0	15	153	VFe	3 NiNaMg	4 0

(to be continued)

II. Three cation sites

No.	Site 1	Site 2	Site 3	No.	Site 1	Site 2	Site 3
154	VNaMg	7 Ca	3 NiFe	18	179 VFe	5 CaNa	5 NiMg
155	VMgFe	6 Ca	3 NiNa	18	180 VFe	5 CaNaMg	6 Ni
156	V	4 CaNa	5 NiMgFe	18	181 VFe	5 Ca	3 NiNaMg
157	V	4 CaFe	3 NiNaMg	18	182 VNaMg	8 CaFe	4 Ni
158	V	4 CaNaMg	6 NiFe	18	183 VNaMg	8 Ca	3 NiFe
159	V	4 CaMgFe	4 NiNa	18	184 VNaFe	7 CaMg	4 Ni
160	VNa	6 CaMg	4 NiFe	19	185 VNaFe	7 Ca	3 NiMg
161	VNa	6 Ca	3 NiMgFe	19	186 VMgFe	6 CaNa	5 Ni
162	VMg	6 CaNa	5 NiFe	19	187 V	5 CaNa	5 NiMgFe
163	VMg	6 Ca	3 NiNaFe	19	188 V	5 CaMg	4 NiNaFe
164	VFe	5 CaNa	5 NiMg	19	189 V	5 CaFe	4 NiNaMg
165	VFe	5 Ca	3 NiNaMg	19	190 V	5 CaNaMg	6 NiFe
166	VNaMg	7 Ca	3 NiFe	19	191 V	5 CaNaFe	5 NiMg
167	VNaFe	7 Ca	3 NiMg	19	192 VNa	7 CaFe	4 NiMg
168	V	5 CaNa	5 NiMgFe	19	193 VNa	7 CaMgFe	5 Ni
169	V	5 CaMg	4 NiNaFe	19	194 VMg	6 CaFe	4 NiNa
170	V	5 CaNaMg	6 NiFe	19	195 VMg	6 CaNaFe	6 Ni
171	V	5 CaNaFe	5 NiMg	19	196 VFe	5 CaNa	5 NiMg
172	VNa	7 CaMg	4 NiFe	20	197 VFe	5 CaMg	5 NiNa
173	VNa	7 CaFe	4 NiMg	20	198 VFe	5 CaNaMg	6 Ni
174	VNa	7 CaMgFe	5 Ni	20	199 VNaMg	8 CaFe	4 Ni
175	VNa	7 Ca	3 NiMgFe	20	200 VNaFe	7 CaMg	5 Ni
176	VMg	6 CaNa	5 NiFe	20	201 VMgFe	7 CaNa	5 Ni
177	VMg	6 CaNaFe	5 Ni	20	202 V	5 CaMg	5 NiNaFe
178	VMg	6 Ca	3 NiNaFe	20			

Note: The valence assignments for the cations are: Na +1, Mg +2, Ca +2, Fe +3, V +5, and Ni +2.

modified the Goldschmidt rules by including the electronegativity of an ion as an additional factor influencing element distribution. The modified Goldschmidt rules are not without problems and various other models were subsequently proposed. DeVore (1955a,b) preferred to interpret trace element geochemistry by adsorption phenomena, kinetics of crystal growth, and disequilibrium processes whereas Burns and Fyfe (1964) and Curtis (1964) employed crystal field theory to interpret transition-metal geochemistry. It should be pointed out that in spite of the limitations of the Goldschmidt rules, they are still the most successful and most widely used model to explain trace element distributions among phases. More recently, Burnham (1990) defended the ionic model, and Faure (1991) also stated that the Goldschmidt rules provides a rational basis for understanding the distribution of trace elements.

For the present study, the Goldschmidt rules were used as a primary tool to evaluate the ionic substitutional possibilities. An ion substitution priority table (Table 5) was created by considering ionic radius, bond characteristic, charge, and coordination. First, all the elements of different valence states and coordinations were listed and the ionic radius (Whittaker and Muntus 1970) and ion-oxide bond character (Smith 1956) data were tabulated. This was followed by calculating the radius and bond character differences among each pair of ions. For each major cation, the minor cations were sorted into a descending order on the basis of radius differences and bond character differences. According to the Goldschmidt rules, two ions are able to replace one another in a crystal structure if the ionic radii do not differ by more than 15 percent. For the present study, the criteria was set to 40 percent for two reasons. First, a 40 percent difference allows aluminum to be included as substitutional for silicon; second, by setting the criteria to a wider range, there is less risk of eliminating a possible substitution. Further elimination was made on the basis of bond criteria and charge criteria. The bond character difference was set to 60 percent. It is used as a secondary criterion on the belief that ionic radius is

Table 5. Ionic substitution priority table

I V				V				V I						
Mg+2	Al+3	Si+4	V+3	V+4	V+5	Cr+3	Fe+2	Fe+3	Ni+2	Na+1	Mg+2	Al+3	Mg+2	Na+1
Ni+2	V+4	V+5	Cr+3	Ti+4	V+4	Fe+3	Mg+2	Cr+3	Mg+2	Mg+2	Ni+2	Al+3	Ni+2	Ca+2
Fe+2	Ti+4	Al+3	Fe+3	Cr+3	Ti+4	Ti+4	Ni+2	Ti+4	V+3	Mn+2	Fe+2	Mn+3	Al+3	Mn+2
V+3	Cr+3	Cr+3	Ti+4	Fe+3	Si+4	V+3	V+3	V+3	Fe+2	Na+1	Mn+3	Cr+3	Cr+3	V+4
Cr+3	Fe+3	Fe+3	Ni+2	V+3	V+3	V+4	Cr+3	V+4	Cr+3	Fe+3	V+3	V+3	V+3	Ti+4
Fe+3	V+3	V+4	V+4	Al+3	Al+3	Ni+2	Fe+3	Ni+2	Fe+3	K+1	Mn+3	Cr+3	V+3	Cr+3
Al+3	Ni+2	Mg+2	Mg+2	V+5	V+5	Mg+2	Mg+2	Mg+2	Al+3	Mg+2	Mn+2	Fe+3	Fe+3	V+3
Si+4	Si+4	Zr+4	Zr+4	Zr+4	Zr+4	Zr+4	Zr+4	Zr+4	Zr+4	Ni+2	Cr+3	Ni+2	Cr+3	Ni+2
Mg+2	Mg+2	Fe+2	Fe+2	Al+3	Al+3	Al+3	Al+3	Al+3	Al+3	Al+3	Si+4	Si+4	Si+4	Si+4
Zr+4	Zr+4	Al+3	Al+3	Fe+2	Fe+2	Fe+2	Fe+2	Fe+2	Fe+2	Ca+2	Mg+2	Mg+2	Mg+2	Mg+2

V I				V II				VIII				I X				X				XII			
Ca+2	V+3	V+4	V+5	Cr+3	Fe+2	Fe+3	Ni+2	Na+1	Ca+2	Na+1	Mg+2	Ca+2	Na+1	Ca+2	Na+1	Ca+2	Na+1						
Na+1	Mn+3	Ti+4	V+4	Ti+4	Mn+2	Mn+3	Mg+2	Ca+2	Na+1	Ca+2	Mn+2	Mg+2	Mn+2	Ca+2	Na+1	Ba+2	Ca+2						
Mn+2	Fe+3	Cr+3	Ti+4	V+3	Mg+2	V+3	Mn+3	Ba+2	Ba+2	Ba+2	Ca+2	Na+1	Mn+2	Ca+2	Ba+2	Ba+2	K+1						
Fe+2	Cr+3	V+3	Zr+4	Mn+3	Ni+2	Cr+3	Fe+3	Mn+2	K+1	K+1	Mn+2	Na+1	Mg+2	K+1	K+1	K+1	Ba+2						
Ba+2	Ti+4	V+5	Si+4	Fe+3	Mn+3	Ni+2	V+3	Mg+2	K+1	Mg+2	Ba+2	Mg+2	Ba+2	K+1	K+1	K+1	Ba+2						
Mg+2	Ni+2	Mn+3	Mn+3	V+4	Fe+3	Ti+4	Cr+3	K+1	K+1	K+1	K+1	K+1	K+1	K+1	K+1	K+1	Ba+2						
K+1	V+4	Fe+3	Fe+3	Ni+2	V+3	V+4	Fe+2	K+1	K+1	K+1	K+1	K+1	K+1	K+1	K+1	K+1	Ba+2						
Ni+2	Mg+2	Al+3	Al+3	Mg+2	Cr+3	Mg+2	Mn+2	K+1	K+1	K+1	K+1	K+1	K+1	K+1	K+1	K+1	Ba+2						
Mn+3	Zr+4	Zr+4	Zr+4	Zr+4	Ca+2	Zr+4	Al+3	K+1	K+1	K+1	K+1	K+1	K+1	K+1	K+1	K+1	Ba+2						
Fe+3	Al+3	Si+4	Si+4	Al+3	Na+1	Fe+2	Ca+2	K+1	K+1	K+1	K+1	K+1	K+1	K+1	K+1	K+1	Ba+2						
V+3	Fe+2	Fe+2	Fe+2	Fe+2	Al+3	Al+3	Na+1	K+1	K+1	K+1	K+1	K+1	K+1	K+1	K+1	K+1	Ba+2						
Mn+2	Mn+2	Mn+2	Mn+2	Mn+2	Al+3	Mn+2	Na+1	K+1	K+1	K+1	K+1	K+1	K+1	K+1	K+1	K+1	Ba+2						
Si+4	Si+4	Si+4	Si+4	Si+4	Al+3	Ca+2	Ca+2	K+1	K+1	K+1	K+1	K+1	K+1	K+1	K+1	K+1	Ba+2						
Ca+2	Ca+2	Ca+2	Ca+2	Ca+2	Ca+2	Ca+2	Ca+2	K+1	K+1	K+1	K+1	K+1	K+1	K+1	K+1	K+1	Ba+2						

Note: 1) Roman numbers are the coordinations; 2) Major ions are listed on top with substitutional ions below in the order of descending probability.

probably more critical than bond character in ionic substitutions. The charge difference was set to more than one. This means that minor ions with charges differing from the major ions by two or more were dropped from the table. The reason is that substitution of ions with such charge differences are uncommon due to charge balance problems. After all the eliminations were completed, the surviving minor ions were considered as possible substitutional candidates. The program for creating Table 5 is listed in Appendix V.

In Table 5, each major ion (bold) is followed by substitutional minor cations in a descending order of probability. On the basis of the table, all the minor cations can be evaluated with respect to the substituted major cations. If the minor cation is not listed under the major cation, it is unlikely that such a substitution would occur and therefore that the formula can be ruled out; if the minor cation is found under the major cation, the proximity of the minor cation to the major cation is considered and the resulting formulae can be compared on the basis of a searching path. The higher the rank, the more likely the formula based on that substitution.

It should be pointed out that in Table 5, major cations are listed under multiple coordination possibilities. The exact coordination that should be used during the screening process is not a straightforward issue. However, there are some constraints to aid in the selection of the most likely coordination number. The calculations relating to ion substitutional process reveal that the phases in the slags include silicates, vanadates, spinels, and simple oxides. In silicates, the coordination for Si is fixed (four). The coordinations for other major cations must be dealt with individually because they vary depending upon the sites they take. In this respect, comparison of unknown compounds with known compounds offers a guide for the selection of coordination number. For example, for a compound with garnet type stoichiometry ($M_1M_2M_3O_{12}$), the coordination numbers can be assigned as 8 to the M1 site, 6 to the M2 site, and 4 to the M3 site respectively. All spinels contain two different cations, or at least two different valences

of the same cation, in the ratio of 2:1. The general formula is AB_2O_4 . Spinel is classified as normal or inverse, depending on where the more abundant of these cations resides. If the more abundant cation occupies the octahedral sites, the spinel is normal. If it is split evenly between the octahedral and tetrahedral sites, the spinel is inverse. In order to get the most likely formula, the distribution of cations must be known for a specific spinel. This can be done by referring to structural sorting diagrams (Price et al. 1982) in which numerous normal and inverse spinels are plotted. For example, $NiAl_2O_4$ can be easily recognized as an inverse spinel. In the screening process, Ni was assigned to octahedral coordination, while Al was assigned to both tetrahedral and octahedral coordination.

After the screening process, the number of potential formulae was reduced dramatically. Table 6 is a short list of chemical formulae for the calcium nickel vanadate phase which passed the ionic substitution test. It can be seen that before the process, there were 202 possible formulae and after the process there are only 33 left. The most likely formula is the first one on the list (marked in bold).

X-ray diffraction confirmation

XRD analysis was conducted to verify the validity of the procedure for determination of inorganic phases in petroleum coke slags. Figure 6 is an example XRD diffraction pattern for a phase assemblage representative of oxidized slags. Standard peak patterns for V_2O_4 , CaV_2O_6 , $NiAl_2O_4$ and $Ni_3V_2O_8$, respectively, are shown below the sample spectrum. By comparing the individual pattern against the bulk sample, it can be seen that the four phases account for most of the peaks in the bulk sample.

Table 6. A short list of calcium nickel vanadate formulae which passed ionic substitution test

Formulae	
(CaNa) ₃ (NiMgFe) ₂ V ₃ O ₁₂	1
(CaNa) ₃ (NiMgFe) ₂ V ₃ O ₁₃	2
(CaNa) ₄ (NiMgFe) ₃ V ₄ O ₁₇	3
(CaNa) ₅ (NiMgFe) ₃ V ₄ O ₁₈	4
(CaNa) ₅ (NiMgFe) ₃ V ₅ O ₁₉	5
(CaNa) ₅ (NiMgFe) ₃ V ₅ O ₂₀	6
(CaMg) ₃ (NiNaFe) ₃ V ₄ O ₁₅	7
(CaMg) ₄ (NiNaFe) ₃ V ₄ O ₁₇	8
(CaMg) ₄ (NiNaFe) ₄ V ₅ O ₁₉	9
(CaMg) ₄ (NiNaFe) ₄ V ₅ O ₂₀	10
(CaMg) ₅ (NiNaFe) ₄ V ₅ O ₂₁	11
(CaNaMg) ₃ (NiFe) ₂ V ₂ O ₉	12
(CaNaMg) ₅ (NiFe) ₂ V ₄ O ₁₇	13
(CaNaMg) ₆ (NiFe) ₂ V ₄ O ₁₈	14
(CaNaMg) ₆ (NiFe) ₂ V ₅ O ₁₉	15
(CaNaMg) ₆ (NiFe) ₂ V ₅ O ₂₀	16
(CaFe) ₂ (NiNaMg) ₃ V ₃ O ₁₂	17
(CaFe) ₃ (NiNaMg) ₄ V ₄ O ₁₆	18
(CaFe) ₃ (NiNaMg) ₄ V ₄ O ₁₇	19
(CaFe) ₃ (NiNaMg) ₄ V ₄ O ₁₈	20
(CaFe) ₄ (NiNaMg) ₅ V ₅ O ₂₀	21
(CaNaFe) ₄ (NiMg) ₂ V ₄ O ₁₅	22
(CaNaFe) ₅ (NiMg) ₃ V ₅ O ₁₉	23
(CaNaFe) ₅ (NiMg) ₃ V ₅ O ₂₀	24
(CaMgFe) ₃ (NiNa) ₂ V ₃ O ₁₂	25
(CaMgFe) ₄ (NiNa) ₃ V ₄ O ₁₆	26
(CaMgFe) ₄ (NiNa) ₃ V ₄ O ₁₇	27
(CaMgFe) ₄ (NiNa) ₃ V ₄ O ₁₈	28
(CaNiNaMgFe) ₃ V ₂ O ₈	29
(CaNiNaMgFe) ₄ V ₂ O ₉	30
(CaNiNaMgFe) ₅ V ₃ O ₁₂	31
(CaNiNaMgFe) ₅ V ₃ O ₁₃	32
(CaNiNaMgFe) ₆ V ₄ O ₁₅	33

*Valences of the cations are Na +1, Mg +2, Ca +2, V +5, Fe +3, and Ni +2.

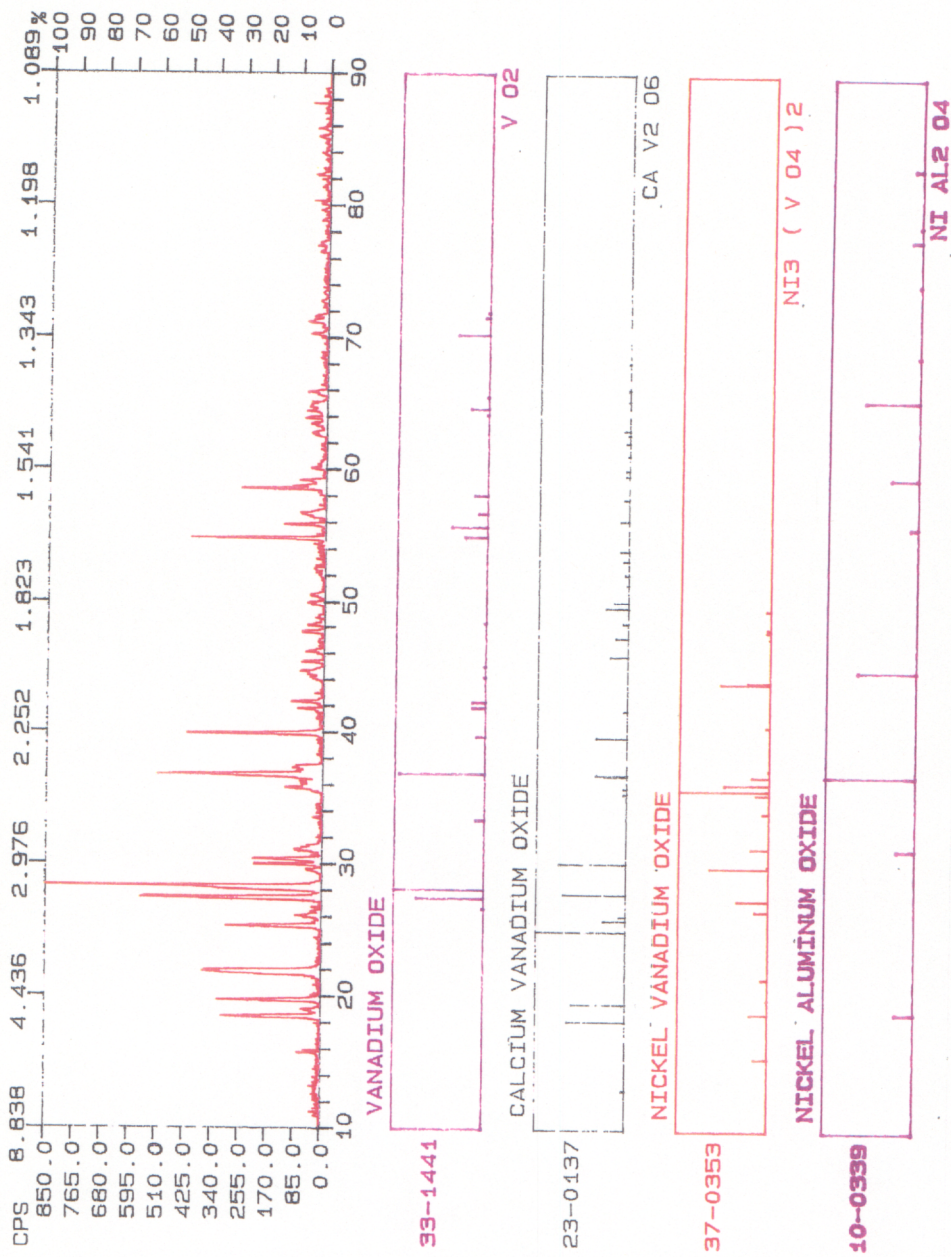


Figure 6. X-ray diffractogram of Type 1 oxidized petroleum coke slags and diffraction patterns of card files of VO_2 , CaV_2O_6 , $\text{Ni}_3(\text{VO}_4)_2$ and NiAl_2O_4 phases.

RESULTS

In the present study, more than 17 phases were determined in reduced slags and oxidized slags with the procedure described and most of major phases have been confirmed through XRD analysis. Their chemical formulae are listed in Table 7. The phases fall into six categories: oxides, silicates, vanadates, sulfides, metal alloys and sulfates. The reduced slags are dominated by V_2O_3 , $(Ca,Na,Mg,Fe,V)_4Si_5O_{12}$, and $(Na,Ca)(Al,V)SiO_4$ whereas the oxidized slags contain mostly V_2O_4 , CaV_2O_6 , $NiAl_2O_4$ and $Ni_3V_2O_8$.

SUMMARY

Determination of the inorganic phases in petroleum coke slags is difficult because of the problems in phase separation, presence of a number of transition elements and extensive ionic substitutions in the phases. This study has taken a comprehensive approach by employing computational methods, thermodynamics, and crystal chemistry to deal with the problem. Electron microprobe analyses, bulk chemical analysis, light microscopy and scanning electron microscopy were all used in this process. The compositional data were subjected to rigorous statistical analysis (Chauvenet's criterion) to eliminate incompatible data. The stable valence states of transition elements (Ti, V, Cr, Mn and Fe) at various temperatures and oxygen pressures were estimated using thermodynamic data for their oxides. Predicted valence states of Ti, Cr, Mn and Fe ions at gasification conditions were compared to those of vanadium, who has valence states determined through the constraints of total oxide weight percentages for simple oxide phases (V_2O_3 and V_2O_4) and calcium vanadate. Vanadium valence states are further constrained by numerical criteria. The possible chemical formulae were calculated on the basis of stoichiometric compound types, integer criteria, and an ion substitutional table. The ion substitutional table is based on ionic radii, charge and bond character. Finally X-ray diffraction was conducted to confirm the identification of many major, and some minor phases. The approach adopted here is

Table 7. Phases present in petroleum coke slags

Phases	Present in reduced slags	Present in oxidized slags
Oxides		
V ₂ O ₃	Major (X)	
V ₂ O ₄		Major (X)
(Fe, Mg)(V, Al) ₂ O ₄	Minor	
(Mg, Fe)(Cr, Al) ₂ O ₄	Minor	
(Ni, Mg)(Al, Cr, V) ₂ O ₄		Major (X)
Cr ₂ O ₃ **	Minor	
Fe ₂ O ₃ **	Minor	
Silicates		
(Ca, Na, Mg, Fe, V) ₄ (Si, Al) ₅ O ₁₂	Major	
(Na, Ca)(Al, Fe)(Si, V) ₃ O ₈	Minor	
(Na, Ca)(Al, V)SiO ₄	Major	
(Ca, Na) ₃ (V, Ti, Mg, Fe) ₂ Si ₃ O ₁₂	Minor (X)	
Vanadates		
Ca, Mg, Fe, Ni, Na)V ₂ O ₆ **	minor	Major (X)
NaV ₂ O ₅ (OH)**	minor	Minor
(Ca, Na) ₃ (Ni, Mg, Fe) ₂ V ₃ O ₁₂ **	minor	Minor (X)
(Ni, Mg, Fe) ₃ (V, Si) ₂ O ₈ **	minor	Major (X)
Sulfides		
FeNiS ₂ -NiS	Minor	
Metal Alloys		
FeNi ₃ -Fe ₂ Ni ₅	Minor	
Sulfates		
CaSO ₄	Minor	

*Major: >10% by volume; Minor: <5% by volume.
X: confirmed by XRD analysis

successful in that most of the major and some minor phases in petroleum coke slags were identified. Such a technique should be applicable to a wide variety of slags, ashes, ceramics, and incinerator solid wastes which are, in general, less complex than petroleum coke slags.

REFERENCES

- Arens, L.H., 1953, The use of ionization potentials: 2. Anion affinity and geochemistry: *Geochim. Cosmochim. Acta*, v. 3, p. 1-29.
- Burnham, C.W., 1990, The ionic model: perceptions and realities in mineralogy: *American Mineralogist*, v. 75, p. 443-463.
- Burns, R.G. and Fyfe, W.S., 1964, Site preference energy and selective uptake of transition-metal ions during magmatic crystallization: *Science*, v. 144, p. 1001-1003.
- Conoco, Inc. and Foster Wheeler Energy Corp., 1981, Phase I: the pipeline gas demonstration plant: *Demonstration plant engineering and design*, v. 3, p. 405.
- Craig, J.R., and Vaughan, D.J., *Ore microscopy and ore petrography*: 1994, New York, John Wiley & Sons, Inc., 434 p.
- Curran, P.F., 1990, Texaco coal gasification: Status and development: *Proceedings (of) evaluation of integrated coal gasification combined cycle for Canadian utility applications*, p. 121-124.
- Curtis, C.D., 1964, Application of the crystal-field theory to the inclusion of trace transition elements in minerals during magmatic crystallization: *Geochim. Cosmochim. Acta*, v. 28, p. 389-402.
- DeVore, G.W., 1955a, The role of adsorption in the fractionation and distribution of elements: *J. Geol.*, v. 63, p. 159-190.
- DeVore, G.W., 1955b, Crystal growth and the distribution of the elements: *J. Geol.*, v. 63, p. 471-484.
- DeVore, G.W., 1957, The association of strongly polarizing anions with weakly polarizing cations as a major influence in element distribution, mineral composition, and crystal growth: *J. Geol.*, v. 65, p. 178-195.
- Evans, R. T, B.H., Hiller, H., Vierrath, H.E., 1985, British Gas/Lurgi Slagging gasifier status, application and economics: *Coaltech'85 London*, p. 659-687.
- Faure, G., 1993, *Principles and applications of inorganic geochemistry*, New York, Macmillan Publishing Company, 626 p.
- Galloway, T.R., Chiramoute, J., Pack, G.E., Patterson, J., 1983, Progress toward the Hercules coke-to-methanol plant: *Proceedings of Intersoc. Energy Convers. Eng. Conf.*, v. 2, p. 437-442.
- Goldschmidt, V.M., 1937, The principles of distribution of chemical elements in minerals and rocks: *J. Chem.*, p. 655-673.

- Groen, J.C., 1992, Microchemical Phase Characterization of Petroleum Coke Gasification Slags: Ph.D Desertation, VPI&SU, 131 p.
- Groen, J.C., and Craig, J.R., 1994, The inorganic geochemistry of coal, petroleum, and their gasification/combustion products: Fuel Processing Technology, v. 40 p. 15-48.
- Klein., C., and Hurlbut, Jr., C.S., 1993, Manual of Mineralogy, New York, John Wiley & Sons, Inc., 681 p.
- Lacey, J.A., Scott, J.E., Thomson, B.H., Lienhard, H., Vierrath, H., 1984, Further development of the British Gas/Lurgi slagging gasifier: Proceedings: third annual EPRI contractors' conference on coal gasification, p. 8.1-8.32.
- Lu, J., Craig, J.R., and Groen, J.C., 1994, Petroleum coke slags: characterization and chemistry of phases: 208th ACS National Meeting, v. 34, No.2.
- Matsunaga, E., 1987, Experience with ammonia manufacture based on the Texaco Coal gasification Process: Proceedings of the fifth advanced coal gasification symposium, p. 12.51-12.58.
- Philips, J.N., Mahagaokar, U., Krewinghaus, A.B., 1992, Shell coal gasification project: Gasification of eleven diverse feeds: EPRI Electric Power Research Institute, Palo Alto, CA, 161 p.
- Price, G.D., Price, S.L., and Burdett, J.K., 1982, The factors influencing cation site-preference in spinels: a new Mendelyevian approach: Phys. Chem. Minerals, v. 8, p. 69-76.
- Revankar, V.V.S., Gokarn, A.N., Doraiswamy, L.K., 1987, Studies in catalytic steam gasification of petroleum coke with special reference to the effect of particle size: Ind. Eng. Chem. Res., v. 26, p. 1018-1025.
- Ringwood, A.E., 1955, The principles governing trace element distribution during magmatic crystallization: Geochem. Cosmochim. Acta, v. 7, p. 189-202.
- Robie, R.A., Hemingway, B.S. and Fisher, J.R., 1978, Thermodynamic properties of minerals and related substances at 298.15K and 1 bar pressure and at higher temperatures: U.S. Geol. Survey Bull. 1452, 456 p.
- Samsnov, G.V., 1982, The Oxide Handbook: Institute of Problems in Materials Science, Academy of Sciences of the Ukrainian SSR, Kiev, USSR, New York, IFI/Plenum, 200 p.
- Schlinger, W.G., 1978, Texaco Coal Gasification Process for manufacture of medium Btu gas: Proceedings of the conference on coal use for California, p. 243-247.
- Siegart, W.R., 1992, Texaco coal gasification: Proceedings of the American Power Conference (United States) v. 54:1, p. 152-153.

- Spencer, D.F. and Gluckman, M.J., 1983, An economic comparison of coal gasification in the United States and an update of the 100 MWe Cool Water Coal Gasification Combined Cycle project: Trip report on second advanced coal gasification symposium, Shanghai, China, p. 15.78-15.106.
- Sueyama, T. and Katagiri, K., 1989, Four year operating experience with Texaco coal gasification process in Ube Ammonia: Eight annual EPRI conference on coal gasification, p. 11.1-11.13.
- Taylor, J.R., 1982, An introduction to error analysis, Mill Valley, California, University Science Books, 270 p.
- Thimsen, D., Pooler, A.R., Pui, D., Kittelson, D., Liu, B.Y.H., Dicks, J.B., 1985, Synthetic fuels gas from petroleum coke-performance in an industrial gasifier: Synfuels and coal energy symposium, p. 167-174.
- Timpe, R.C., Kulas, R.W., hauserman, W.B., 1990, Characterization of gasification coal tar: Seven annual international Pittsburg coal conference, p. 10-14.
- Whittaker, E.J.W., and Muntus, R., 1970, Ionic radii for use in geochemistry: *Geochim. et Cosmochim. Acta*, v. 34, p. 945-956.
- Whitten, K.W., Gailey, K.D., and Davis, R.E., 1988, General Chemistry, New York, Saunders Golden Sunburst Series, Saunders College Publishing, 884 p.

CHAPTER 3. PETROLEUM COKE SLAGS: PHASE ASSEMBLAGES AND TEXTURES

INTRODUCTION

The petroleum coke gasification process was described in Chapter 2. Petroleum coke slags, which are generated during gasification, have been studied from the aspect of determination of inorganic phases. Identification of phases present has the highest priority because it is basic for almost any application. To further understand the nature of the petroleum coke slags, knowledge of phase assemblages and textures help in understanding the sequence of phase formation, the nature of elemental partitioning, and the interpretation and prediction of dissolution kinetics. Knowledge of formation mechanisms may permit subtle modification of operational parameters such as temperature, pressure, or additives to minimize the formation of undesirable phases or to enhance the formation of desirable ones. This chapter considers the phase assemblages, textures and their formation mechanisms.

METHODS

The samples were obtained and prepared as described in Chapter 2. Reflected and transmitted light microscopic, and scanning electron microscopic examinations were conducted to observe phase assemblages and textures at various scales. Elemental distributions within phases were investigated using electron microprobe analysis and X-ray elemental mapping. Bulk compositional data of slags were used to aid in the interpretation of formation mechanisms of various phase assemblages.

PHASE ASSEMBLAGES, TEXTURES AND THEIR FORMATION MECHANISMS

Phase assemblages

Texaco gasifiers are generally operated at temperatures of approximately 1400°C. Cooling the gasifier with an inert gas preserves the reduced slag phases. The preservation of glass in many of the current slag samples, as well as samples from other studies (Groen and Craig 1994), indicates that liquid phases were super cooled into glasses without crystallizing during cooling. Some fractional crystallization is evident by the presence of tiny spheres of crystalline aggregates oriented in flow patterns in some of the glasses, but these crystals are readily distinguished from larger, presumably primary crystals. Although silicate melts commonly solidify as glasses on cooling, sulfide melts are almost never preserved as glasses (Vaughan and Craig 1978). Because the upper thermal stability of FeS is 1190°C, it is apparent that the (Fe, Ni)S phases observed in the reduced slags must have crystallized during cooling. Textural evidence suggests that the (Fe, Ni)S grains were merely trapped equilibrium droplets of melt that retained their positions in the matrices of the other crystals as they solidified. They do not appear to have undergone any chemical reaction with the neighboring phases. The oxidized slags were identical to the reduced slags until an oxygen-bearing atmosphere was passed through the gasifier during cooling. In the presence of oxygen, oxidation completely changed the phase assemblages throughout the samples. The phase assemblages that occur in the reduced slags and oxidized slags are summarized in Table 1.

Slags formed under reduced conditions

Megascopically, the reduced slag samples are black, fine grained, and porous somewhat resembling the texture of a sponge. Careful megascopic and microscopic examination reveals that samples extracted from the walls of the gasifier can be divided into

Table 1. Phases present in petroleum coke slags

Compound Categories	Phases	Reduced slags				Oxidized slags	
		Zone 1	Zone 2	Zone 3	Zone 4	Type 1	Type 2
Oxides	V2O3	**	**	**		**	
	V2O4		*			**	*
	(Fe, Mg)(V, Al)2O4						
	(Mg, Fe)(Cr, Al)2O4	*				**	*
	(Ni, Mg)(Al, Cr, V)2O4					**	*
Cr2O3	*						
Fe2O3				*			
Silicates	(Ca, Na, Mg, Fe, V)4Si5O12	**	*	**			
	(Na, Ca)(Al, Fe)(Si, V)3O8				**		
	(Na, Ca)(Al, V)SiO4	**	**	**			
	(Ca, Na)3(V, Ti, Mg, Fe)2Si3O12	*	**				
Vanadates	(CaMg, Fe, Ni, Na)V2O6				**	**	*
	NaV2O5(OH)					*	
	(Ca, Na)3(Ni, Mg, Fe)2V3O12				*		
Sulfides	(Ni, Mg, Fe)3(V, Si)2O8				**	**	*
	FeNiS2-NiS	*	*	*			
Metal Alloys	FeNi3-Fe2Ni5	*	*	*			
	CaSO4				*		
Sulfate							
Glass						*	**

** Abundant phases (>10% by volume)

* Significant phases (1-10% by volume)

four zones that developed as layers parallel to the walls of the gasifier as the slag accumulated from the refractory surface inward (Figure 1). The causes of the zonation are not known, but possibilities include variations in compositions of the feedstock, in feeding rate, or modification of operating parameters. The iron-nickel sulfides with compositions between FeNiS_2 and NiS are scattered throughout all the zones. Within the sulfide grains, various compositions of Fe-Ni alloy occur, ranging from FeNi_3 to Fe_2Ni_5 . The complex sulfide textures will be discussed in detail later. Zone 1, in contact with the refractory lining, makes up about 40 percent by volume of the reduced slags. The bulk of the zone is composed of euhedral 10-30 mm V_2O_3 crystals with interstitial, intergrown $(\text{Ca}, \text{Na}, \text{Mg}, \text{Fe}, \text{V})_4(\text{Si}, \text{Al})_5\text{O}_{12}$ and subordinate NaAlSiO_4 (Figure 2a). Minor amounts of $\text{Ca}_3\text{V}_2\text{Si}_3\text{O}_{12}$ occur as irregular fringes along the rims of V_2O_3 crystals. At the points of direct contact with the refractory surface, fragments of refractory (MgCr_2O_4) are occasionally engulfed in the slag (Figure 2b). At the refractory-slag interface, a unique assemblage exists, consisting of elongate skeletal V_2O_3 crystals rimmed by $\text{Ca}_3\text{V}_2\text{Si}_3\text{O}_{12}$ (Figure 2c).

Zone 2, which makes up about 10 percent by volume of the reduced slags, also contains euhedral crystals of V_2O_3 as the dominant phase, but the interstitial phases and textures are different. The interstitial phases display distinctive graphic textures which are composed of lamellae of $\text{Ca}_3\text{V}_2\text{Si}_3\text{O}_{12}$ and NaAlSiO_4 (Figure 3a). In addition, a $(\text{Fe}, \text{Mg})(\text{V}, \text{Al})_2\text{O}_4$ spinel phase occurs as well-developed euhedral to subhedral crystals scattered throughout the zone (Figure 3b).

Zone 3, which makes up about 45 percent by volume of the reduced slags, is similar to Zone 1 in that the major phases include euhedral 10-30 mm V_2O_3 crystals and interstitial, intergrown $(\text{Ca}, \text{Na}, \text{Mg}, \text{Fe}, \text{V})_4(\text{Si}, \text{Al})_5\text{O}_{12}$ and subordinate NaAlSiO_4 . The difference is that the amount of $\text{Ca}_3\text{V}_2\text{Si}_3\text{O}_{12}$ phase is insignificant in Zone 3.

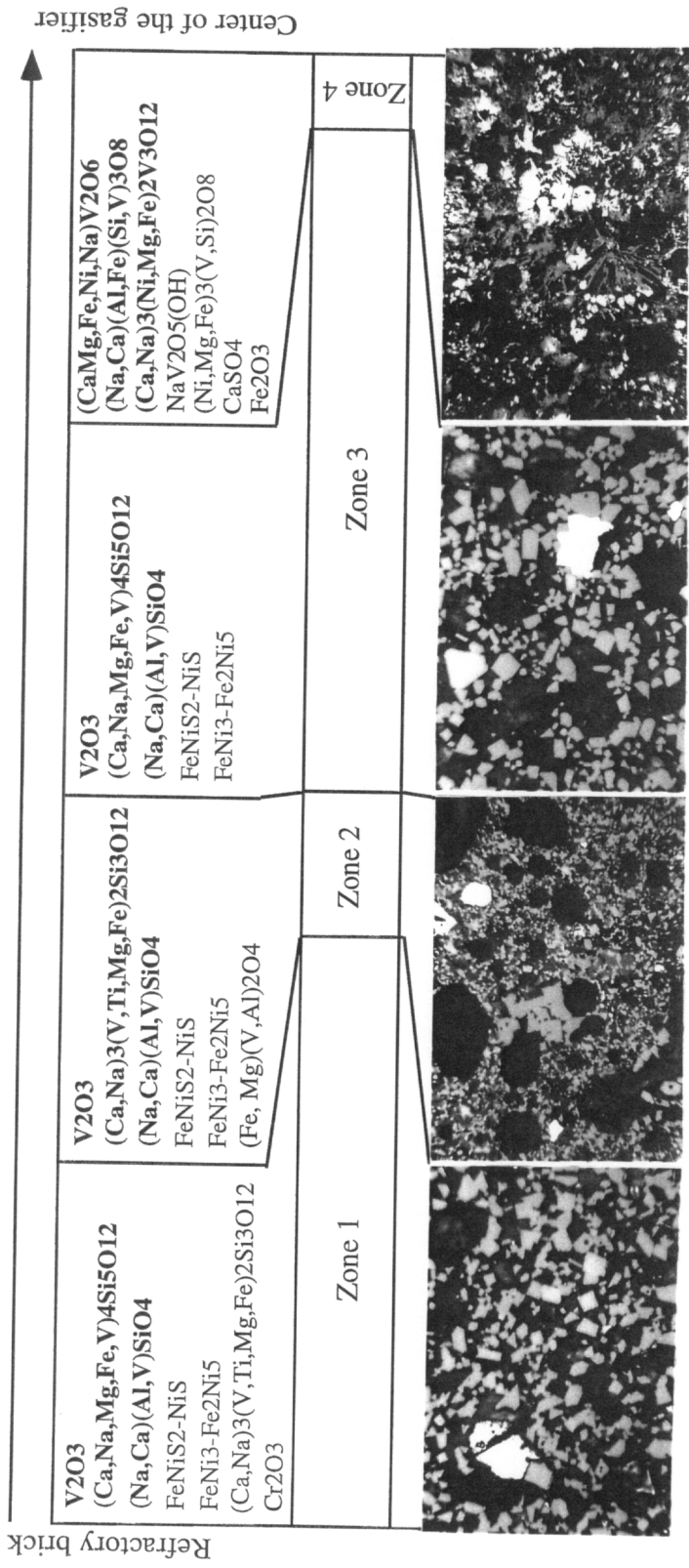


Figure 1. Four zones in reduced petroleum coke slags, their phase assemblages and their textures (see text for discussions). The total thickness for the four zones is about 10 centimeters. The field of views of the photo micrographs are 0.75, 1.5, 0.75 and 3 mm in for Zone 1, Zone 2, Zone 3 and Zone 4 respectively.

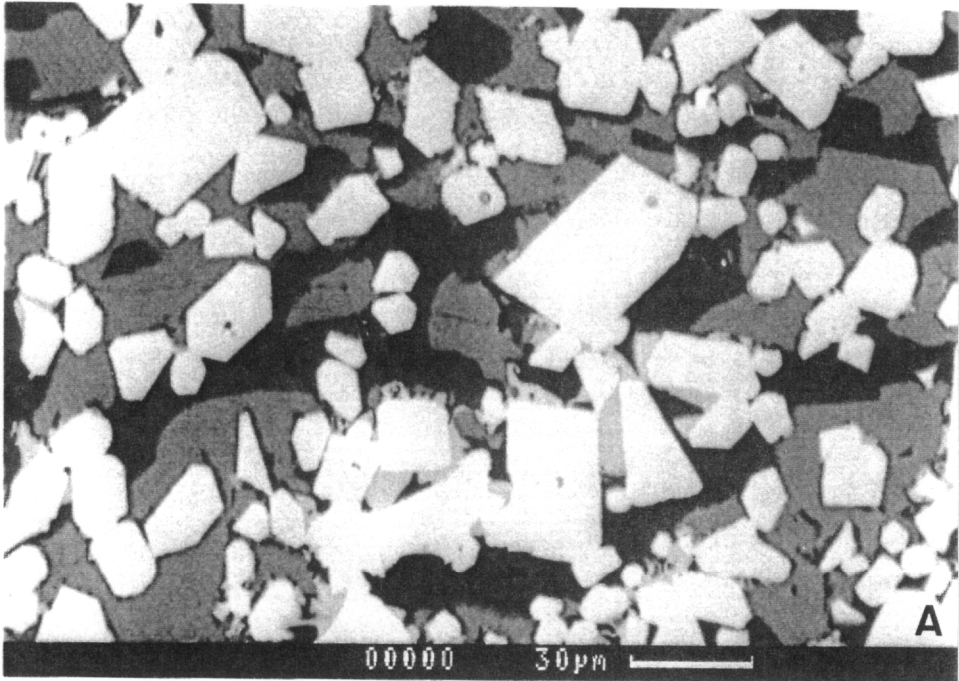


Figure 2. Various phases in Zone 1 of reduced petroleum coke slags (scale bars are all 1 mm). (a) Typical assemblage: V_2O_3 (euhedral, brightest), $Ca_3V_2Si_3O_{12}$ (second brightest, lower middle), $(Ca, Na, Mg, Fe, V)_4(Si, Al)_5O_{12}$ (gray), $NaAlSiO_4$ (black); (b) Refractory brick fragments (red); (c) Phases occurring in the interface between the refractory brick and slag: V_2O_3 (black, lenty), $Ca_3V_2Si_3O_{12}$ (greenish yellow), $(Ca, Na, Mg, Fe, V)_4(Si, Al)_5O_{12}$ (white).

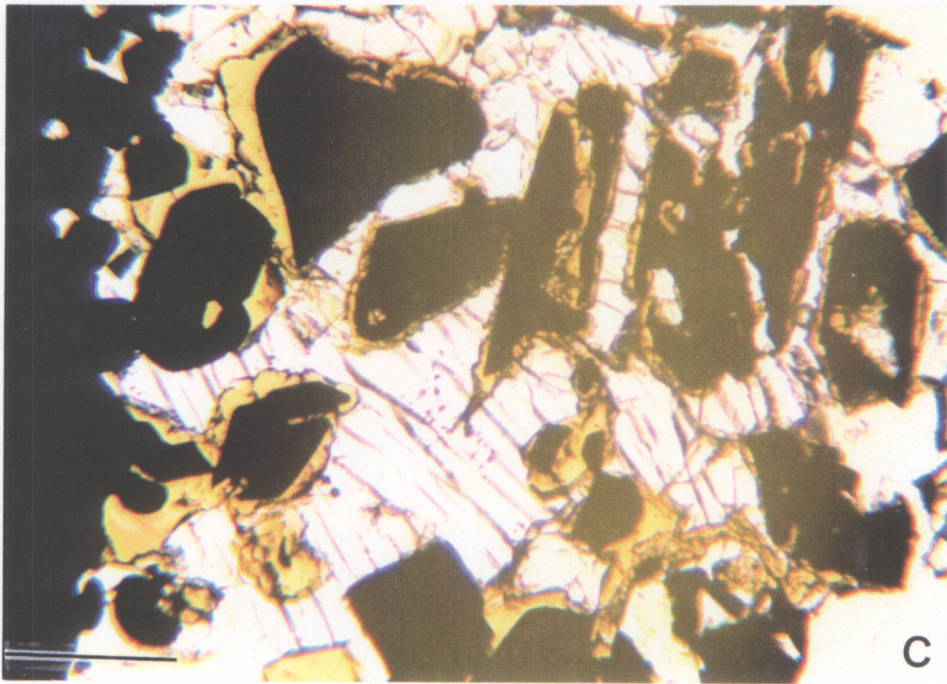
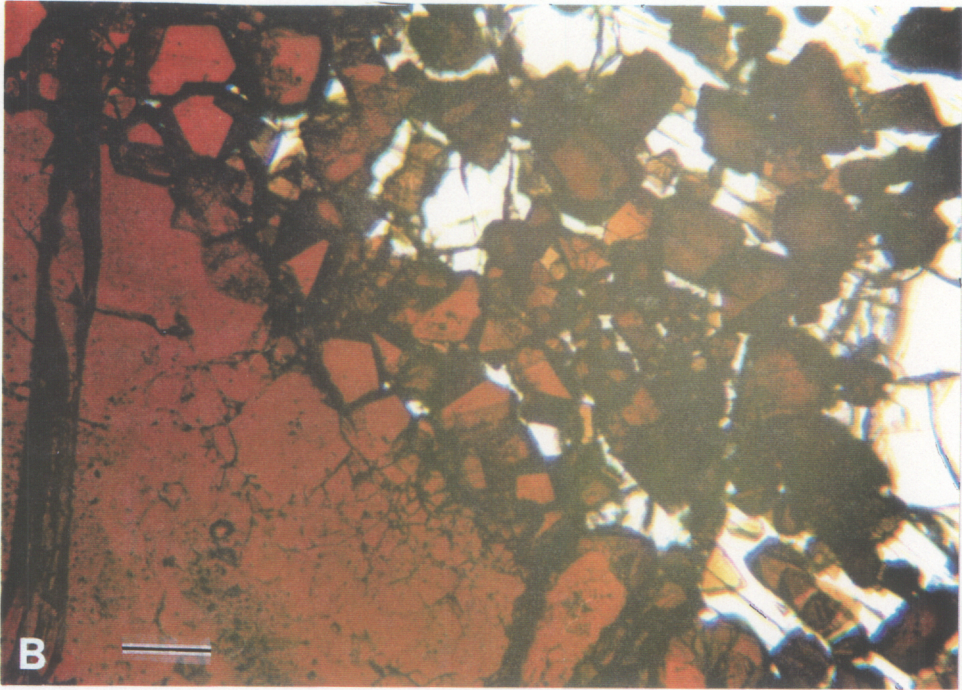


Figure 2 (concluded)

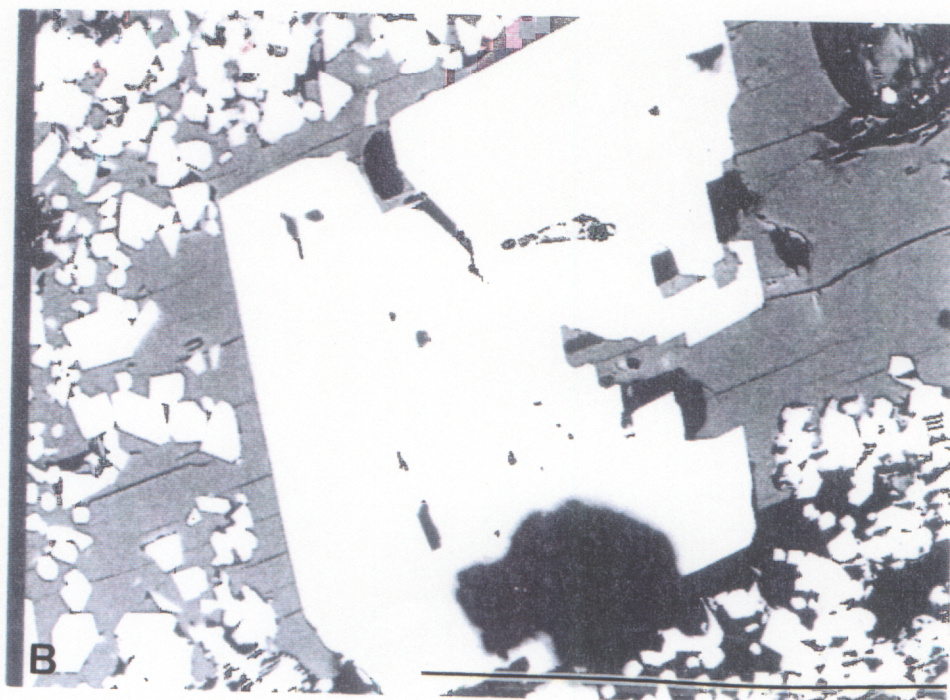
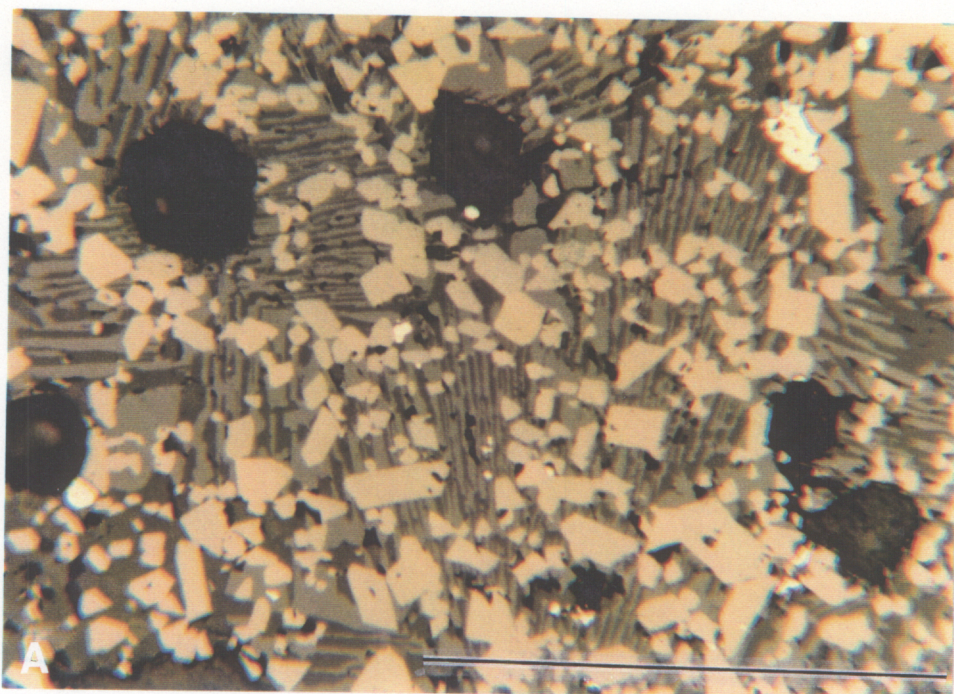


Figure 3. Various phases in Zone 2 of reduced petroleum coke slags (scale bars are all 1 mm). (a) Typical assemblage: V_2O_3 (euhedral, yellow), $Ca_3V_2Si_3O_{12}$ (gray, lamella), $NaAlSiO_4$ (dark gray, lamella), nickel-iron sulfides (upper right, brightest); (b) FeV_2O_4 (euhedral, white).

Zone 4 is a thin crust resulting from some minor oxidation of the slags during cooling. This zone only makes up about 5 percent of the reduced slags, but the phase assemblage is very complex. Phases present include $(\text{Na,Ca})(\text{Al,Fe})\text{Si}_3\text{O}_8$, CaV_2O_6 , $\text{NaV}_2\text{O}_5(\text{OH})$, $(\text{Ca,Na})_3(\text{Ni,Mg,Fe})_2\text{V}_3\text{O}_{12}$, $\text{Ni}_3\text{V}_2\text{O}_8$, CaSO_4 , and Fe_2O_3 . Figure 4 shows the typical textures found in this zone. $(\text{Na,Ca})(\text{Al,Fe})\text{Si}_3\text{O}_8$ crystals occur as aggregates of radiating laths (Fig 4a), $(\text{Ca,Na})_3(\text{Ni,Mg,Fe})_2\text{V}_3\text{O}_{12}$ as euhedral crystals which have hexagonal outlines in cross section (Figure 4b, the big crystal on the right), $\text{Ni}_3\text{V}_2\text{O}_8$ as euhedral laths (Figure 4b, upper left corner), CaSO_4 as euhedral laths (Figure 4c, dark gray crystals throughout the picture), and Fe_2O_3 as elongate aggregate (Figure 4d, lower part of the picture). Along the contact between Zone 3 and Zone 4, the transition from reduced phases to oxidized phases can be seen. As shown in Figure 5a, a single original grain of iron-nickel sulfide has been converted to a number of isolated grains with various oxidized phases distributed immediately around the sulfide grains ($(\text{Ca,Na})_3(\text{Ni,Mg,Fe})_2\text{V}_3\text{O}_{12}$, grey) or scattered nearby the grains ($\text{Ni}_3\text{V}_2\text{O}_8$, euhedral, light grey; CaSO_4 , euhedral, black). Figure 5b shows V_2O_3 crystals which have been oxidized to form V_2O_4 along the rims.

Slags formed under oxidized conditions

As mentioned earlier, the oxidized slag samples were collected from the quench vessel located under the gasifier. Although these are random samples, the fully penetrative oxidation process and coincident slag homogenization via mixing as it flows from the gasifier suggest that all samples would be similar, and representative of the oxidized slags in general. Microscopic examinations revealed that there are two general types, named here as Type 1 and Type 2, in the order of their abundance (Figure 6). Type 1, which makes up about 90 percent of the oxidized slags, is composed of 80 percent crystalline phases and 20 percent glass. Type 2, which makes up only 5-10 percent by volume of the oxidized slags,

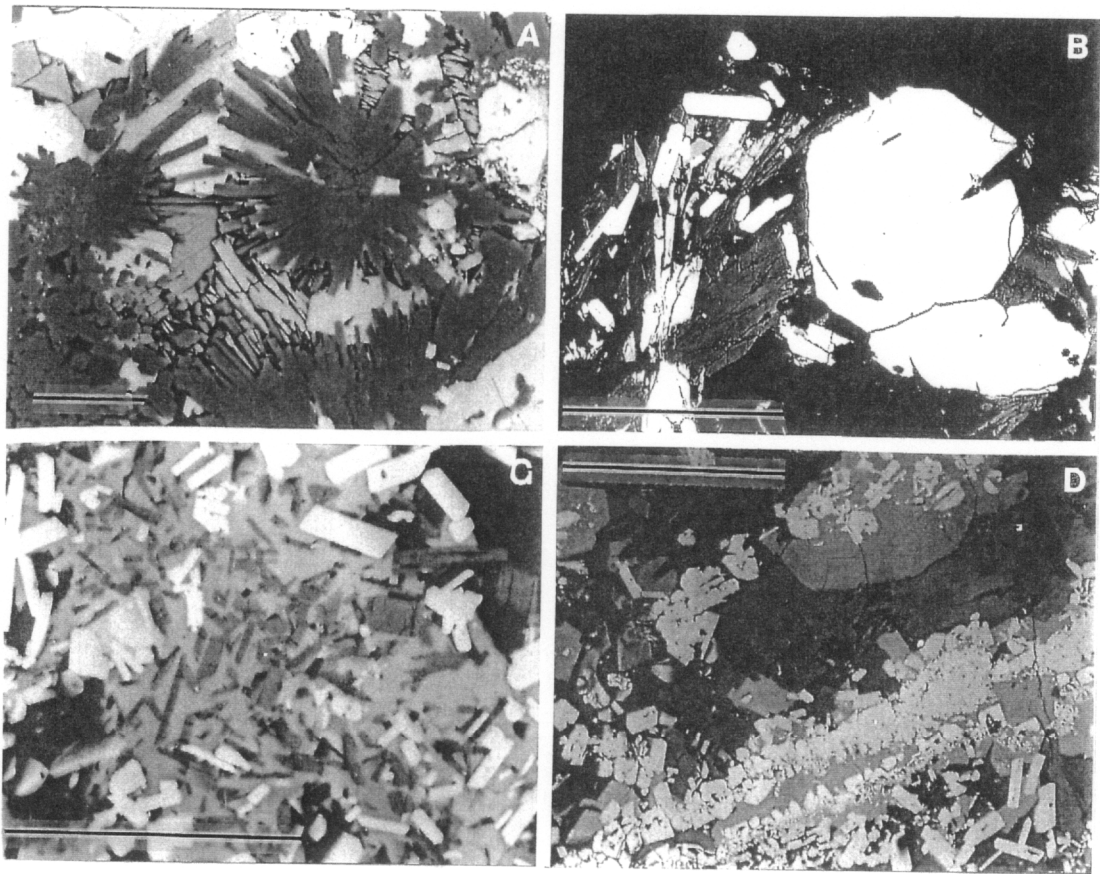


Figure 4. Various phases and their physical mode of occurrence in Zone 4 of reduced petroleum coke slags (scale bars are all 1 mm). (a) $\text{NaAlSi}_3\text{O}_8$ (dark gray, radiating aggregate); (b) $(\text{Ca,Na})_3(\text{Ni,Mg,Fe})_2\text{V}_3\text{O}_{12}$ (the biggest euhedral crystal on the right), $(\text{Ni,Mg,Fe})_3(\text{V,Si})_2\text{O}_8$ (white, lengthly euhedral crystals on the upper left), $(\text{CaMg,Fe,Ni,Na})\text{V}_2\text{O}_6$ (dark gray, columnar); (c) CaSO_4 (gray needle), $(\text{Ni,Mg,Fe})_3(\text{V,Si})_2\text{O}_8$ (white, lengthly euhedral); (d) Fe_2O_3 (bright gray, irregular lengthly masses on the lower part of the picture).

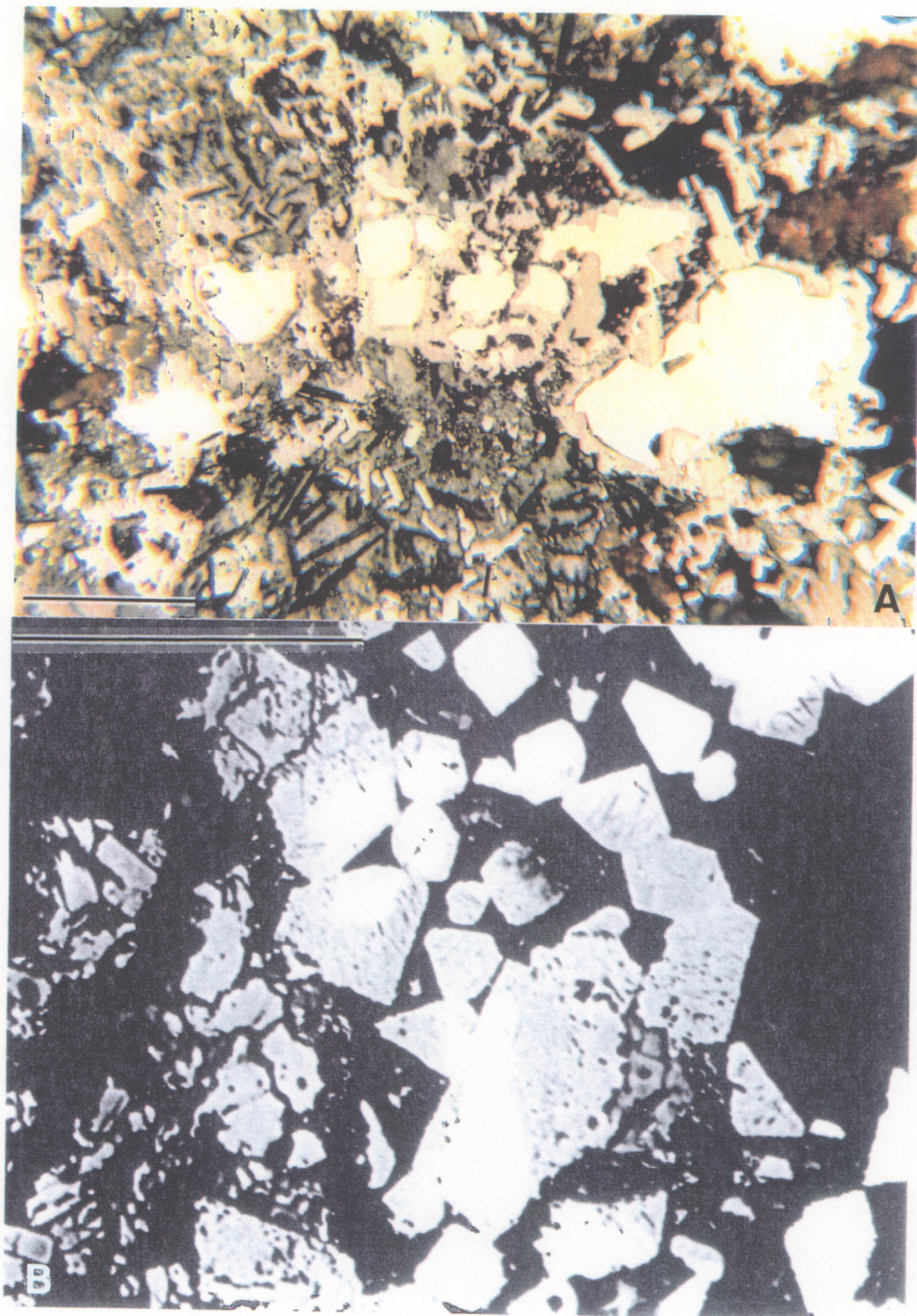


Figure 5. Textures resulting from oxidation (scale bars are all 1 mm). (a) oxidation of sulfides: nickel-iron sulfides (bright yellow), $(\text{Ca,Na})_3(\text{Ni,Mg,Fe})_2\text{V}_3\text{O}_{12}$ (bright gray rims around sulfides), $(\text{Ni,Mg,Fe})_3(\text{V,Si})_2\text{O}_8$ (bright gray, euhedral laths), CaSO_4 (black needles scattered near the center); (b) oxidation of V_2O_3 : V_2O_3 (white), V_2O_5 (gray, oxidation product of V_2O_3).

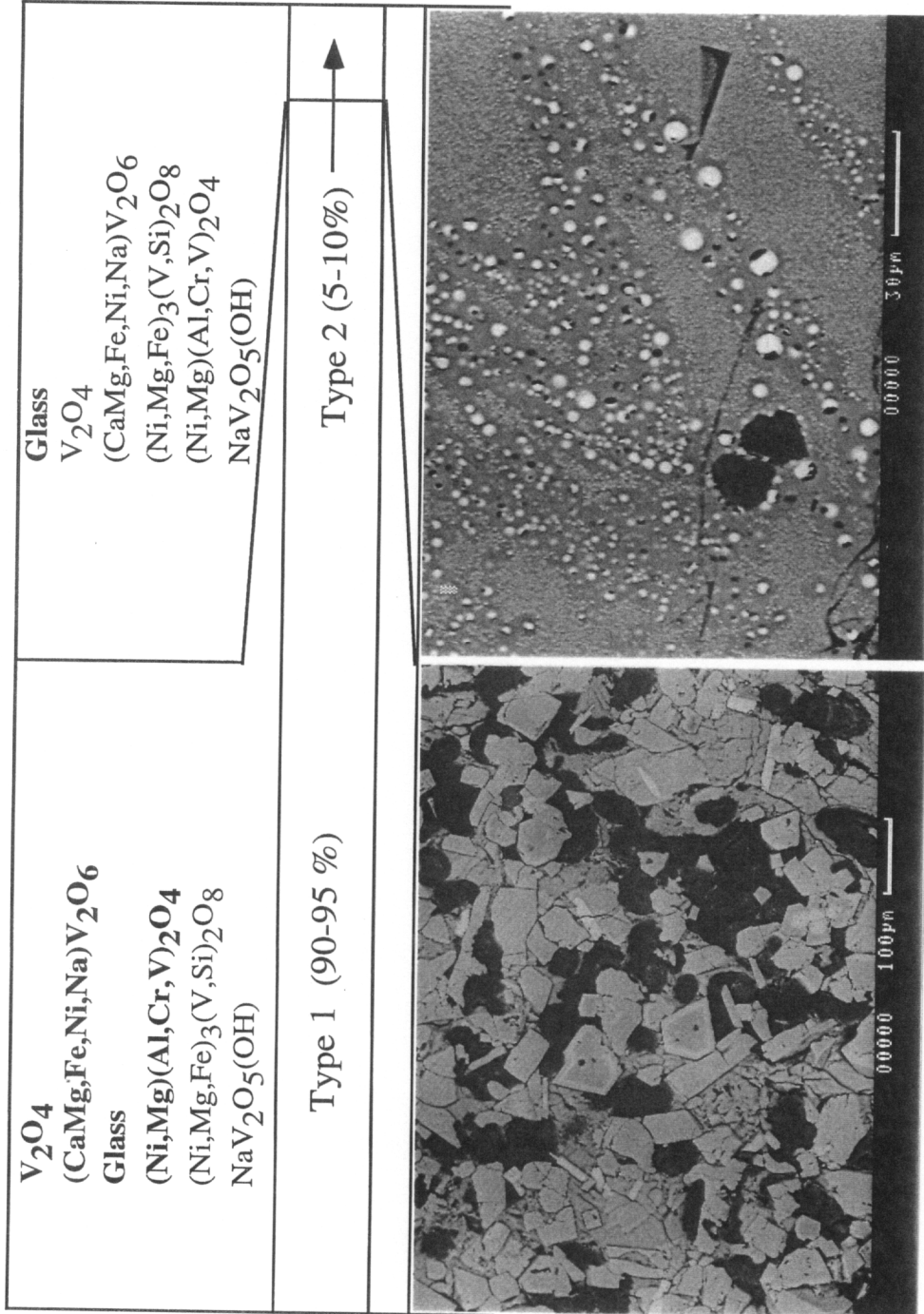


Figure 6. Oxidized petroleum coke slags, their phase assemblages and their textures (see text for discussions).

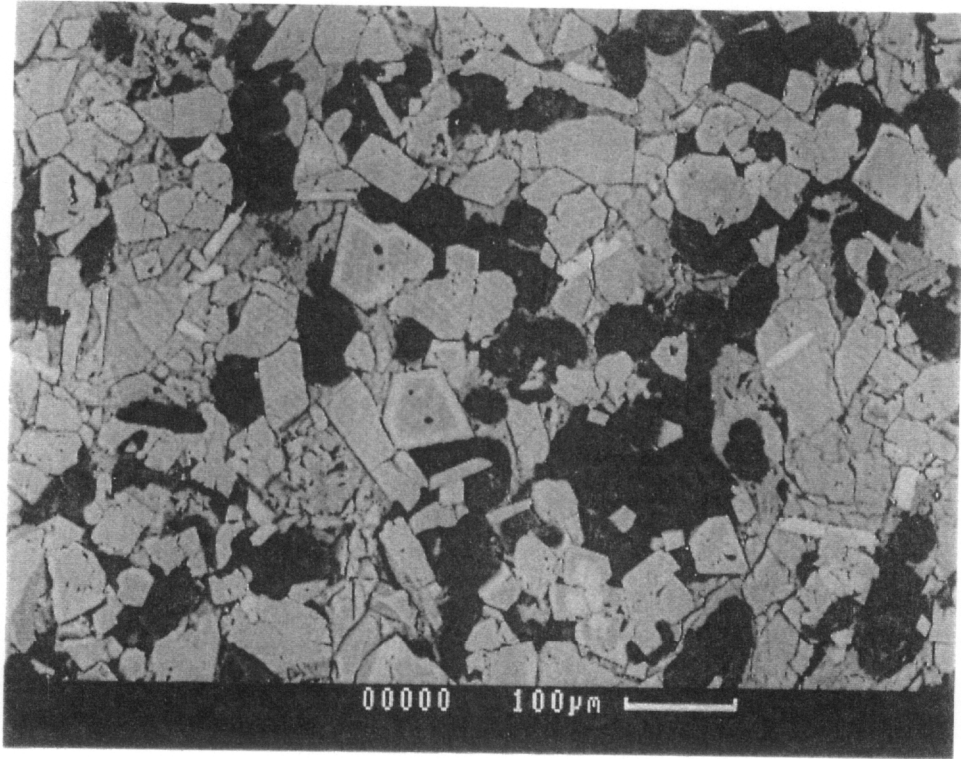


Figure 7. Various phases in Type 1 oxidized petroleum coke slags: V_2O_4 (gray, columar to equigranular), $Ni_3V_2O_8$ (light gray, needle shaped), $NiAl_2O_4$ (gray with light gray rims, equigranular), CaV_2O_6 (gray, rough surface, occurring in matrix) and glass (black).

is composed of 10 percent polycrystalline clusters and 90 percent glass. The phases in Type 1 slag include V_2O_4 , $(Ca,Mg,Fe,Ni,Na)V_2O_6$, $(Ni,Mg,Fe)_3(V,Si)_2O_8$, $(Ni,Mg)(Al,Cr,V)_2O_4$, and $NaV_2O_5(OH)$ (Figure 7). V_2O_4 occurs as subhedral to euhedral laths with fractures perpendicular to the direction of elongation (white); $(Ni,Mg,Fe)_3(V,Si)_2O_8$ occurs as euhedral laths (white); $(Ni,Mg)(Al,Cr,V)_2O_4$ occurs as equigranular euhedral crystals (gray); and $(Ca,Mg,Fe,Ni,Na)V_2O_6$ and $NaV_2O_5(OH)$ occur as matrix. The clusters in Type 2 slags are composed of V_2O_4 , $(Ni,Mg)(Al,Cr,V)_2O_4$, $(Ni,Mg,Fe)_3(V,Si)_2O_8$, $(Ca,Mg,Fe,Ni,Na)V_2O_6$, and $NaV_2O_5(OH)$ (Figure 8a, b). The textures of the clusters are the same as those of Type 1 slags, except that the spinel crystals possess distinctive zoning, which will be discussed in detail later. The glass in Type 2 slags displays flow textures which are defined by fine grains of crystalline aggregate (Figure 8c, d). Compositions of the glass in both types of slags vary substantially from sphere to sphere in the same type of slags and from spot to spot within the same sphere. Table 2 shows the major and minor elements that occur in the glass, and their ranges of concentration. These variations result from fractional crystallization, which will be discussed in detail later.

Formation mechanisms

From the descriptions above, it is apparent there are significant differences in the phase assemblages from zone to zone in reduced slags, from type to type in oxidized slags, and especially between the reduced and oxidized slags. To summarize, reduced slags are composed of all crystalline phases including V_2O_3 , $(Ca, Na, Mg, Fe, V)_4(Si, Al)_5O_{12}$, $NaAlSiO_4$ and nickel sulfides. In contrast, the oxidized slags contain the crystalline phases V_2O_4 , $(Ca,Mg,Fe,Ni,Na)V_2O_6$, $(Ni,Mg,Fe)_3(V,Si)_2O_8$, and $(Ni,Mg)(Al,Cr,V)_2O_4$ as well as glass of highly variable composition. In as much as the initial components of the

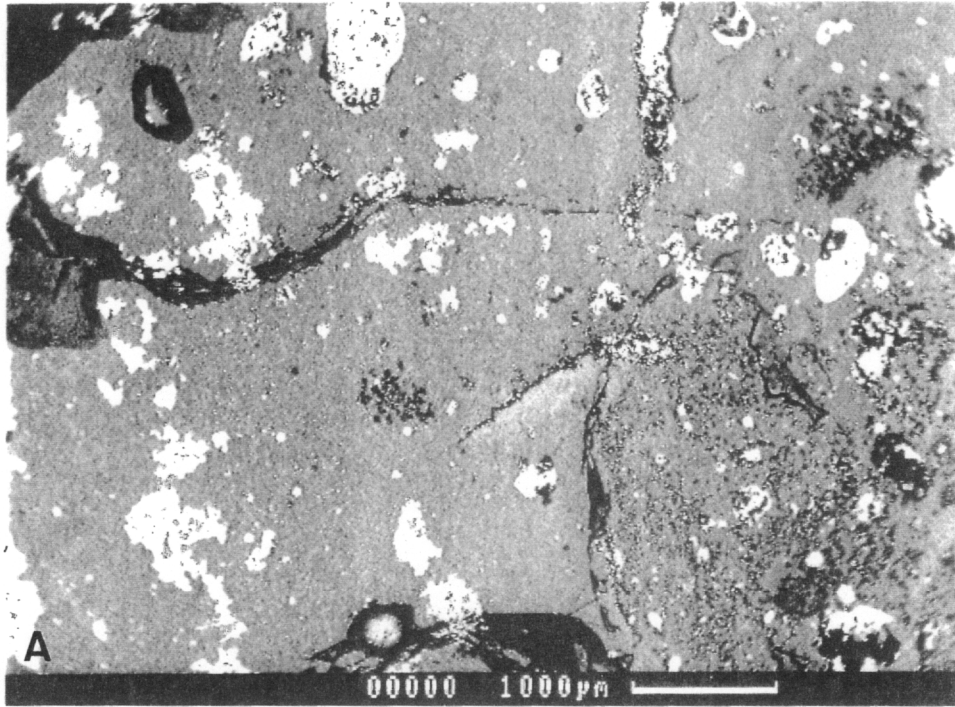


Figure 8. Various textures in Type 2 oxidized petroleum coke slags. (a) gray area is glass and the white masses are polycrystalline aggregates; (b) flow patterns in the glass (transmitted light): the black spheres and the tiny brown dots are the polycrystalline assemblages crystallized out of the glass; the white area is glass after the heavy metals are extracted; (c) Back-scattered image of glass: the heavy metals were extracted out of the glass leaving a large contrast in atomic weights between the glass and the polycrystalline spheres; (d) phase assemblage of the polycrystalline masses: V_2O_4 (white laths), $(Ni,Mg)(Al,Cr,V)_2O_4$ (euhedral, well zoned), $(CaMg,Fe,Ni,Na)V_2O_6$ (gray, blocky laths), glass (black, round to irregular masses).

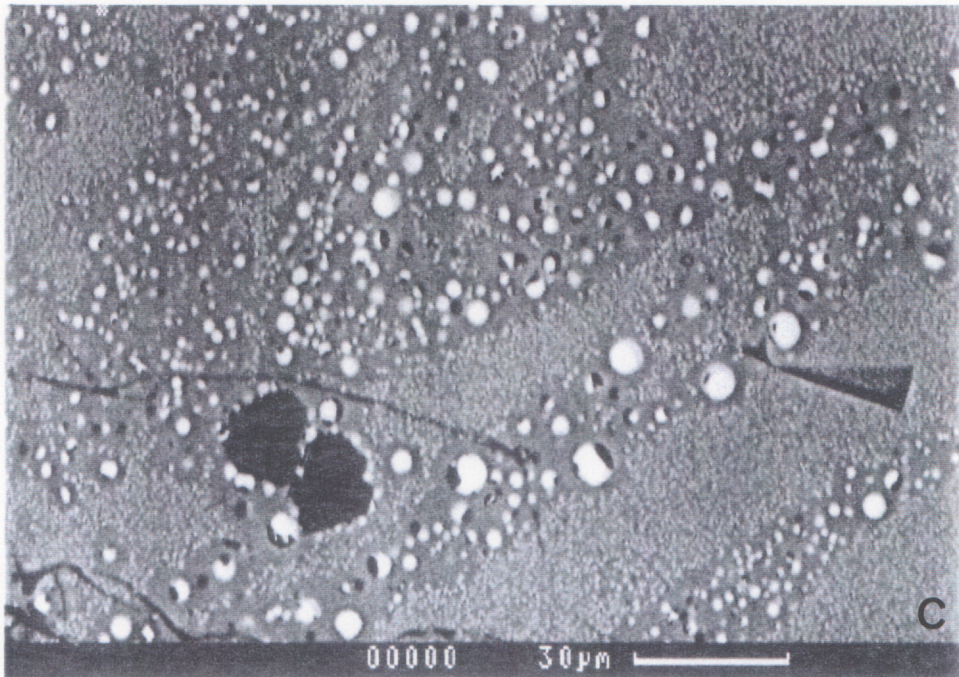
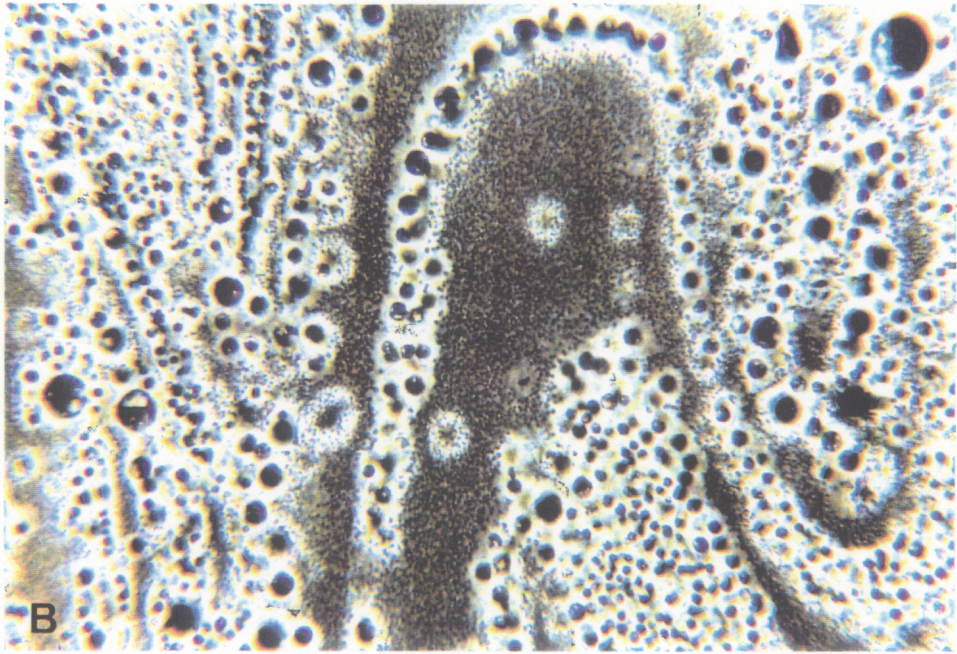


Figure 8 (continued)

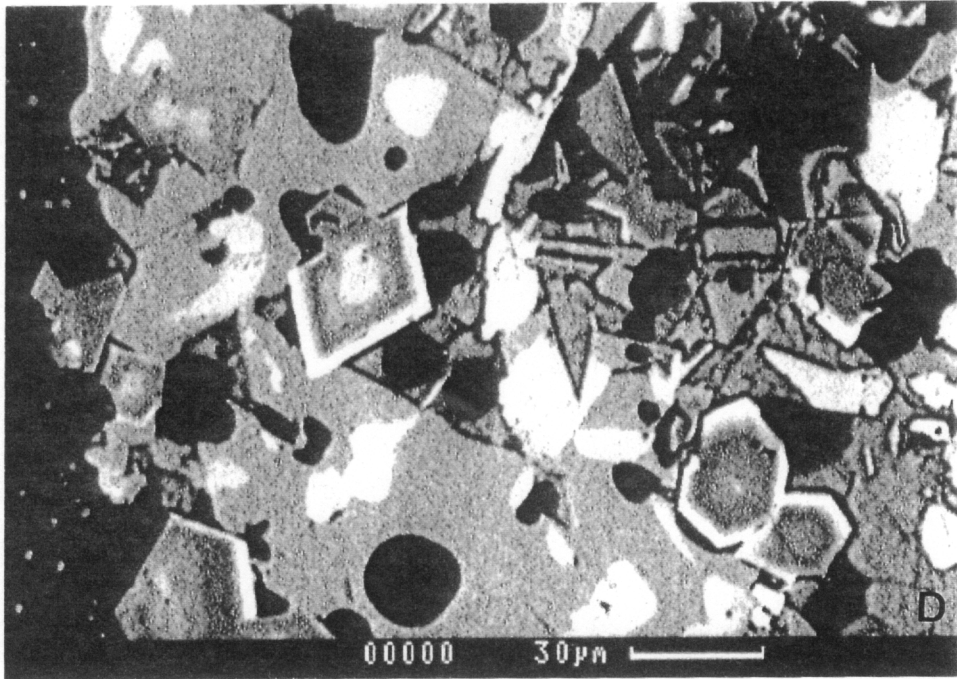


Figure 8 (concluded)

Table 2. The glass compositions of oxidized petroleum coke slags (wt%)

	Si	Al	V	Ca	Na	Ni	Fe	Mg	Ti
Average	72.4	10.2	7.6	1.7	0.9	0.4	0.4	0.3	0.3
Maximum	94.9	15.5	15.2	3.9	1.4	2.1	0.8	0.8	0.7
Minimum	57.5	1.4	0.3	0.1	0.2	0.0	0.0	0.0	0.0

* The data were obtained using electron probe microanalysis.

reduced and oxidized slags were the same, the differences arise from the increase in oxygen pressure during generation of the oxidized slags.

Goldschmidt's (1937) geochemical classification of elements has been widely used as a guide in predicting and explaining chemical behavior during the process of crystallization of igneous rocks. According to Goldschmidt, elements can be divided into four groups, siderophile, chalcophile, lithophile, and atmophile, wherein elements of the same group tend to combine to form specific compounds or alloys.

Table 3 shows the results of bulk chemical analyses of reduced slags. To evaluate the relative importance of the elements in formation of major phases, weight percents (Bulk 1) have been converted into relative atomic proportions (excluding oxygen) (Bulk 2). Figure 9 illustrates the chemical behavior of elements and phase formation under reduced and oxidized conditions. It can be seen that the major slag-forming elements are V, Si, Al, Ca, Na, Fe, Ni, S. Among these elements, V, Si, Al, Ca, Na are typical lithophile; S, chalcophile; and Fe and Ni, primarily siderophile and possibly chalcophile and lithophile. Among the lithophile elements, vanadium and silicon can occur either as the simple compounds, V_xO_y and SiO_2 , respectively, or oxyanion compounds, that is, vanadates and silicates, respectively. Occurrence of other cations (Al, Ca, Na) in vanadium or silicon compounds depends upon redox conditions. Under reduced conditions, vanadium is trivalent (V^{+3}) in V_2O_3 ; and vanadates, which requires pentavalent vanadium, do not occur. The formation of silicates is controlled by the concentration of silicon relative to other cations (e.g. Ca, Na). In the present study, all the silicon is combined with other cations to form silicates such as $(Ca, Na, Mg, Fe, V)_4(Si, Al)_5O_{12}$ and $NaAlSiO_4$ and therefore a discrete silica phase does not occur. Sulfur, a chalcophile element, does not have any typical chalcophile element (Pb, Cu, Zn etc.) to associate with; however, the chemical affinity of iron and nickel depends on the availability of sulfur relative to other anions like O^{2-} . When significant amounts of sulfur and low amounts of oxygen exist in

Table 3. Bulk chemical analyses of reduced petroleum coke slags

Elements	#1* (wt %)	#2 (wt %)	#3 (wt %)	Bulk 1* (wt %)	Bulk 2 (atomic proportion)
V	26.80	38.00	29.60	36.46	44.79
Si	7.84	6.68	7.50	6.83	15.24
Al	4.57	5.46	3.03	5.25	12.19
Ca	5.55	5.26	4.95	5.27	8.24
Na	2.94	2.94	4.13	3.00	8.17
Fe	3.19	2.35	2.66	2.45	2.75
Ni	0.45	2.60	5.00	2.51	2.67
S	0.45	1.03	1.45	0.99	1.94
Mg	1.13	0.55	0.48	0.61	1.57
Cr	4.54	0.40	0.28	0.81	0.97
Ti	0.77	0.65	0.41	0.65	0.85
As	0.26	0.33	0.37	0.33	0.27
K	0.07	0.07	0.07	0.07	0.11
Mn	0.06	0.03	0.03	0.03	0.04
Be	0.01	0.00	0.01	0.00	0.03
Ag	0.05	0.05	0.05	0.05	0.03
Ba	0.05	0.06	0.07	0.06	0.03
Bi	0.08	0.07	0.06	0.07	0.02
Sb	0.02	0.04	0.05	0.04	0.02
Co	0.01	0.02	0.02	0.02	0.02
Zr	0.09	0.02	0.02	0.03	0.02
Mo	0.01	0.02	0.04	0.02	0.01
Sr	0.01	0.02	0.01	0.02	0.01
Nb	0.01	0.01	0.01	0.01	0.01
Y	0.01	0.01	0.01	0.01	0.01

* B, P, Sc, Cu, Zn, Cd, Sn, W, and Pb are analysed but all below detection limit.

*Three sequential samples were taken for bulk chemical analyses. #1 sample is on the side of refractory wall and represents 10% of the total reduced slags; #2 sample is from the middle and represents 85% of the total reduced slags; #3 sample is from the outermost side and represents 5% of the total reduced slags.

*Bulk 1 are the weighted average weight percents and Bulk 2, relative atomic proportion (excluding oxygen).

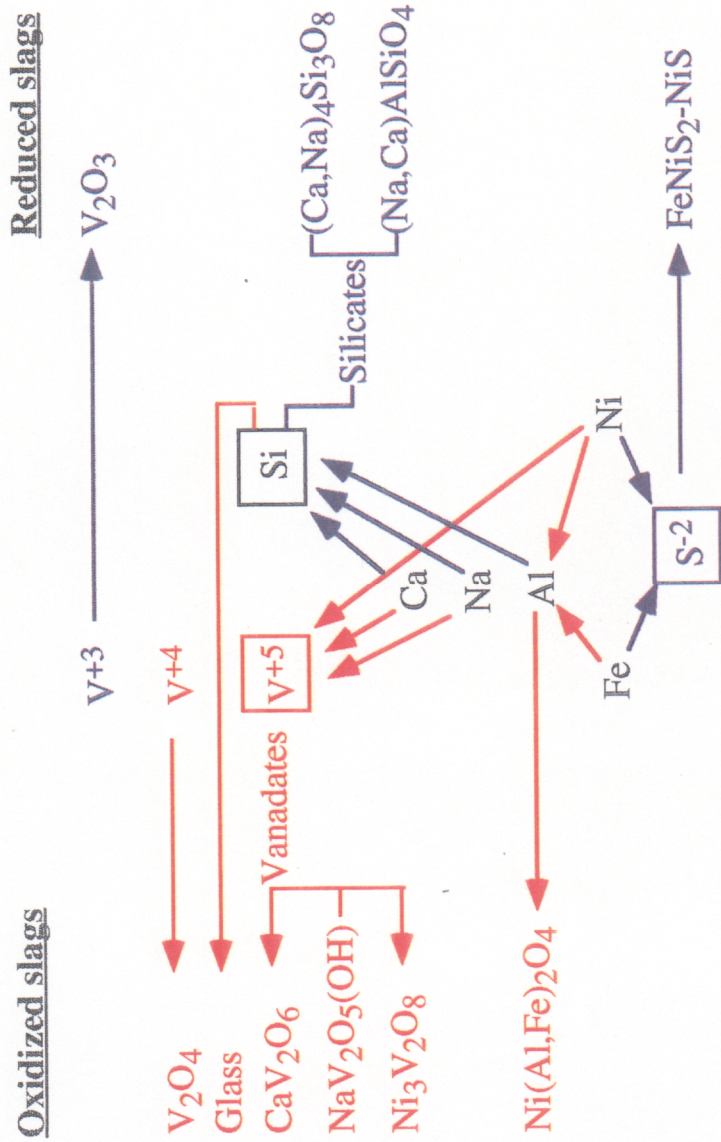


Figure 9. Diagram showing chemical behavior of elements and phase formation under reduced and oxidized conditions.

the slag, as in this case, iron and nickel become chalcophile and combine with sulfur to form iron-nickel sulfides.

The oxidized slags are the same as the reduced slags in terms of bulk chemical compositions except that oxygen has reacted with them and the sulfur originally present as sulfide has been driven off. The remaining elements are all lithophile except iron and nickel. Under these conditions, vanadium was oxidized to higher valence states (V^{+4} and V^{+5}) which created different environments for cation arrangements. V^{+4} occurs in vanadium oxide (V_2O_4) and V^{+5} occurs in vanadates. The presence of vanadates presents a chemically competitive situation between vanadates and silicates for other cations. The thermodynamic data for the silicate and vanadate phases present in the slags are not available, but it seems certain that under the oxidized condition, vanadates are more stable than silicates. Silica, which occurs as silicates in reduced slags, is left as an uncombined component. The presence of substantial amounts of impurities, which significantly lowered the melting point, allowed silica to form a melt phase while other components formed crystalline phases. During the quenching process, the silica melt was preserved as glass.

Textures

Refractory - slag reaction:

The large sample of reduced slag revealed that the slag underwent limited reaction with the refractory lining that contains chromium-magnesium spinel ($MgCr_2O_4$). X-ray dot maps (Figure 10) show that along the margin of the spinel, magnesium and chromium have been replaced by iron, vanadium, aluminum and titanium. More rigorous evaluation of the elemental exchange was made by conducting electron microprobe analyses along a traverse as shown in Figure 11. This traverse shows chromium and vanadium to exhibit a distinct reciprocal relationship. From the unaffected refractory lining side (right) to the interface

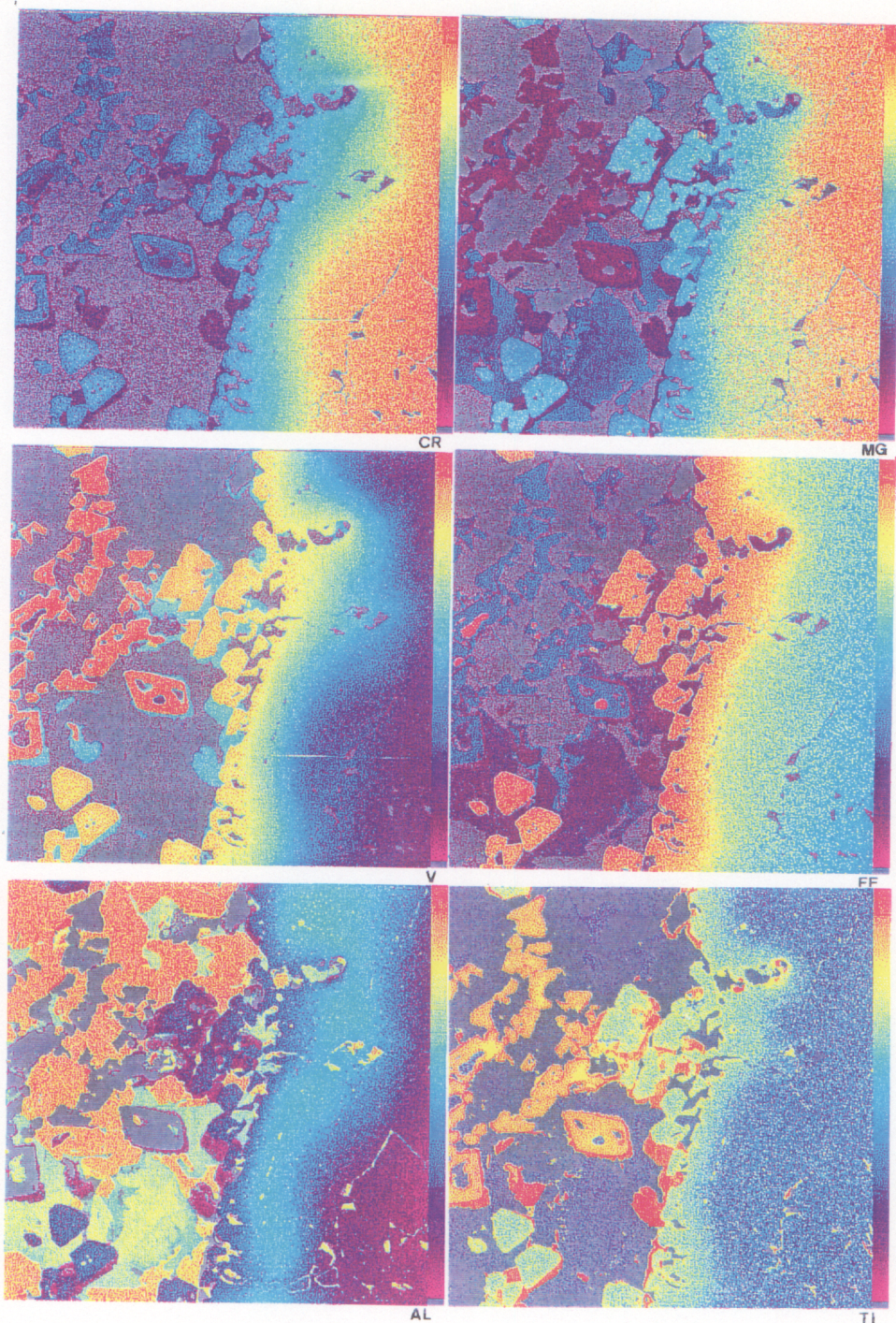


Figure 10. Electron probe X-ray maps of of altered refractory brick (MgCr_2O_4) for Cr, Mg, Fe, V, Al and Ti. The color bar on the right indicates the relative intensity from red (highest) to purple (lowest). The field of views of maps are 1.2 cm.

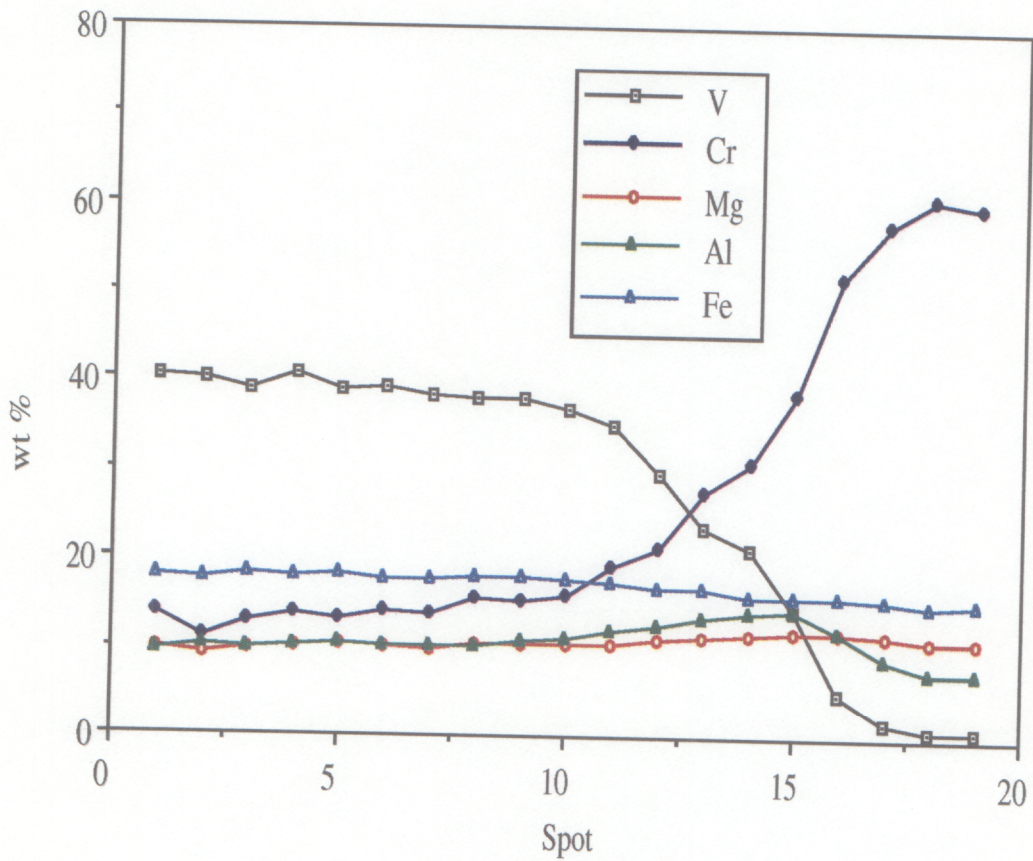


Figure 11. An electron probe traverse analysis of altered spinel brick. The left side is the unaltered brick ($MgCr_2O_4$) and toward the right, the $MgCr_2O_4$ spinel shows gradual compositional changes. The most involved elements in the alteration process are chromium and vanadium which exhibit distinct reverse relationship.

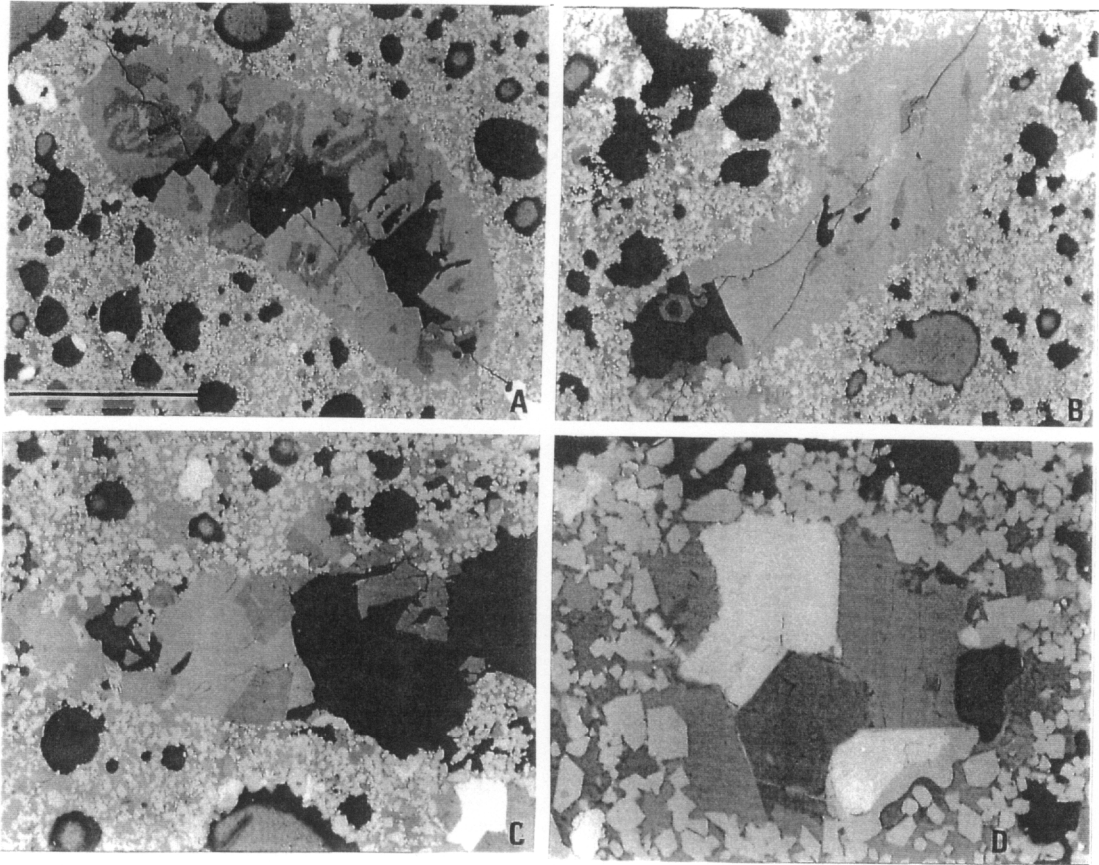


Figure 12. Various cavity filling textures in reduced petroleum coke slags. The gray phase in the cavity is $(Ca, Na, Mg, Fe, V)_4(Si, Al)_5O_{12}$; the dark gray phase is $NaAlSiO_4$; the white phase (d) is nickel-iron sulfide and the black areas are the unfilled cavities.

(left) between the refractory fragment and the slag, the concentration of chromium decreases while that of vanadium increases. The concentration of the other three elements (Mg, Al, and Fe) remain relatively constant with slight depletion of magnesium and slight increase of aluminum and iron towards the interface.

Cavity filling

In the reduced slags, patches of polycrystalline aggregates are common (Figure 12). These aggregates consist primarily of $(\text{Ca,Na,Mg,Fe,V})_4(\text{Si,Al})_5\text{O}_{12}$ and NaAlSiO_4 , and their crystal sizes are several times larger than their counterparts in the host. V_2O_3 is either non-existent or rare in these cavities. Where V_2O_3 is present, the crystals are almost always skeletal, with silicate or sulfide filled cores (Figure 13a). In a few of the cavities, V_2O_3 crystals of significantly larger size line the walls of the cavities (Figure 13b). The aggregates are mostly oval in shape. A comparison of empty, partially filled, and completely filled voids strongly suggests that these oval cavities were originally gas bubbles which were infilled sometime after crystallization of the bulk slag. There would appear to be two possible modes for the melt to get into the gas bubbles: diffusion and/or infiltration. However, at the present time, it is not certain whether one or both of these processes are responsible for the formation of the filling phases.

Eutectic or eutectoid textures

Eutectic or eutectoid textures are common in the phase assemblages in Zone 2 of the reduced slags. In Zone 1 and Zone 3, the major silicate phases are NaAlSiO_4 and $(\text{Ca,Na,Mg,Fe,V})_4(\text{Si,Al})_5\text{O}_{12}$. In Zone 2, however, the $(\text{Ca,Na,Mg,Fe,V})_4(\text{Si,Al})_5\text{O}_{12}$ phase virtually disappears; instead, the $\text{Ca}_3\text{V}_2\text{Si}_3\text{O}_{12}$ and NaAlSiO_4 phases form in colonies, a metallurgical term for phases displaying subparallel lamellar intergrowths as shown in Figure 3a. Also notice that FeV_2O_4 crystals are scattered throughout Zone 2

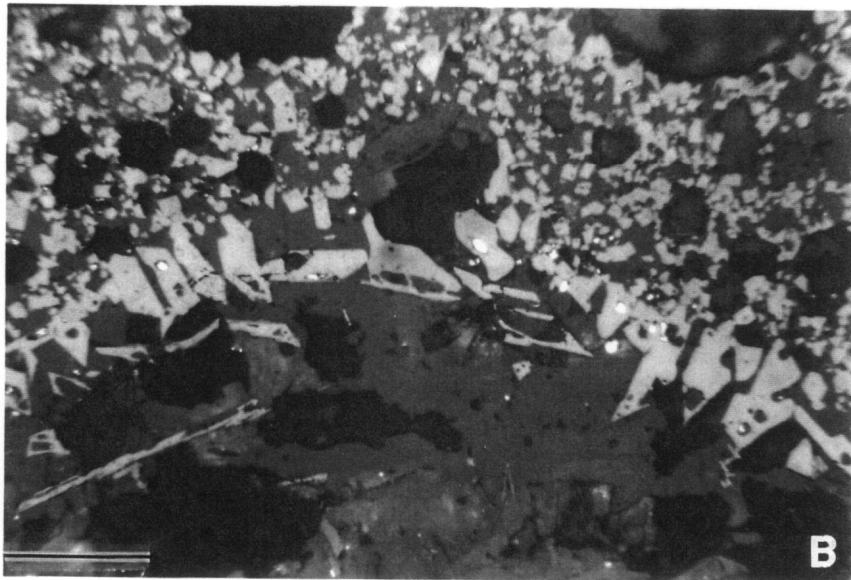
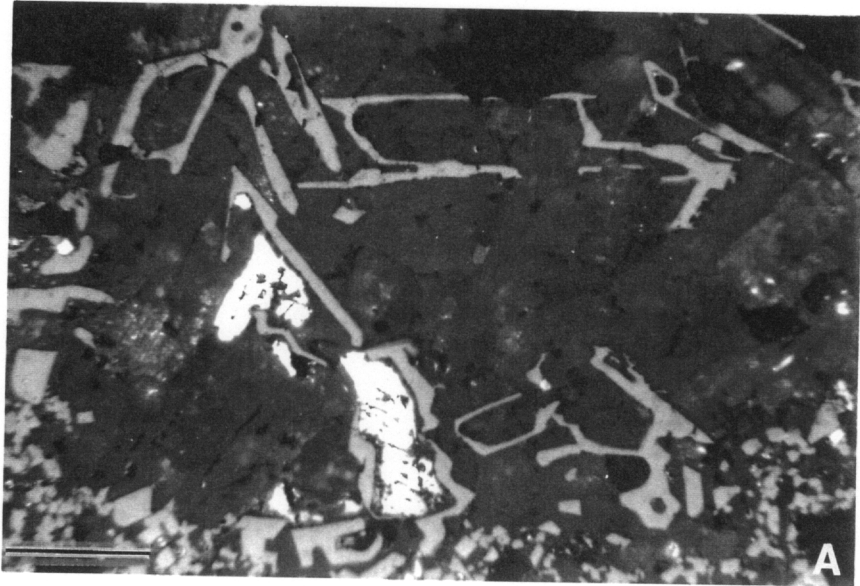


Figure 13. The occurrence of V_2O_3 phase in the cavities in reduced petroleum coke slags. (a) V_2O_3 occurs as skeletal crystals with core filled with silicates or sulfides; (b) V_2O_3 crystals of much bigger size line along the wall of the cavities.

(Figure 3b). On the basis of the texture observed in Zone 1, it is certain that NaAlSiO_4 and $(\text{Ca,Na, Mg,Fe,V})_4(\text{Si,Al})_5\text{O}_{12}$ crystallized after V_2O_3 . The electron microprobe analyses demonstrate that there is no significant amount of vanadium present in these silicate phases. The intergrown lamellae of NaAlSiO_4 and $\text{Ca}_3\text{V}_2\text{Si}_3\text{O}_{12}$ were most likely formed under eutectic conditions because the texture is perfectly analogous to that found in eutectic or eutectoid alloy systems (Figure 14).

Sulfides, metals and textures

Iron-nickel sulfides occur throughout all four zones of the reduced slags but are completely absent from the oxidized slags. Typically, iron-nickel alloys occur as a complex intergrowth with FeNi sulfides as shown in Figure 15. There are frequently distinctive zones to the intergrowths: a central zone with coarser nickel-iron alloy cubes or irregular masses, and a peripheral zone composed of nickel-iron sulfides that exhibit fine grained to lamellar intergrowth textures.

The intimate intergrowth of the iron-nickel sulfides of different compositions appears to be the result of exsolution that occurred during or after crystallization, once the gasifier had cooled sufficiently for these phases to crystallize. However, exsolution is not the sole mechanism responsible for the formation of the iron-nickel alloy cubes. Figure 15c is a good example. It can be seen that where the iron-nickel alloy cube occurs, there is no depletion Zone surrounding it. It is believed that these alloys are primary.

Fractional crystallization

Glass does not occur in reduced slags, but is a common component of the oxidized slags, and has been preserved due to the sudden temperature drop caused by water quenching. Detailed light microscopic and SEM examinations show that the glass has undergone varying degrees fractional crystallization. The fractional crystallization occurs

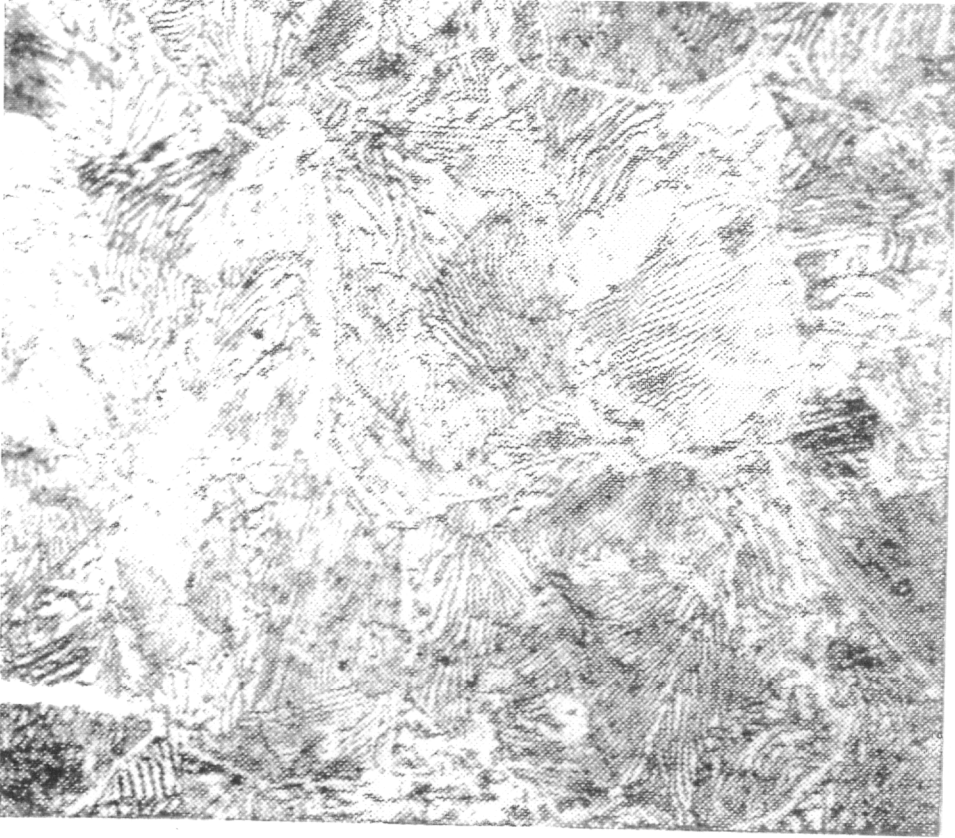


Figure 14. Hypereutectoid steel, 1.2% C. Thin bands of proeutectoid cementite (Fe_3C), light gray, outline the grains of pearlitic eutectoid constituent ($\alpha + \text{Fe}_3\text{C}$). Magnification 1250 (after Rhines 1956).

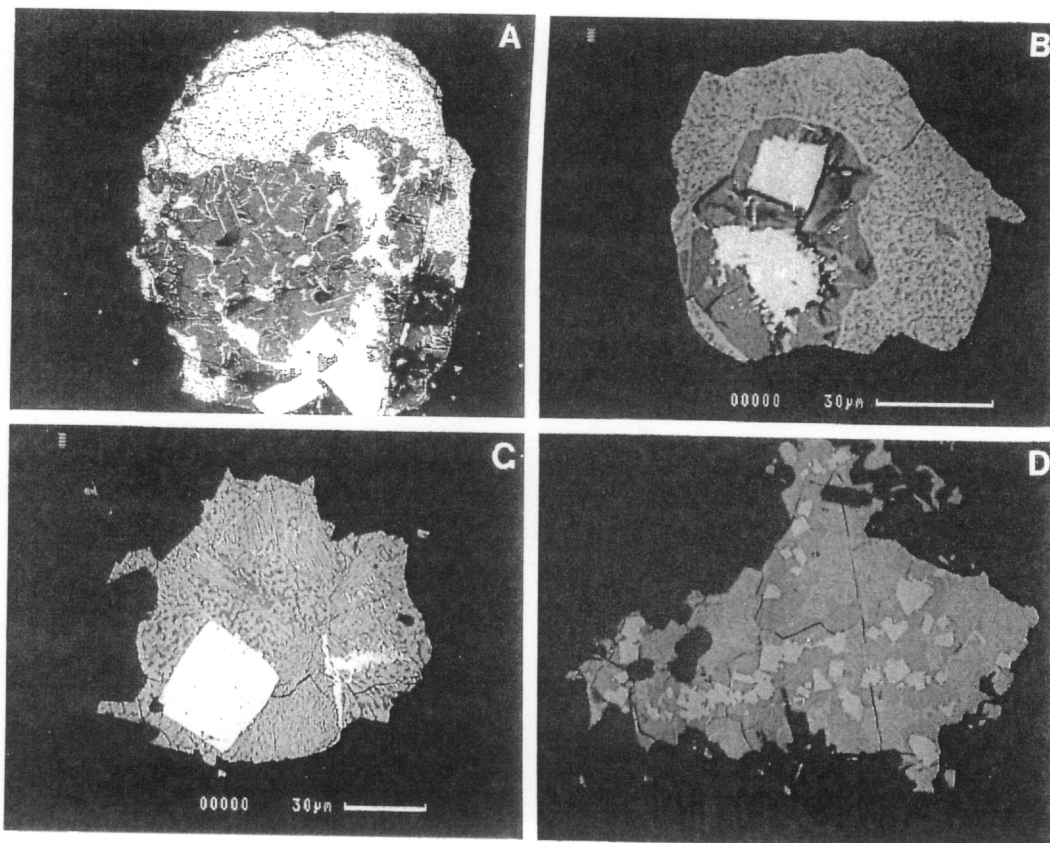


Figure 15. Various forms of sulfides in reduced petroleum coke slags: Ni-Fe alloy (white cubes and lamella), FeNiS_2 -NiS (gray and networked area).

throughout the glass, especially along flowbands. The black and brown spheres visible in Figure 8b consist of polycrystalline assemblages of V_2O_4 , $NiAl_2O_4$, CaV_2O_6 , and $Ni_3V_2O_8$ that crystallized from the glass host. The white areas are glass which has lost most of its calcium and transition metals through crystallization of discrete phases. Figure 8c is a back-scattered image of some of the glass. It shows that during fractional crystallization, the heavier elements are extracted from the glass and incorporated into crystalline oxides (i.e. the bright crystals that have a high average atomic number) yielding a large BSE signal contrast between the glass host and the polycrystalline spheres.

Spinel zonation

There are three spinel phases in the slags: $MgCr_2O_4$, FeV_2O_4 and $NiAl_2O_4$. $MgCr_2O_4$ and FeV_2O_4 occur in reduced slags and do not display any zoning except where $MgCr_2O_4$ (refractory) fragments were engulfed in the normal slags and altered along their margins. $NiAl_2O_4$ occurs in both types of oxidized slags (Type 1 and Type 2) and displays various zoning patterns. The zonation is particularly distinctive in Type 2 oxidized slags where glass is far more abundant than the crystalline phases. The close correlation between the extent of zonation in spinel and the abundance of glass indicates that as more glass formed (i.e. the faster the melt solidified), the more distinctive zones were developed in spinel.

Figure 16 is a back-scattered image of a spinel crystal shown in Figure 8d. The image shows that the core and the margin are enriched with metals of relatively high atomic number. Figure 17 is an electron probe traverse for the six major elements (Cr, Ni, Al, Fe, Mg, V) in that crystal. It shows that the bright core results from enrichment of chromium, and the bright margin from nickel and iron enrichment.

The early intake of chromium into the spinel phase and the sharp increase of iron observed at the margin, may both be explained with crystal field theory. Details about the

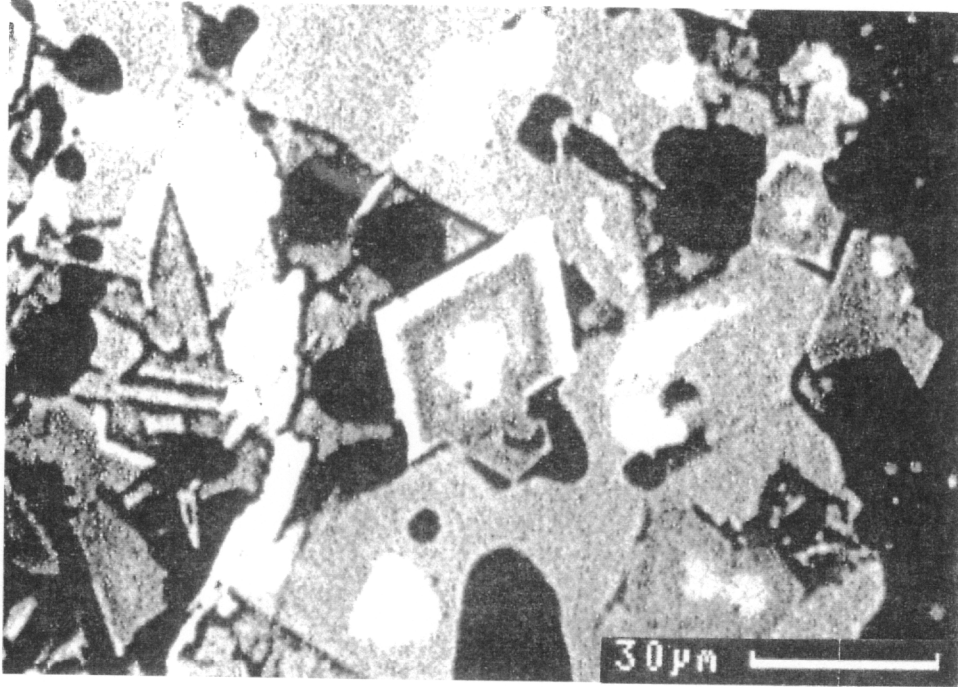


Figure 16. Back-scattered image of one of spinel crystals from Figure 8d. The image shows that the core and the margin are relatively enriched with chromium and iron.

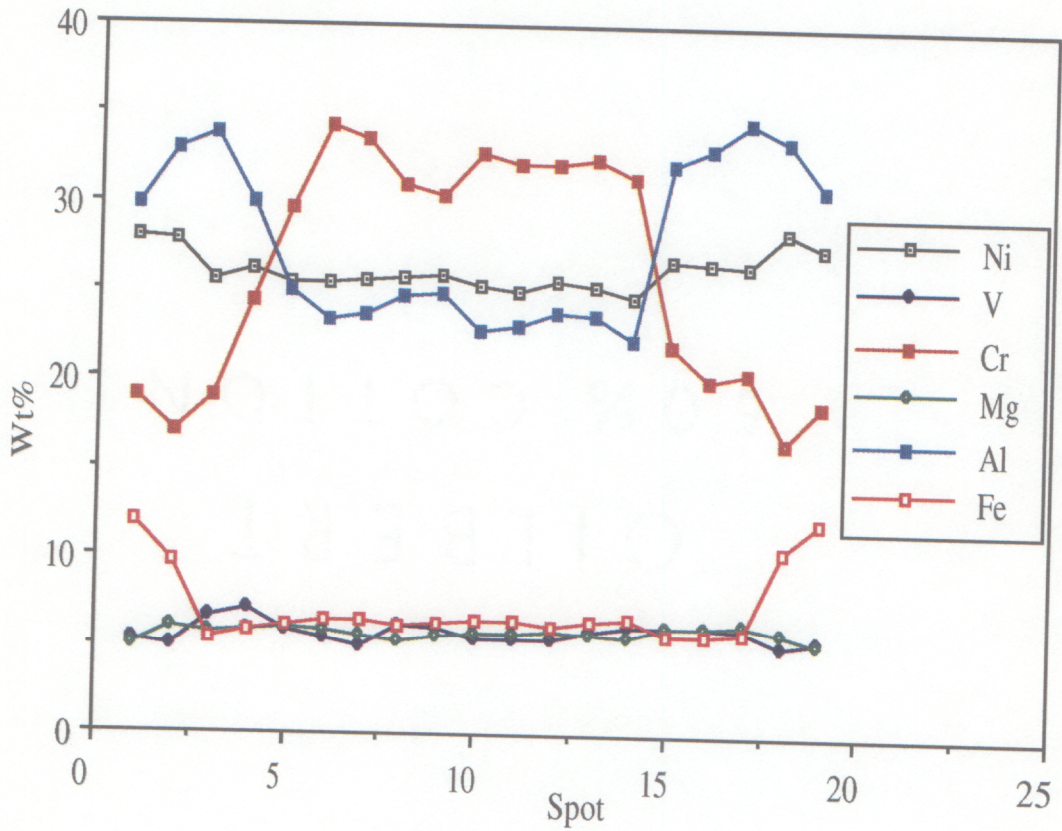


Figure 17. An electron probe traverse analysis of a chemically zoned spinel. The traverse starts at the edge of one side of the crystal and ends at the edge of the other side of the crystal. The bright core seen in Figure 15 obviously results from enrichment of chromium and the bright margin, from nickel and iron.

theory can be found in most texts of general chemistry (e.g. Ebbing and Wrighton, 1990) and mineralogy. Based on this theory, the order of incorporation of transition elements into a growing crystal is controlled by the element's relative octahedral "site preference energy". Dunitz and Orgel (1957) calculated octahedral "site preference energy" for most divalent and trivalent transition metals. It turned out that the octahedral site preference energy for chromium (+3) is the highest ($37.7 \text{ kcal mole}^{-1}$) and iron (+3), the lowest (0).

SUMMARY

The phase assemblages and textures of petroleum coke gasification slags were studied using light microscopic observations and microbeam techniques. The two types of slags, reduced and oxidized, have very different phase assemblages and textures. The reduced slags are zoned and the bulk is composed of predominantly V_2O_3 , with interstitially intergrown $(\text{Ca,Na,Mg,Fe,V})_4(\text{Si,Al})_5\text{O}_{12}$ and subordinate NaAlSiO_4 ; Fe Ni sulfides are scattered throughout the reduced slags and they display very complex exsolution textures. There are two types of oxidized slags, namely Type 1 and Type 2. Type 1 slags make up more than 90% of the oxidized slags. Their major phases include V_2O_4 , $(\text{Ca,Mg,Fe,Ni,Na})\text{V}_2\text{O}_6$, $(\text{Ni,Mg,Fe})_3(\text{V,Si})_2\text{O}_8$, $(\text{Ni,Mg})(\text{Al,Cr,V})_2\text{O}_4$, and $\text{NaV}_2\text{O}_5(\text{OH})$ with glass spheres scattered throughout. Type 2 slags make up only 5-10 % of the oxidized slags. The major component of Type 2 slags is glass of variable composition; there is also small amounts of V_2O_4 , $(\text{Ca,Mg,Fe,Ni,Na})\text{V}_2\text{O}_6$, $(\text{Ni,Mg,Fe})_3(\text{V,Si})_2\text{O}_8$, $(\text{Ni,Mg})(\text{Al,Cr,V})_2\text{O}_4$, and $\text{NaV}_2\text{O}_5(\text{OH})$ occurring in spherical, polycrystalline aggregates that developed through fractional crystallization. The major factor affecting the phase assemblage is the oxygen pressure at which different slags are generated.

A variety of textures were observed in reduced slags and oxidized slags including refractory-slag reaction, cavity filling, sulfide exsolution, eutectic intergrowths, fractional

crystallization, and spinel zonation. The identification and understanding of these textures are of great value in assessment of petroleum coke slags from various perspectives including resource reclamation, environmental application and gasification engineering.

REFERENCES

- Dunitz, J. D., and Orgel, L.E., 1957, *Journal of Physics and Chemistry of Solids*: v.3, p 317.
- Ebbing, D. D., and Wrighton, M.S., 1990, *General Chemistry*, Houston Mifflin Company, 1035p.
- Groen, J.C., and Craig, J.R., 1994, *The inorganic geochemistry of coal, petroleum, and their gasification/combustion products: Fuel Processing Technology*, v. 40, p. 15-48.
- Vaughan, D.J. and Craig, J.R., 1978, *Mineral chemistry of metal sulfides*: Cambridge, Cambridge University Press, 493 p.

CHAPTER 4. PETROLEUM COKE SLAG: POTENTIAL RESOURCE RECLAMATION

INTRODUCTION

The petroleum coke gasification process was described in Chapter 2. Petroleum coke slag generated during gasification, was characterized in Chapters 2 and 3. This chapter assesses petroleum coke slags with respect to potential resource reclamation, using the knowledge of the phases, phase assemblages, and textures developed in Chapters 2 and 3; as well as the results of aqueous dissolution experiments.

METHODS

Characterization of petroleum coke slags

The chemical compositions, phase assemblages, and textures were investigated in Chapters 2 and 3 using various methods including bulk chemical analysis, light microscopy, micro-beam compositional analysis, X-ray diffraction and computational methods. To summarize, the major elements in the petroleum coke slags analyzed are V, Si, Al, Ca, Na, Fe, and Ni. In reduced slags, sulfur is also present. The major phases in the reduced slags are V_2O_3 , $(Ca,Na,Mg,Fe,V)_4(Si,Al)_5O_{12}$, $NaAlSiO_4$ and iron-nickel sulfides; while those in the oxidized slags are crystalline phases (V_2O_4 , $(Ca,Mg,Fe,Ni,Na)V_2O_6$, $(Ni,Mg,Fe)_3(V,Si)_2O_8$, and $(Ni,Mg)(Al,Cr,V)_2O_4$) and glass.

Dissolution experiments

Long term dissolution experiments

Long term dissolution experiments (eight months) were conducted on samples of the oxidized slags to determine approximate concentrations resulting from long term dissolution of slags in aqueous solutions. The slag sample was ground to the -100 mesh for the dissolution experiments. Six 10 gram samples of slag were placed in separate 250 mL glass flasks along with 200 mL of solution. The flasks were plugged with rubber

stoppers, which contained a 4 mm diameter hole that was packed loosely with silica wool to allow air to enter the flask. The flasks were maintained at a constant temperature of 25°C by immersing them into a thermostated water bath. The initial pH of the solutions was 7 (deionized water) but the pH was periodically measured and adjusted by adding acid (1 M HCl) or base (1 M NaOH) to obtain final pH values ranging between 4 and 9. The solutions were judged to be equilibrated when consecutive pH measurements taken at one day intervals differed by less than 0.1 pH units. Only one solution sample was collected from each flask at the end of the experiment. The dissolution residues were dried, cast into polished sections and examined with both reflected and transmitted light to investigate how the remnant phases in the dissolution residues altered in response to long term contact with aqueous solutions.

Kinetics experiments

Dissolution rate experiments were conducted using both reduced and oxidized slag samples. The slag samples were prepared in the same way as for long term dissolution experiments. The specific surface area of the crushed slag sample was determined from a three-point N₂ BET isotherm using a Nova 1000 Surface Area Analyzer. For each measurement, approximately 0.2 g of sample was outgassed in a vacuum at 50°C for 24 hours. The specific surface area of the unreacted, oxidized and reduced slag samples was found to be 0.73 m²/g and 0.27 m²/g, respectively (Appendix VI). Five 10 gram samples of each of these powders were placed in separate 250 mL glass flasks along with 200 mL of solution. The flasks were plugged with rubber stoppers, which contained a 4 mm diameter hole that was packed loosely with silica wool to allow air to contact the solutions. A constant reaction temperature of 25°C was maintained by immersing the flasks in a thermostated water bath. The initial pH was 7 (deionized water) and one solution sample was collected from each flask at time intervals of 1 hour, 3 hours, 24 hours, 72 hours and 168 hours.

RESULTS

Elements of significance

The bulk chemical analyses of petroleum coke slags are shown in Table 1. It can be seen that the concentrations of V, Si, Ca, Al, Na, Fe, Ni, Cr, S, Mg, Ti and As are above 0.3% ; Bi, K, Ba, Ag, Zr, Mn, Sb, Mo, Co and Sr range between 700 and 100 ppm; Y, Be and Nb range between 100 and 30 ppm; B, Sn, W, Cu Sc, Zn, Cd and Pb range between 30 and 1 ppm.

To assess the resource reclamation potential, the enrichment of the elements in the slags relative to average rocks is illustrated in Figure 1. The solid oblique line represents equal concentrations in both materials; the dashed lines represent order of magnitude enrichments of elements in the slags relative to the crustal rocks. The shaded area indicates the most significant elements in the slags because of their high absolute abundance and their enrichment over average crustal abundances. Although many elements are enriched in the slags relative to crustal rocks, vanadium, nickel, chromium, sulfur and arsenic (in the shaded area) are especially noteworthy. Among these elements, vanadium is the most significant.

Dissolution behavior

Long term dissolution

The original oxidized slag phase assemblage (before dissolution) is shown in Figure 2a. The slag phases include V_2O_4 (gray, columnar to equigranular), $Ni_3V_2O_8$ (light gray, needle shaped), $NiAl_2O_4$ (gray with light gray rims, equigranular), CaV_2O_6 (gray, rough surface, occurring in matrix) and glass (black). After dissolution (Figure 2b), the remaining phases are V_2O_4 (white), $Ni_3V_2O_8$ (white, center of photo), $NiAl_2O_4$ (white, indistinguishable from V_2O_4 on back scattered images) and glass (black with gray rims). The residue shown here is from an experiment adjusted to pH 7.5, but the phases

Table 1. Bulk chemical analyses of reduced petroleum coke slags

Elements	#1* (wt %)	#2 (wt %)	#3 (wt %)	Bulk 1* (wt %)	Bulk 2 (atomic proportion)
V	26.80	38.00	29.60	36.46	44.79
Si	7.84	6.68	7.50	6.83	15.24
Al	4.57	5.46	3.03	5.25	12.19
Ca	5.55	5.26	4.95	5.27	8.24
Na	2.94	2.94	4.13	3.00	8.17
Fe	3.19	2.35	2.66	2.45	2.75
Ni	0.45	2.60	5.00	2.51	2.67
S	0.45	1.03	1.45	0.99	1.94
Mg	1.13	0.55	0.48	0.61	1.57
Cr	4.54	0.40	0.28	0.81	0.97
Ti	0.77	0.65	0.41	0.65	0.85
As	0.26	0.33	0.37	0.33	0.27
K	0.07	0.07	0.07	0.07	0.11
Mn	0.06	0.03	0.03	0.03	0.04
Be	0.01	0.00	0.01	0.00	0.03
Ag	0.05	0.05	0.05	0.05	0.03
Ba	0.05	0.06	0.07	0.06	0.03
Bi	0.08	0.07	0.06	0.07	0.02
Sb	0.02	0.04	0.05	0.04	0.02
Co	0.01	0.02	0.02	0.02	0.02
Zr	0.09	0.02	0.02	0.03	0.02
Mo	0.01	0.02	0.04	0.02	0.01
Sr	0.01	0.02	0.01	0.02	0.01
Nb	0.01	0.01	0.01	0.01	0.01
Y	0.01	0.01	0.01	0.01	0.01

* B, P, Sc, Cu, Zn, Cd, Sn, W, and Pb are analysed but all below detection limit.

*Three sequential samples were taken for bulk chemical analyses. #1 sample is on the side of refractory wall and represents 10% of the total reduced slags; #2 sample is from the middle and represents 85% of the total reduced slags; #3 sample is from the outermost side and represents 5% of the total reduced slags.

*Bulk 1 are the weighted average weight percents and Bulk 2, relative atomic proportion (excluding oxygen).

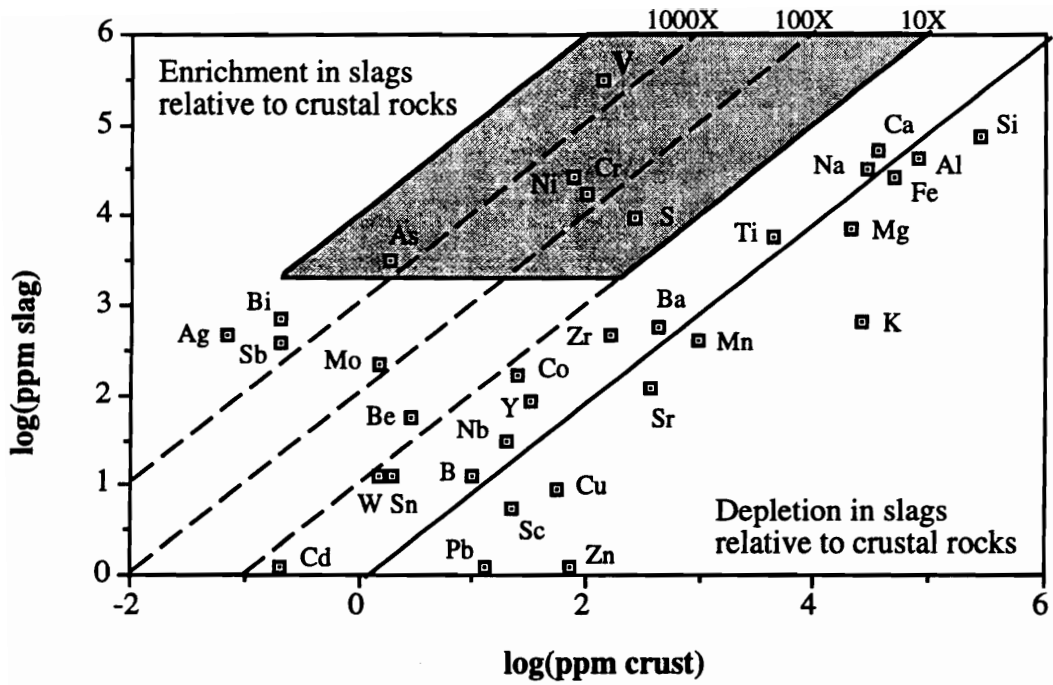


Figure 1. Log-log diagram for concentrations of elements in petroleum coke slags versus elemental abundance in the earth's crust. The solid oblique line represents equal concentrations in both materials; the dashed lines represents order of magnitude of enrichments of elements in slags relative to the crustal rocks. The shaded area include the most significant elements in the slags.

remaining in residues from solutions with other pH values are more or less the same as that at pH 7.5. It appears that the calcium vanadate, which made up 40% of the original phase assemblage, was largely responsible for the vanadium dissolution because it was completely dissolved. It is also apparent that all the reacted glass particles display brighter rims in the back scattered images (Figure 2b). This indicates that dissolution was selective, with lighter components (Si, Al) dissolving more than heavier ones (V, Cr, Fe).

The dissolution results are listed in Table 2 and plotted in Figure 3. It can be seen that the concentrations of vanadium in the long term experiments are pH dependent. At both high and low pH the concentrations are high, while the minimum concentration occurs near pH 6.

Dissolution kinetics

Concentration versus time data for the short term dissolution kinetics experiments are listed in Table 3 and plotted in Figure 4. The apparent rates of vanadium dissolution in pure water for oxidized slag and reduced slag were estimated to be $1.28 \times 10^{-4} \text{ mol m}^{-2} \text{ sec}^{-1}$ and $3.08 \times 10^{-5} \text{ mol m}^{-2} \text{ sec}^{-1}$, respectively, using the initial rate method (Rimstidt and Newcomb 1992). These rates are quite rapid compared to the rate of dissolution of common silicate minerals which range from about 10^{-7} to $10^{-13} \text{ mol m}^{-2} \text{ sec}^{-1}$.

DISCUSSION

Although vanadium is relatively abundant (~135 ppm) in the earth's crust, it is widely dispersed and rarely concentrated into minable ores. Although vanadium forms numerous minerals, almost 95% of the world vanadium reserves occur distributed in just three major types of deposits (titaniferous magnetite, phosphorite or phosphatic shale, and crude petroleum and tar sands) in which vanadium occurs only as a minor element (Gupta 1992). The current mining grades for vanadium are mostly below 1% and a grade of around 0.4% is very common.

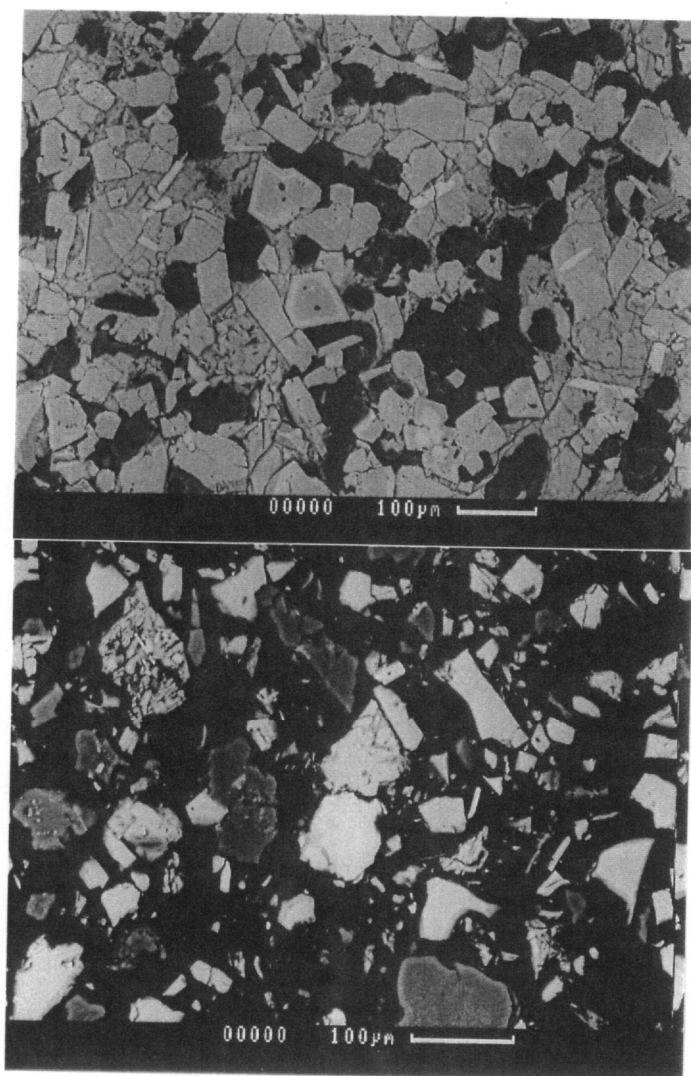


Figure 2. Comparison between phase assemblages in Type 1 oxidized petroleum coke slags before dissolution and after dissolution . a) Before dissolution: phases include V_2O_4 (gray, columnar to equigranular), $Ni_3V_2O_8$ (light gray, needle shaped), $NiAl_2O_4$ (gray with light gray rims, equigranular), CaV_2O_6 (gray, rough surface, occurring in matrix) and glass (black). b) After dissolution (for solution of pH 7.5): phases remaining are V_2O_3 (white) and $Ni_3V_2O_8$ (white, center of the photo), and glass (black with gray rims).

**Table 2: Results of the long term dissolution experiments
using oxidized petroleum coke slags**

pH	(ppm)	(molal)
4.0	3840	0.075
5.2	2490	0.049
5.9	1510	0.030
6.3	1830	0.036
7.7	4430	0.087
8.4	4390	0.086

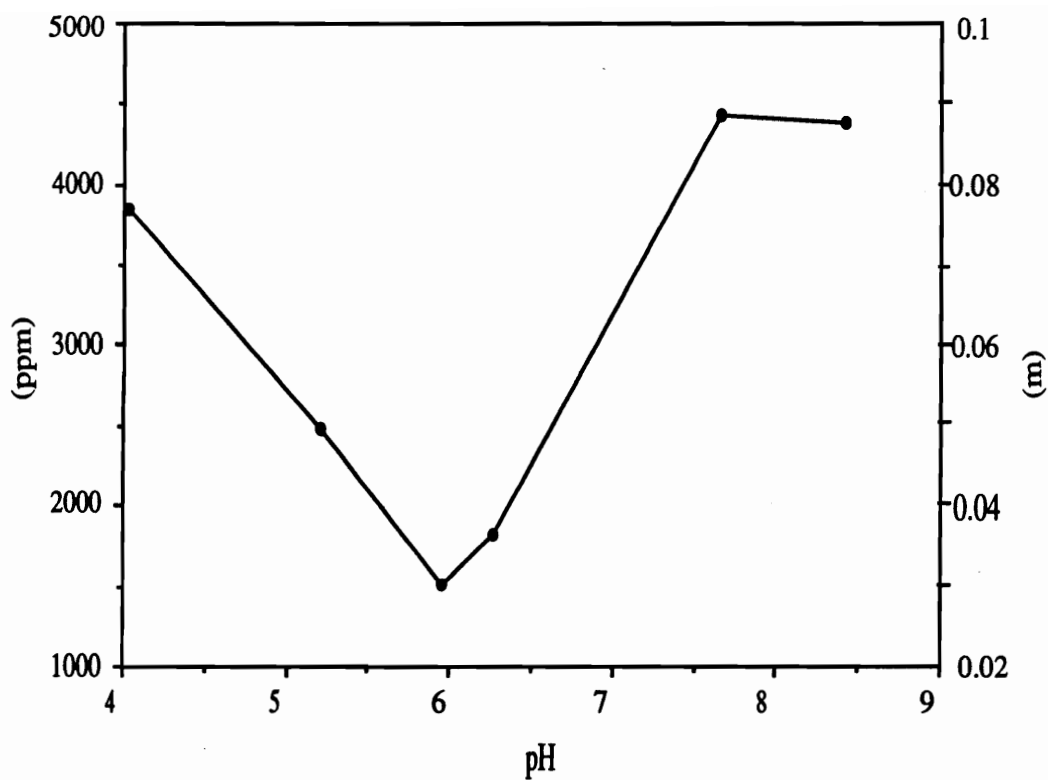


Fig. 3. Concentrations of vanadium in solutions that remained in contact with oxidized petroleum coke slags for 8 months at various pH values (25°C, in contact with atmosphere).

Table 3: Vanadium concentrations vs time for reduced and oxidized petroleum coke slags.

Hours	Oxidized slags		Reduced slags	
	(ppm)	(molal)	(ppm)	(molal)
1	246	0.0048	39.0	0.0008
3	276	0.0054	45.8	0.0009
24	461	0.0090	88.3	0.0017
72	600	0.0118	138.0	0.0027
168	785	0.0154	231.0	0.0045

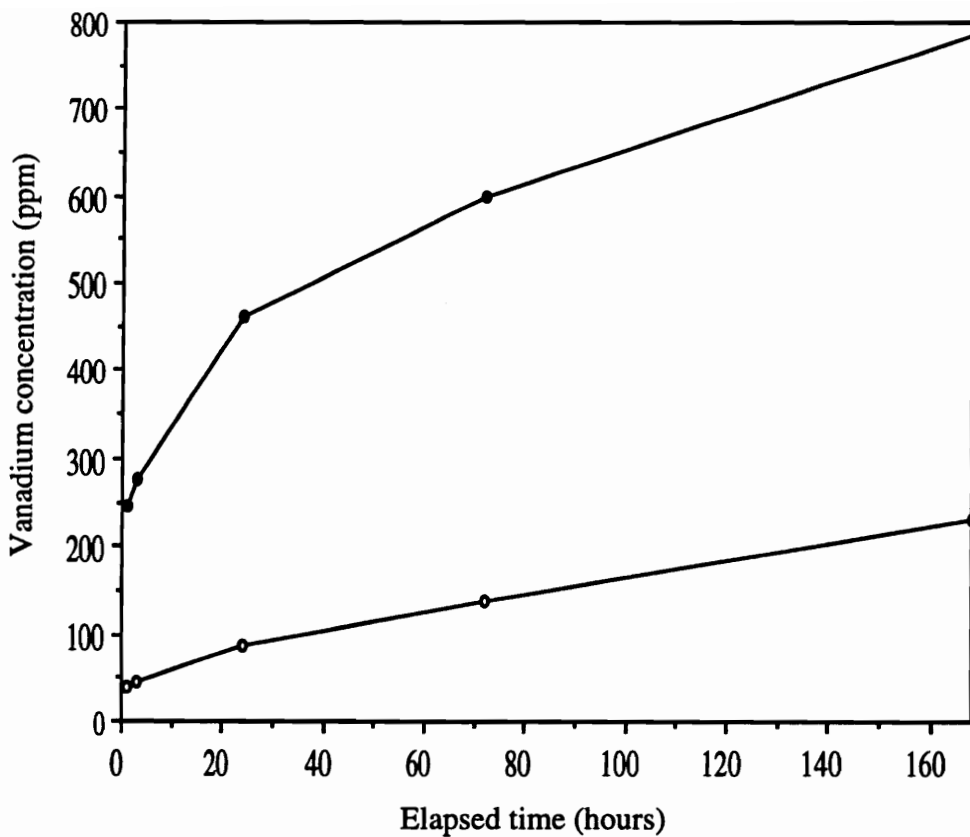


Figure 4. Concentration of vanadium versus time at 25°C.

Vanadium has in recent years found increasing applications in various fields and has been viewed as a strategic metal (Goldberg et al. 1992) for several reasons. First, vanadium is an additive that provides high strength and durability in steel, particularly in high-strength low-alloy steels used in the manufacture of gas and oil pipelines, automotive components, engineering structural steels and rails and in the aircraft industry. Secondly, minable resources of ores containing vanadium are unevenly distributed. They are confined to less than 10 countries, three of which (South Africa, the Soviet Union, and China), have more than 97 percent of the world total. Finally, vanadium is an important element because it cannot be substituted for technologically or economically.

The concentration of vanadium in petroleum coke slags can range up to 38 wt % as demonstrated in this study. It is primarily contained in V_2O_3 in reduced slags, and in V_2O_4 , calcium vanadate, and nickel vanadate in oxidized slags. Compared with vanadium ores, petroleum coke gasification slags have extremely high concentrations of vanadium, no mining costs, and none of the environmental impacts of mining. All of these factors suggest that recovery of vanadium is not only economically attractive, but also an environmentally sound strategy.

CONCLUSIONS

Petroleum coke slags are by-products of petroleum coke gasification. Comparison of the chemical composition of petroleum coke slag with average crustal rocks shows that vanadium is the most significant element in these slags from a perspective of resource reclamation. Long term dissolution experiments demonstrate that dissolved vanadium concentrations, although pH dependent, are extremely high at all pH conditions. The concentrations range from 1500 ppm to 5000 ppm with minimum solubilities around pH 6, and high concentrations both at low pH and high pH. The kinetics experiments show that the rate of vanadium dissolution is also quite high. In view of the strategic nature of vanadium and the fact that the concentration of vanadium in slags is almost two orders of

magnitude higher than the current mining grades, petroleum coke slags have great potential as an important resource for vanadium.

REFERENCES

- Goldberg, B.I, Hammerbeck, E.C.I., Labuschagne, L.S., and Rossouw, C., 1992, International strategic inventory summary report-vanadium: U.S. Geological Survey Circular 930-K, 45 p.
- Rimstidt, J.D., and Newcomb, 1992, Measurement of analysis of rate data: The rate of reaction of ferric iron with pyrite: *Geochimica et Cosmochimica Acta*, v. 57, p. 1919-1934.

Appendix I. Bulk chemical analyses of reduced petroleum coke slags

VIRGINIA TECH
ATTN: JUN LU

TSL/ASSAYERS Laboratories

1270 FEWSTER DRIVE, UNIT 3 MISSISSAUGA, ONTARIO L4W-1M4
PHONE #: (416)625-1544 FAX #: (416)206-0513

REPORT No. : M3047
Page No. : 1 of 1
File No. : DC22MA
Date : DEC-18-1993

I.C.A.P. PLASMA SCAN
Aqua-Regia Digestion

SAMPLE #	Ag	As	B	Bi	Cd	Co	Cu	Mo	Mn	Pb	Sb	Sn	W	Zn
	ppm	ppm	ppm	ppm	ppm	ppm	ppm	ppm	ppm	ppm	ppm	ppm	ppm	ppm
01	450	2600	< 50	800	< 5	90	< 5	140	4500	< 5	200	< 50	< 50	< 5
02	470	3300	< 50	680	< 5	190	5	200	9999	< 5	400	< 50	< 50	< 5
03	530	3700	< 50	600	< 5	240	20	350	9999	25	530	< 50	< 50	< 5

A .5 gm sample is digested with 2 ml of 3:1 HCL/HNO3
at 95 C for 90 min and diluted to 10 ml with DI H2O
This method is partial for many oxide materials

TSL/93

SIGNED :

VIRGINIA TECH
ATTN: JUN LU

TSL/ASSAYERS Laboratories
1270 FEWSTER DRIVE, UNIT 3 MISSISSAUGA, ONTARIO L4W-1M1
PHONE #: (416)625-1544 FAX #: (416)206-0513

REPORT No. : M3047
Page No. : 1 of 1
File No. : DC21RA
Date : DEC-18-1993

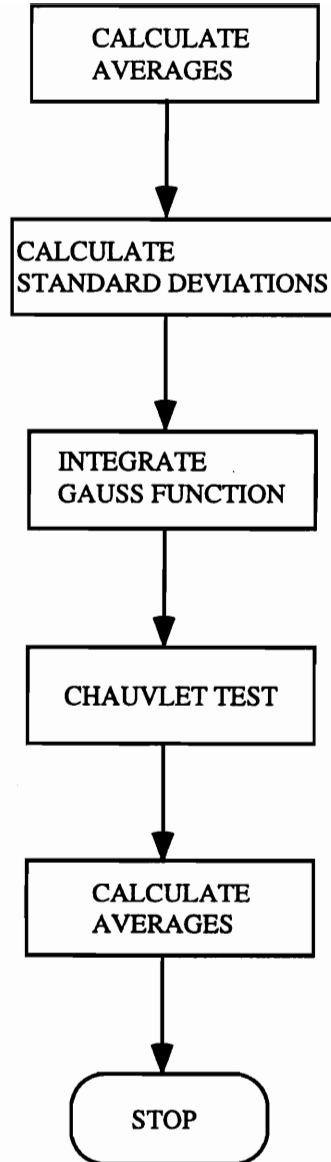
I.C.A.P. TOTAL OXIDE ANALYSIS
Lithium HeteroBorate Fusion

SAMPLE #	SiO2	Al2O3	Fe2O3	CaO	MgO	Na2O	K2O	TiO2	MnO	P2O5	Ba	Sr	Zr	Y	Sc	Nb	Be	Ni	Cr	V	LOI TOTAL	
	%	%	%	%	%	%	%	%	%	%	ppm	ppm	ppm	ppm	ppm	ppm	ppm	ppm	ppm	ppm	%	
01	16.76	8.64	4.56	7.76	1.88	3.96	0.08	1.28	0.08	0.08	480	80	920	80	80	120	68	4500	45360	99999	<0.04	45.00
02	14.28	10.32	3.36	7.36	0.92	3.96	0.08	1.08	0.04	0.08	560	160	200	96	80	120	40	26000	40000	99999	<0.04	41.36
03	16.04	5.72	3.80	6.92	0.80	5.56	0.08	0.68	0.04	0.08	680	120	240	72	40	120	60	50000	28200	99999	<0.04	39.72

SIGNED : 

TSL/93

Appendix II. Excel macro for data rejection



DATA REJECTION

*min=minimal value (wt%) set to bypass rejection process

min=5

=DIRECTORY("jl:probe:misc")

=OPEN("formula sheet")

=DIRECTORY("jl:probe:data0")

=SET.NAME("fl",FILES())

=FOR("Index",1, COLUMNS(fl))

= SET.NAME("next",INDEX(fl,1,Index))

= OPEN(next)

m=GET.DOCUMENT(10)

n=GET.DOCUMENT(12)

= IF(m=2)

= CLOSE()

= GOTO(another)

= END.IF()

*noa=No. of total analyses

noa=m

*****Add the sum column

na=n+1

= SELECT("r1c"&na)

= FORMULA("SUM")

= SELECT("r2c"&na)

= FORMULA("=SUM(RC3:RC"&n&")")

= SELECT("R2C"&na)

= COPY()

= SELECT("R3C"&na&":R"&m&"C"&na)

= PASTE()

*****Calculate averages

ma=m+1

= SELECT("r"&ma&"c2")

= FORMULA("AVERAGE")

= SELECT("r"&ma&"c3")

= FORMULA("=AVERAGE(r2c:r"&m&"c)")

= SELECT("r"&ma&"c3")

= COPY()

= SELECT("R"&ma&"C4:R"&ma&"C"&na)

```

= PASTE()
= SELECT("R"&ma&"C3:R"&ma&"C"&na)
= COPY()
= SELECT("R"&ma&"C3:R"&ma&"C"&na)
= PASTE.SPECIAL(3,1,FALSE,FALSE)
****Calculate standard deviation
ms=ma+1
= SELECT("r"&ms&"c2")
= FORMULA("STDEV")
= SELECT("r"&ms&"c3")
= FORMULA("=2*stdev(r2c:r"&m&"c)")
= SELECT("r"&ms&"c3")
= COPY()
= SELECT("R"&ms&"C4:R"&ms&"C"&na)
= PASTE()
= SELECT("R"&ms&"C3:R"&ms&"C"&na)
= COPY()
= SELECT("R"&ms&"C3:R"&ms&"C"&na)
= PASTE.SPECIAL(3,1,FALSE,FALSE)
****Loops for rejecting bad data
count=0
= FOR("a",3,n)
=   SELECT("r"&ma&"c"&a)
=   mean=ACTIVE.CELL()
=   SELECT("r"&ms&"c"&a)
=   stdd=ACTIVE.CELL()
=   IF(mean<min)
=     ****go to next column
=     GOTO(g)
=   END.IF()
= FOR("b",2,m)
=   SELECT("r"&b&"c"&a)
=   susp=GET.CELL(5)
=   IF(OR(susp>(mean+stdd),susp<(mean-stdd)))
=     t=ABS((susp-mean)/stdd)
=     ****integrate Gauss function
=     div=100
=     lim1=-(t)

```

```

lim2=t
q=(lim2-lim1)/(div-1)
sum=0
= FOR("i", 1, div-1)
    term=EXP(-0.5*(lim1+i*q)*(lim1+i*q))
    sum=sum+term
= NEXT()
total=0.5*q*(EXP(-lim1*lim1/2)+2*sum+EXP(-lim2*lim2/2))
prob=total*(1/SQRT(2*PI()))
out=(1-prob)*(m-1)
*****Chauvelet criterian
= IF(out>0.5)
=     SELECT("r"&b)
=     EDIT.DELETE(2)
    b=b-1
    m=m-1
    ma=ma-1
    ms=ms-1
    count=count+1
= END.IF()
= END.IF()
    *****h
= NEXT()
    *****G
= NEXT()
    *****Average after the data evaluation
ma2=ms+1
= SELECT("r"&ma2&"c2")
= FORMULA("AVERAGE")
= SELECT("r"&ma2&"c3")
= FORMULA("=AVERAGE(r2c:r"&m&"c)")
= COPY()
= SELECT("R"&ma2&"c3:r"&ma2&"C"&na)
= PASTE()
    *****Delete the sum column
= SELECT("c"&na)
= EDIT.DELETE(2)
= SELECT("R"&ma2+1&"c2")

```

```

= FORMULA("No. of rej.")
= SELECT("R"&ma2+1&"c3")
= FORMULA(noa-m)
= DIRECTORY("jl:probe:data")
= SAVE.AS(next&"/g")
*****Data transposition to formula sheets
= SELECT("r"&ma2&"c3:r"&ma2&"c"&n)
= COPY()
= ACTIVATE("formula sheet")
= SELECT("r4c6")
= PASTE.SPECIAL(3,1,FALSE,TRUE)
= SELECT("r4c7:r"&4+n-3&"c7")
= COPY()
= SELECT("r4c7:r"&4+n-3&"c7")
= PASTE.SPECIAL(3,1,FALSE,FALSE)
= DIRECTORY("jl:probe:total")
= SAVE.AS(next&"/t")
= CLOSE(TRUE)
= CLOSE(TRUE)
= DIRECTORY("jl:probe:misc")
= OPEN("formula sheet")
*****another
= DIRECTORY("jl:probe:data0")
= SET.NAME("fl",FILES())
=NEXT()
=CLOSE(FALSE)
=CLOSE(FALSE)
/=CLOSE(FALSE)
*****Register rejection results
=OPEN("jl:probe:misc:register")
=SELECT("r2c2")
=FORMULA("No. of Rej.")
=SELECT("r2c3")
=FORMULA("No. of Ana.")
=SELECT("r2c4")
=FORMULA("Rej. Rate")
count=0
=DIRECTORY("jl:probe:data")

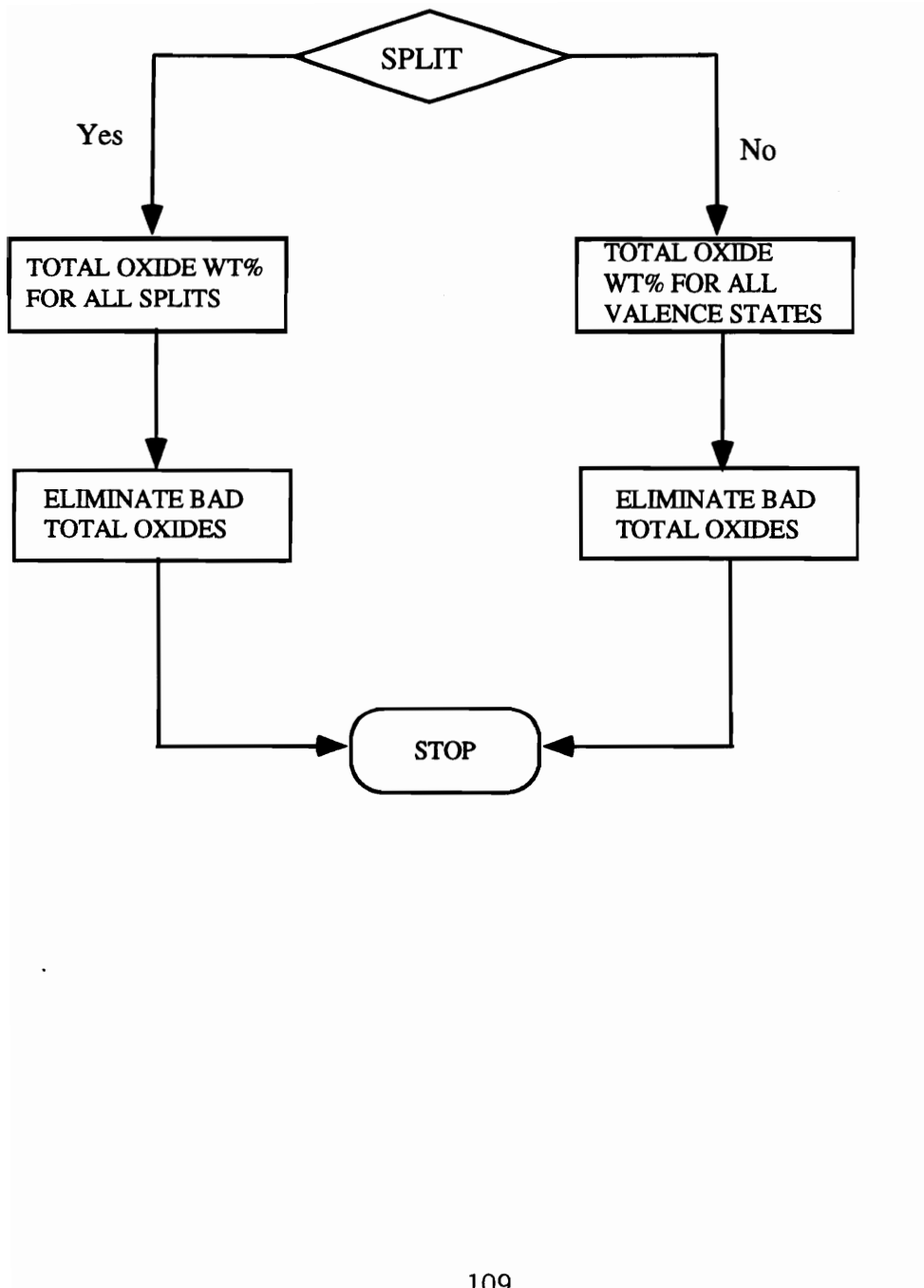
```

```

=SET.NAME("fl",FILES())
=FOR("Index",1, COLUMNS(fl))
= SET.NAME("next",INDEX(fl,1,Index))
= OPEN(next)
  m=GET.DOCUMENT(10)
  n=GET.DOCUMENT(12)
= SELECT("r"&m&"c3")
  x=GET.CELL(5)
  count=count+1
= ACTIVATE("register")
= SELECT("r2c1")
= SELECT(OFFSET(SELECTION(),count,0))
= FORMULA(next)
= SELECT(OFFSET(SELECTION(),0,1))
= FORMULA(x)
= SELECT(OFFSET(SELECTION(),0,1))
= FORMULA(x+m-5)
= SELECT(OFFSET(SELECTION(),0,1))
= FORMULA(x/(x+m-5)*100)
= ACTIVATE(next)
= CLOSE(FALSE)
= DIRECTORY("jl:probe:data")
= SET.NAME("fl",FILES())
=NEXT()
=SELECT("c4")
=FORMAT.NUMBER(0)
=CLOSE(TRUE)
=CLOSE(FALSE)
=RETURN()

```

Appendix III. Excel macro for transition element valence state calculation



OPTIMIZATION OF TOTAL OXIDE WEIGHT PERCENTAGE

```
*rn3=row no. of the last cation excluding H
rn3=25
*****first row containing cation
rn0=4
*****Specify variables for ion splitting
*If split, 1; if nonsplit, 0
split=0
*If valence known, tiew; if valence unknown, 0
ti0=tiew
v0=0
cr0=crew
mn0=0
fe0=0
*****Specify valence range
*if the valence is fixed, set the starting and ending valence the same
ti3=4
ti4=4
v3=3
v5=5
cr3=3
cr6=3
mn2=2
mn4=4
fe2=2
fe3=3
*****Open files
=DIRECTORY("jl:probe:total")
=SET.NAME("fl",FILES())
=FOR("Index",1, COLUMNS(fl))
= SET.NAME("next",INDEX(fl,1,Index))
= OPEN(next)
  rn0=4
  *****Look for Ti, V, Cr, Mn and Fe and record their locations
= FOR("a",4,rn3)
= SELECT("r"&a&"c1")
= IF(ACTIVE.CELL()="TI")
```

```

tir=GET.CELL(2)
tic=GET.CELL(3)
tiw=GET.CELL(5,OFFSET(ACTIVE.CELL(),0,6))
= ELSE.IF(ACTIVE.CELL()="V")
  vr=GET.CELL(2)
  vc=GET.CELL(3)
  vew=GET.CELL(5,OFFSET(ACTIVE.CELL(),0,6))
= ELSE.IF(ACTIVE.CELL()="CR")
  crr=GET.CELL(2)
  crc=GET.CELL(3)
  crew=GET.CELL(5,OFFSET(ACTIVE.CELL(),0,6))
= ELSE.IF(ACTIVE.CELL()="MN")
  mnr=GET.CELL(2)
  mnc=GET.CELL(3)
  mnew=GET.CELL(5,OFFSET(ACTIVE.CELL(),0,6))
= ELSE.IF(ACTIVE.CELL()="FE")
  fer=GET.CELL(2)
  fec=GET.CELL(3)
  feew=GET.CELL(5,OFFSET(ACTIVE.CELL(),0,6))
= END.IF()
= NEXT()
= SELECT("r"&m3+1&"c7")
ew=ACTIVE.CELL()
= IF(split=1)
= GOTO(ionsplit)
= END.IF()
*****titanium
= FOR("ti",ti3,ti4)
= IF(ti=3)
= SELECT("r"&tir&"c"&tic+2)
= FORMULA("2")
= SELECT("r"&tir&"c"&tic+3)
= FORMULA("3")
= ELSE.IF(ti=4)
= SELECT("r"&tir&"c"&tic+2)
= FORMULA("1")
= SELECT("r"&tir&"c"&tic+3)
= FORMULA("2")

```

```

= END.IF()
*****vanadium
= FOR("v",v3,v5)
= IF(v=3)
= SELECT("r"&vr&"c"&vc+2)
= FORMULA("2")
= SELECT("r"&vr&"c"&vc+3)
= FORMULA("3")
= ELSE.IF(v=4)
= SELECT("r"&vr&"c"&vc+2)
= FORMULA("1")
= SELECT("r"&vr&"c"&vc+3)
= FORMULA("2")
= ELSE.IF(v=5)
= SELECT("r"&vr&"c"&vc+2)
= FORMULA("2")
= SELECT("r"&vr&"c"&vc+3)
= FORMULA("5")
= END.IF()
*****chromium
= FOR("cr",cr3,cr6,3)
= IF(cr=3)
= SELECT("r"&cr&"c"&crc+2)
= FORMULA("2")
= SELECT("r"&cr&"c"&crc+3)
= FORMULA("3")
= ELSE.IF(cr=6)
= SELECT("r"&cr&"c"&crc+2)
= FORMULA("1")
= SELECT("r"&cr&"c"&crc+3)
= FORMULA("3")
= END.IF()
*****manganese
= FOR("mn",mn2,mn4)
= IF(mn=2)
= SELECT("r"&mnr&"c"&mnc+2)
= FORMULA("1")
= SELECT("r"&mnr&"c"&mnc+3)

```

```

=          FORMULA("1")
=      ELSE.IF(mn=3)
=          SELECT("r"&mnr&"c"&mnc+2)
=          FORMULA("2")
=          SELECT("r"&mnr&"c"&mnc+3)
=          FORMULA("3")
=      ELSE.IF(mn=4)
=          SELECT("r"&mnr&"c"&mnc+2)
=          FORMULA("1")
=          SELECT("r"&mnr&"c"&mnc+3)
=          FORMULA("2")
=      END.IF()
*****iron
=      FOR("fe",fe2,fe3)
=          IF(fe=2)
=              SELECT("r"&fer&"c"&fec+2)
=              FORMULA("1")
=              SELECT("r"&fer&"c"&fec+3)
=              FORMULA("1")
=          ELSE.IF(fe=3)
=              SELECT("r"&fer&"c"&fec+2)
=              FORMULA("2")
=              SELECT("r"&fer&"c"&fec+3)
=              FORMULA("3")
=          END.IF()
*****cycle
=          SELECT("r"&rn0&"c14")
=          FORMULA("V"&v&"Mn"&mn&"Fe"&fe)
=          SELECT("r"&rn3+1&"c8")
=          COPY()
=          SELECT("r"&rn0&"c15")
=          PASTE.SPECIAL(3,1,FALSE,FALSE)
=          rn0=rn0+1
=      NEXT()
=  NEXT()
=  NEXT()
=  NEXT()
=  NEXT()

```

```

= SELECT("r4c14:r"&m0&"c15")
= SORT(1,"r4c15",2)
= FOR("total",4,m0)
=   SELECT("r"&total&"c15")
=     x=GET.CELL(5)
=     IF(ABS(x-100)>3)
=       SELECT("r"&total&"c14:r"&total&"c15")
=       EDIT.DELETE(2)
=       m0=m0-1
=       total=total-1
=     END.IF()
= NEXT()
= GOTO(file)

```

*****ionsplit

*****titanium

```

= IF(ti3<>ti4)
= SELECT("r"&tir)
= COPY()
= SELECT("r"&m3+1&"c1")
= PASTE()
= FORMULA("TI3", "r"&tir&"c1")
= FORMULA(2, "r"&tir&"c3")
= FORMULA(3, "r"&tir&"c4")
= FORMULA("TI4", "r"&m3+1&"c1")
= FORMULA(1, "r"&m3+1&"c3")
= FORMULA(2, "r"&m3+1&"c4")
= SELECT("r"&m3+1&"c7")
= FORMULA("="&tiew&"-"&"r"&tir&"c7")
= END.IF()

```

*****vanadium

```

= IF(v3<>v5)
= SELECT("r"&vr)
= COPY()
= SELECT("r"&m3+2&"c1")
= PASTE()
= FORMULA("V4", "r"&vr&"c1")

```

```

= FORMULA(1, "r"&vr&"c3")
= FORMULA(2, "r"&vr&"c4")
= FORMULA("V5", "r"&m3+2&"c1")
= FORMULA(2, "r"&m3+2&"c3")
= FORMULA(5, "r"&m3+2&"c4")
= SELECT("r"&m3+2&"c7")
= FORMULA("=&vew&-"&"r"&vr&"c7")
= END.IF()

```

*****chromium

```

= IF(cr3<>cr6)
= SELECT("r"&cr)
= COPY()
= SELECT("r"&m3+3&"c1")
= PASTE()
= FORMULA("CR3", "r"&cr&"c1")
= FORMULA(2, "r"&cr&"c3")
= FORMULA(3, "r"&cr&"c4")
= FORMULA("CR6", "r"&m3+3&"c1")
= FORMULA(1, "r"&m3+3&"c3")
= FORMULA(3, "r"&m3&"c4")
= SELECT("r"&m3+3&"c7")
= FORMULA("=&crew&-"&"r"&cr&"c7")
= END.IF()

```

*****manganese

```

= IF(mn2<>mn4)
= SELECT("r"&mnr)
= COPY()
= SELECT("r"&m3+4&"c1")
= PASTE()
= FORMULA("MN3", "r"&mnr&"c1")
= FORMULA(2, "r"&mnr&"c3")
= FORMULA(3, "r"&mnr&"c4")
= FORMULA("MN4", "r"&m3+4&"c1")
= FORMULA(1, "r"&m3+4&"c3")
= FORMULA(2, "r"&m3+4&"c4")
= SELECT("r"&m3+4&"c7")

```

```
= FORMULA("=&mnew& "-"&r"&mnr&"c7")
= END.IF()
```

```
*****iron
```

```
= IF(fe2<>fe3)
= SELECT("r"&fer)
= COPY()
= SELECT("r"&rn3+5&"c1")
= PASTE()
= FORMULA("FE2", "r"&fer&"c1")
= FORMULA(1, "r"&fer&"c3")
= FORMULA(1, "r"&fer&"c4")
= FORMULA("FE3", "r"&rn3+5&"c1")
= FORMULA(2, "r"&rn3+5&"c3")
= FORMULA(3, "r"&rn3+5&"c4")
= SELECT("r"&rn3+5&"c7")
= FORMULA("=&few& "-"&r"&fer&"c7")
= END.IF()
```

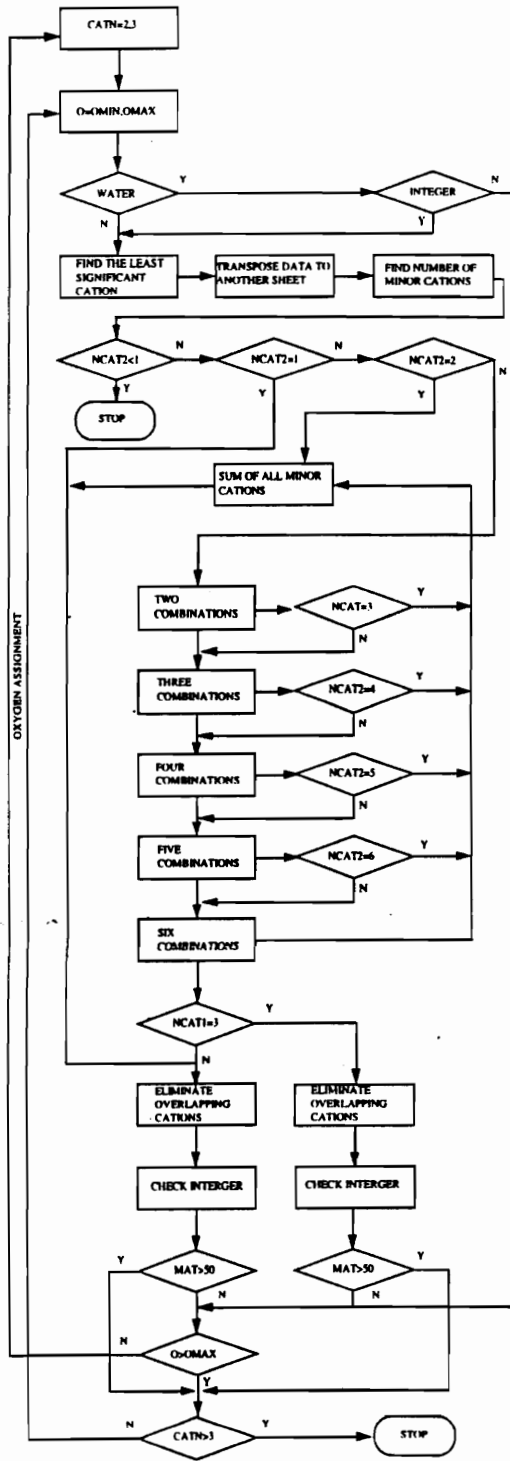
```
= FOR("ti",ti0,tiew)
=   FORMULA(ti,"r"&tir&"c7")
=   FOR("v",v0,vew)
=     FORMULA(v,"r"&vr&"c7")
=     FOR("cr",cr0,crew)
=       FORMULA(cr,"r"&crr&"c7")
=       FOR("mn",mn0,mnew)
=         FORMULA(mn,"r"&mnr&"c7")
=         FOR("fe",fe0,feew)
=           FORMULA(fe,"r"&fer&"c7")
=           SELECT("r"&rn3+8&"c8")
=           x=GET.CELL(5)
=           IF(ABS(x-100)<3)
=             SELECT("r"&rn0&"c14")
=             tival=ROUND(ti,2)
=             vval=ROUND(v,2)
=             crval=ROUND(cr,2)
=             mnval=ROUND(mn,2)
=             feval=ROUND(fe,2)
```

```

=          FORMULA("Ti"&tival&"V"&vval&"Cr"&crval&"Mn"&mnval&"Fe"
=          FORMULA(x,"r"&m0&"c15")
          m0=m0+1
=          END.IF()
=          NEXT()
=          NEXT()
=          NEXT()
=          NEXT()
=          NEXT()
=          NEXT()
          *****file
=          SELECT("c14")
=          COLUMN.WIDTH(15)
=          CLOSE(TRUE)
=          DIRECTORY("jl:probe:total")
=          SET.NAME("fl",FILES())
=NEXT()
=RETURN()

```

Appendix IV. Excel macro for chemical formula deviation



```

CHEMICAL FORMULA DERIVATION
=ECHO(FALSE)
time1=NOW()
=DIRECTORY("jl:probe:total")
=SET.NAME("fl",FILES())
=FOR("Index",1, COLUMNS(fl))
=SET.NAME("next",INDEX(fl,1,Index))
=OPEN(next)
=SELECT("r27c2")
*no. of major cations
catn1=GET.CELL(5)
=SELECT("r28c2")
*no. of major cations
catn2=GET.CELL(5)
=SELECT("r29c2")
*omin=lower limit of no. of oxygen
omin=GET.CELL(5)
=SELECT("r30c2")
*omax=higher limit of no. of oxygen
omax=GET.CELL(5)
=NEW(1)
=SAVE.AS("jl:probe:formula:"&next&"/")
=ACTIVATE(next)
*count1=counter for no. of offset
count1=0
*count2=counter for no. of matchments for major2
count2=0
*count3=counter for no. of matchments for major3
count3=0
*r3=row no. of the last cation excluding H
r3=25
*min=least significant cation taken into account
min=0.005
*fa=tolarence for integers
fa=0.11
*mat=no. of matches needed
mat=100
*****loop for major cation assignments

```

```

****cation number
=FOR("catn",catn1,catn2)
  *ncat1=no. of major cations
  ncat1=catn
  ****oxygen number
=   FOR("o",omin,omax)
=   SELECT("R"&4&"C1:R"&m3-1&"c"&cn1)
=   SORT(1,"R"&4&"c"&cn1,2)
  *num=smallest number used for minor cations
  num=min*o/3
  sp=0
=   SELECT("r3c12")
=   FORMULA("="&o)
****assign aluminum to si site
=   FOR("si",4,catn+3)
=     SELECT("r"&si&"c1")
=     sic=GET.CELL(5)
=     IF(sic="SI")
=       sicr=GET.CELL(2)
=       SELECT("r"&si&"c13")
=       siv=GET.CELL(5)
=       tem1=TRUNC(siv)
=       tem2=siv-tem1
=       IF(AND(siv>1,tem2<siv*0.05))
=         GOTO(water)
=       ELSE()
=         tem3=1-tem2
=         GOTO(aluminum)
=       END.IF()
=     END.IF()
=   NEXT()
=     GOTO(water)
****aluminum
=   FOR("al",4,m1)
=     SELECT("r"&al&"c1")
=     alc=GET.CELL(5)
=     IF(alc="AL")
=       alcr=GET.CELL(2)

```

```

=      SELECT("r"&alcr&"c13")
      alv=GET.CELL(5)
=      BREAK()
=      END.IF()
=      NEXT()
=      IF(alv>num)
          sp=1
=      SELECT("r"&alcr)
=      COPY()
=      SELECT("r19")
=      PASTE()
=      SELECT("r19c1")
=      FORMULA("A6")
=      SELECT("r19c7")
=      FORMULA(0)
=      SELECT("r4c13:r"&m3&"c13")
=      COPY()
=      SELECT("r4c14:r"&m3&"c14")
=      PASTE.SPECIAL(3,1,FALSE,FALSE)
=      SELECT("r19c14")
=      FORMULA(alv-tem3)
=      SELECT("r"&sicr&"c14")
=      IF(alv>tem3)
          FORMULA(tem1+1)
=      ELSE()
          FORMULA(siv+alv)
=      END.IF()
=      SELECT("r"&alcr&"c14")
=      FORMULA(0)
=      SELECT("R"&4&"C1:R"&m3-1&"c"&cn1+1)
=      SORT(1,"R"&4&"c"&cn1+1,2)
=      END.IF()
****water
****check if water is present
=      SELECT("r"&m3&"c13")
      water1=GET.CELL(5)
=      IF(water1=0)
=      GOTO(nowater)

```

```

= ELSE()
    water2=ROUND(water1,0)
= IF(ABS(water1-water2)>water1*fa)
= GOTO(oxygen)
= ELSE()
= GOTO(nowater)
= END.IF()
= END.IF()
*****nowater
*****Look for the 1st cell containing "minimum"
= FOR("a1", ncat1+4,m3)
= IF(sp=1)
= SELECT("r"&a1&"c"&cn1+1)
= ELSE()
= SELECT("r"&a1&"c"&cn1)
= END.IF()
= IF(ACTIVE.CELL()<num)
    *m1=row no. of the 1st minor cation accepted
    m1=GET.CELL(2)-1
    *ncat2=no. of minor cations
    ncat2=m1-ncat1-3
= IF(ncat2>7)
    ncat2=7
    m1=ncat2+ncat1+4
= END.IF()
= GOTO(transpose)
= END.IF()
= NEXT()
*****transpose
*****Transpose the data to another sheet
= SELECT("r"&4&"c1:r"&m1&"c1")
= COPY()
= ACTIVATE(next&"/")
= SELECT("R1C1")
= PASTE.SPECIAL(3,1,FALSE,TRUE)
= ACTIVATE(next)
= IF(sp=1)
= SELECT("r"&4&"c"&cn1+1&":r"&m1&"c"&cn1+1)

```

```

= ELSE()
= SELECT("r"&4&"c"&cn1&":r"&rn1&"c"&cn1)
= END.IF()
= COPY()
= ACTIVATE(next&"/")
= SELECT("R2C1")
= PASTE.SPECIAL(3,1,FALSE,TRUE)
****Loops for calculations
*n=no. of the 1st blank column
n=ncat1+ncat2+1
= IF(ncat2<1)
= GOTO(file)
= ELSE.IF(ncat2=1)
= GOTO(setup)
= ELSE.IF(ncat2=2)
= GOTO(minorsum)
= END.IF()
*****two combinations
= FOR("b1",ncat1+1,ncat1+ncat2-1)
= FOR("b2",b1+1,ncat1+ncat2)
= SELECT("r2c"&n)
= FORMULA("=r2c"&b1&"+r2c"&b2)
= SELECT("r1c"&b1)
= x1=GET.CELL(5)
= SELECT("r1c"&b2)
= x2=GET.CELL(5)
= SELECT("r1c"&n)
= FORMULA(x1&x2)
= n=n+1
= NEXT()
= NEXT()
= IF(ncat2=3)
= GOTO(minorsum)
= END.IF()
*****three combinations
= FOR("b1",ncat1+1,ncat1+ncat2-2)
= FOR("b2",b1+1,ncat1+ncat2-1)
= FOR("b3",b2+1,ncat1+ncat2)

```

```

=          SELECT("r2c"&n)
=          FORMULA("=r2c"&b1&"r2c"&b2&"r2c"&b3)
=          SELECT("r1c"&b1)
=          x1=GET.CELL(5)
=          SELECT("r1c"&b2)
=          x2=GET.CELL(5)
=          SELECT("r1c"&b3)
=          x3=GET.CELL(5)
=          SELECT("r1c"&n)
=          FORMULA(x1&x2&x3)
=          n=n+1
=          NEXT()
=          NEXT()
=          NEXT()
=          IF(ncat2=4)
=              GOTO(minorsum)
=          END.IF()
=          *****four combinations
=          FOR("b1",ncat1+1,ncat1+ncat2-3)
=              FOR("b2",b1+1,ncat1+ncat2-2)
=                  FOR("b3",b2+1,ncat1+ncat2-1)
=                      FOR("b4",b3+1,ncat1+ncat2)
=                          SELECT("r2c"&n)
=                          FORMULA("=r2c"&b1&"r2c"&b2&"r2c"&b3&"r2c"&b4)
=                          SELECT("r1c"&b1)
=                          x1=GET.CELL(5)
=                          SELECT("r1c"&b2)
=                          x2=GET.CELL(5)
=                          SELECT("r1c"&b3)
=                          x3=GET.CELL(5)
=                          SELECT("r1c"&b4)
=                          x4=GET.CELL(5)
=                          SELECT("r1c"&n)
=                          FORMULA(x1&x2&x3&x4)
=                          n=n+1
=                          NEXT()
=                      NEXT()
=                  NEXT()
=              NEXT()
=          NEXT()

```

```

=      NEXT()
=      IF(ncat2=5)
=          GOTO(minorsum)
=      END.IF()
*****five combinations
=      FOR("b1",ncat1+1,ncat1+ncat2-4)
=          FOR("b2",b1+1,ncat1+ncat2-3)
=              FOR("b3",b2+1,ncat1+ncat2-2)
=                  FOR("b4",b3+1,ncat1+ncat2-1)
=                      FOR("b5",b4+1,ncat1+ncat2)
=                          SELECT("r2c"&n)
=                          FORMULA("=r2c"&b1&"&r2c"&b2&"&r2c"&b3&"&r2c"&b4
=                          SELECT("r1c"&b1)
=                          x1=GET.CELL(5)
=                          SELECT("r1c"&b2)
=                          x2=GET.CELL(5)
=                          SELECT("r1c"&b3)
=                          x3=GET.CELL(5)
=                          SELECT("r1c"&b4)
=                          x4=GET.CELL(5)
=                          SELECT("r1c"&b5)
=                          x5=GET.CELL(5)
=                          SELECT("r1c"&n)
=                          FORMULA(x1&x2&x3&x4&x5)
=                          n=n+1
=                      NEXT()
=                  NEXT()
=              NEXT()
=          NEXT()
=      NEXT()
=      IF(ncat2=6)
=          GOTO(minorsum)
=      END.IF()
*****six combinations
=      FOR("b1",ncat1+1,ncat1+ncat2-5)
=          FOR("b2",b1+1,ncat1+ncat2-4)
=              FOR("b3",b2+1,ncat1+ncat2-3)
=                  FOR("b4",b3+1,ncat1+ncat2-2)

```

```

=          FOR("b5",b4+1,ncat1+ncat2-1)
=          FOR("b6",b5+1,ncat1+ncat2)
=              SELECT("r2c"&n)
=              FORMULA("=r2c"&b1&"r2c"&b2&"r2c"&b3&"r2c"&
=              SELECT("r1c"&b1)
=              x1=GET.CELL(5)
=              SELECT("r1c"&b2)
=              x2=GET.CELL(5)
=              SELECT("r1c"&b3)
=              x3=GET.CELL(5)
=              SELECT("r1c"&b4)
=              x4=GET.CELL(5)
=              SELECT("r1c"&b5)
=              x5=GET.CELL(5)
=              SELECT("r1c"&b6)
=              x6=GET.CELL(5)
=              SELECT("r1c"&n)
=              FORMULA(x1&x2&x3&x4&x5&x6)
=              n=n+1
=          NEXT()
=      NEXT()
=  NEXT()
=  NEXT()
=  NEXT()
=  NEXT()
=  NEXT()
=  IF(ncat2=7)
=      GOTO(minorsum)
=  END.IF()
*****minorsum
    chminor=""
    vaminor=0
=  FOR("t",ncat1+1,ncat1+ncat2)
=      SELECT("r1c"&t)
=      chv=GET.CELL(5)
=      chminor=chminor&chv
=      SELECT("r2c"&t)
=      vav=GET.CELL(5)
=      vaminor=vaminor+vav

```

```

=      NEXT()
=      SELECT("r1c"&n)
=      FORMULA(chminor)
=      SELECT("r2c"&n)
=      FORMULA(vaminor)
=      *****setup
=      n=n+1
=      SELECT("r1c"&n)
=      FORMULA("NO")
=      SELECT("r2c"&n)
=      FORMULA(0)
=      IF(ncat1=3)
=      GOTO(major3)
=      END.IF()
=      SELECT("r1c1")
ch1=GET.CELL(5)
=      SELECT("r2c1")
v1=GET.CELL(5)
=      SELECT("r1c2")
ch2=GET.CELL(5)
=      SELECT("r2c2")
v2=GET.CELL(5)
=      FOR("a",ncat1+1,n)
=      SELECT("r1c"&a)
cha=GET.CELL(5)
=      SELECT("r2c"&a)
va=GET.CELL(5)
=      FOR("b",ncat1+1,n)
=      SELECT("r1c"&b)
chb=GET.CELL(5)
=      SELECT("r2c"&b)
vb=GET.CELL(5)
=      *****loop for eliminating ion overlapping
=      IF(a=b)
=      GOTO(minor1)
=      END.IF()
=      ch=cha&chb
=      y=LEN(ch)

```

```

=          IF(y<ncat2*2)
=            GOTO(minor1)
=          END.IF()
=          x=y-2
=          IF(y>=ncat2*2)
=            FOR("e",1,x)
=              che=MID(ch,e,2)
=              g=e+2
=            FOR("f",g,y)
=              IF(MID(ch,f,2)=che)
=                GOTO(minor1)
=              END.IF()
=            f=f+1
=          NEXT()
=          e=e+1
=        NEXT()
=      END.IF()
=    FOR("h",1,y)
=      IF(AND(MID(ch,h,2)="NO",y<ncat2*2+2))
=        GOTO(minor1)
=      END.IF()
=      h=h+1
=    NEXT()
=    *****check if all assignments have integer values
=    va1=v1+va
=    vb2=v2+vb
=    s1=ROUND(va1,0)
=    s2=ROUND(vb2,0)
=    IF(AND(ABS(va1-s1)<va1*fa,ABS(vb2-s2)<vb2*fa))
=      cha1=ch1&cha
=      chb2=ch2&chb
=      count1=count1+1
=    SELECT("R5c1")
=    SELECT(OFFSET(SELECTION(),count1,0))
=    FORMULA(cha1)
=    SELECT(OFFSET(SELECTION(),0,1))
=    FORMULA(s1)
=    SELECT(OFFSET(SELECTION(),0,1))

```

```

=          FORMULA(chb2)
=          SELECT(OFFSET(SELECTION(),0,1))
=          FORMULA(s2)
=          IF(water1>0)
=              on=o-water2
=              SELECT(OFFSET(SELECTION(),0,1))
=              FORMULA("O")
=              SELECT(OFFSET(SELECTION(),0,1))
=              FORMULA(on)
=              SELECT(OFFSET(SELECTION(),0,1))
=              FORMULA("OH")
=              SELECT(OFFSET(SELECTION(),0,1))
=              FORMULA(o)
=          ELSE()
=              SELECT(OFFSET(SELECTION(),0,1))
=              FORMULA("O")
=              SELECT(OFFSET(SELECTION(),0,1))
=              FORMULA(o)
=          END.IF()
=              *****Counting no. of matches made
=                  count2=count2+1
=          IF(count2>mat)
=              GOTO(major)
=          END.IF()
=          END.IF()
=          *****minor1
=          NEXT()
=          NEXT()
=          GOTO(oxygen)
=          *****major3
=          SELECT("r1c1")
=          ch1=GET.CELL(5)
=          SELECT("r2c1")
=          v1=GET.CELL(5)
=          SELECT("r1c2")
=          ch2=GET.CELL(5)
=          SELECT("r2c2")
=          v2=GET.CELL(5)

```

```

=      SELECT("r1c3")
ch3=GET.CELL(5)
=      SELECT("r2c3")
v3=GET.CELL(5)
=      FOR("a",ncat1+1,n)
=          SELECT("r1c"&a)
cha=GET.CELL(5)
=          SELECT("r2c"&a)
va=GET.CELL(5)
=      FOR("b",ncat1+1,n)
=          SELECT("r1c"&b)
chb=GET.CELL(5)
=          SELECT("r2c"&b)
vb=GET.CELL(5)
=      FOR("d",ncat1+1,n)
=          SELECT("r1c"&d)
chd=GET.CELL(5)
=          SELECT("r2c"&d)
vd=GET.CELL(5)
*****loop for eliminating ion overlapping
=      IF(OR(a=b, a=d, b=d))
=          GOTO(minor2)
=      END.IF()
ch=cha&chb&chd
y=LEN(ch)
=      IF(y<ncat2*2)
=          GOTO(minor2)
=      END.IF()
x=y-2
=      IF(y>=ncat2*2)
=      FOR("e",1,x)
che=MID(ch,e,2)
g=e+2
=      FOR("f",g,y)
=          IF(MID(ch,f,2)=che)
=          GOTO(minor2)
=      END.IF()
f=f+1

```

```

=          NEXT()
          e=e+1
=          NEXT()
=          END.IF()
=          FOR("h",1,y)
=              IF(AND(MID(ch,h,2)="NO",y<>ncat2*2+2))
=                  GOTO(minor2)
=              END.IF()
=                  h=h+1
=          NEXT()
          *****check if all assignments have integer values
          va1=v1+va
          vb2=v2+vb
          vd3=v3+vd
          s1=ROUND(va1,0)
          s2=ROUND(vb2,0)
          s3=ROUND(vd3,0)
=          IF(AND(ABS(va1-s1)<va1*fa,ABS(vb2-s2)<vb2*fa,ABS(vd3-s3)<vd
              cha1=ch1&cha
              chb2=ch2&chb
              chd3=ch3&chd
              count1=count1+1
=          SELECT("r5c1")
=          SELECT(OFFSET(SELECTION(),count1,0))
=          SELECT("R5c1")
=          SELECT(OFFSET(SELECTION(),count1,0))
=          FORMULA(cha1)
=          SELECT(OFFSET(SELECTION(),0,1))
=          FORMULA(s1)
=          SELECT(OFFSET(SELECTION(),0,1))
=          FORMULA(chb2)
=          SELECT(OFFSET(SELECTION(),0,1))
=          FORMULA(s2)
=          SELECT(OFFSET(SELECTION(),0,1))
=          FORMULA(chd3)
=          SELECT(OFFSET(SELECTION(),0,1))
=          FORMULA(s3)
=          IF(water1>0)

```

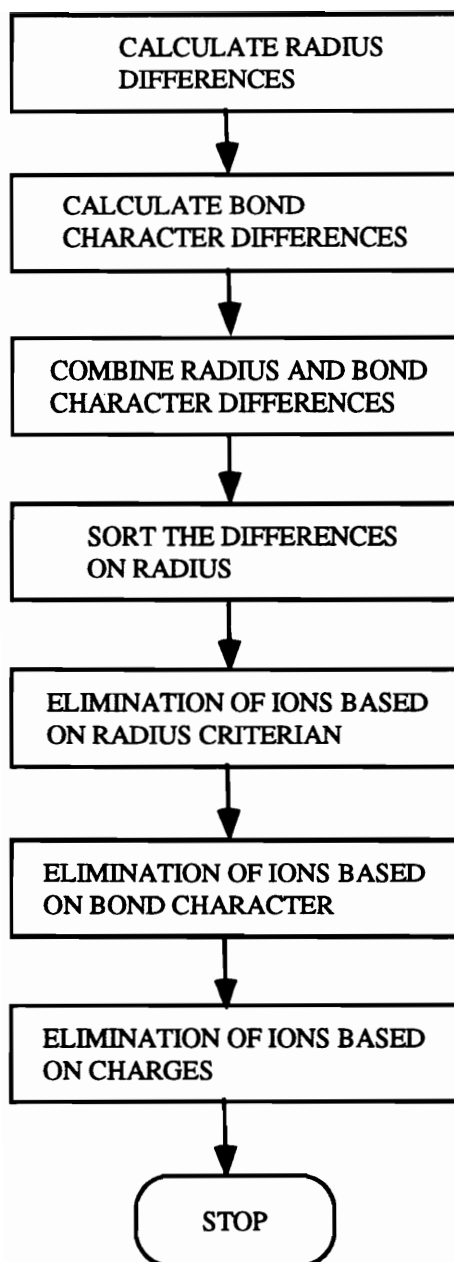
```

on=o-water2
= SELECT(OFFSET(SELECTION(),0,1))
= FORMULA("O")
= SELECT(OFFSET(SELECTION(),0,1))
= FORMULA(on)
= SELECT(OFFSET(SELECTION(),0,1))
= FORMULA("OH")
= SELECT(OFFSET(SELECTION(),0,1))
= FORMULA(o)
= ELSE()
= SELECT(OFFSET(SELECTION(),0,1))
= FORMULA("O")
= SELECT(OFFSET(SELECTION(),0,1))
= FORMULA(o)
= END.IF()
****Counting no. of matches made
count3=count3+1
= IF(count3>mat)
= GOTO(file)
= END.IF()
= END.IF()
****minor2
= NEXT()
= NEXT()
= NEXT()
****oxygen
= ACTIVATE(next)
= NEXT()
****major
= ACTIVATE(next)
= NEXT()
****file
= ACTIVATE(next&"/")
= CLOSE(TRUE)
= CLOSE(FALSE)
= DIRECTORY("jl:probe:total")
= SET.NAME("fl",FILES())
=NEXT()

```

```
time2=NOW()
time=time2-time1
h=HOUR(time)
m=MINUTE(time)
s=SECOND(time)
time=h&" "&m&" "&s
=CLOSE(FALSE)
=RETURN()
```

Appendix V. Excel macro for ion substitution priority



ION SUBSTITUTION PRIOTITY

*****Calculating the radius and bond character differences

```
=ECHO(FALSE)
=DIRECTORY("jl:probe:ionsub0")
=SET.NAME("fl",FILES())
=FOR("Index",1, COLUMNS(fl))
=SET.NAME("next",INDEX(fl,1,Index))
=OPEN(next)
m=GET.DOCUMENT(10)
n=GET.DOCUMENT(12)
=FOR("a",3,n)
= SELECT("r1c"&a)
  x=GET.CELL(5)
= FOR("b",3,m)
= SELECT("r"&b&"c1")
  y=GET.CELL(5)
= FORMULA("=abs("&x&"-"&y&")/((("&x&"+"&y&")/2)*100","r"&b&"c"&a)
= NEXT()
=NEXT()
=CLOSE(TRUE)
=DIRECTORY("jl:probe:ionsub0")
=SET.NAME("fl",FILES())
=NEXT()
=RETURN()
```

*****Sorting the radius and bond differences by ions

```
=DIRECTORY("jl:probe:ionsub0")
=OPEN("radi")
=OPEN("bond")
m=GET.DOCUMENT(10)
n=GET.DOCUMENT(12)
*****copy ion names to a worksheet
=DIRECTORY("jl:probe:ionsub1")
=OPEN("sub/s")
=ACTIVATE("radi")
=SELECT("c2")
=COPY()
=ACTIVATE("sub/s")
=FOR("a",1,3*(n-2)-2,3)
```

```

= SELECT("c"&a)
= PASTE()
=NEXT()
****copy ion radius to a worksheet
nv=0
=ACTIVATE("radi")
=FOR("b",3,n)
= SELECT("c"&b)
= COPY()
= ACTIVATE("sub/s")
  nv=nv+3
= SELECT("c"&nv-1)
= PASTE()
= ACTIVATE("radi")
=NEXT()
****copy ion bond character to a worksheet
nv=0
=ACTIVATE("bond")
=FOR("b",3,n)
= SELECT("c"&b)
= COPY()
= ACTIVATE("sub/s")
  nv=nv+3
= SELECT("c"&nv)
= PASTE()
= ACTIVATE("bond")
=NEXT()
=ACTIVATE("sub/s")
=SAVE()
****sort the differences on radius
m=GET.DOCUMENT(10)
n=GET.DOCUMENT(12)
=FOR("d",1,n,3)
= SELECT("r3c"&d&":r"&m&"c"&d+2)
= SORT(1,"r3c"&d+1,1)
=NEXT()
****format the sheet
=PAGE.SETUP("&F","Page &P",0.75,0.75,1,1,FALSE,TRUE,FALSE,FALSE,2,,100,1,

```

```

=SELECT("r1C1:r"&m&"c"&n)
=FORMAT.NUMBER("##0.00")
=ALIGNMENT(2)
=COLUMN.WIDTH(6)
=CLOSE(TRUE)
=CLOSE(FALSE)
=CLOSE(FALSE)
  =RETURN()
****Eliminate ions based on preset radius and bond character criteria
*rv=maximum radius difference allowed
rv=40
*rv=maximum bond difference allowed
bv=60
=DIRECTORY("jl:probe:ionsub1")
=OPEN("sub/s")
m=GET.DOCUMENT(10)
n=GET.DOCUMENT(12)
=FOR("a",2,n,3)
=  SELECT("r2c"&a)
  chion=GET.CELL(5)
  ch1=RIGHT(chion,2)
  ch=MID(chion,4,1)
  ch=VALUE(ch)
  mv=m
  count=0
  ****eliminate based on radius
=  FOR("b",3,mv)
=    SELECT("r"&b&"c"&a)
    v=ACTIVE.CELL()
=    IF(v>rv)
=      SELECT("r"&b&"c"&a-1&":r"&mv&"c"&a+1)
=      EDIT.DELETE(2)
      mv=count+2
=    END.IF()
    count=count+1
=  NEXT()
  ****eliminate based on coordination
=  FOR("b",3,mv)

```

```

= SELECT("r"&b&"c"&a-1)
ch2=GET.CELL(5)
ch2=RIGHT(ch2,2)
= IF(ch2<>ch1)
= SELECT("r"&b&"c"&a-1&":r"&b&"c"&a+1)
= EDIT.DELETE(2)
b=b-1
mv=mv-1
= END.IF()
= NEXT()
****eliminate based on bond character
= FOR("b",3,mv)
= SELECT("r"&b&"c"&a+1)
v=ACTIVE.CELL()
= IF(v>bv)
= SELECT("r"&b&"c"&a-1&":r"&b&"c"&a+1)
= EDIT.DELETE(2)
b=b-1
mv=mv-1
= END.IF()
= NEXT()
****eliminate based on charge balance
= FOR("b",3,mv)
= SELECT("r"&b&"c"&a-1)
ch3=GET.CELL(5)
ch3=MID(ch3,4,1)
ch3=VALUE(ch3)
char=ABS(ch-ch3)
= IF(char>1)
= SELECT("r"&b&"c"&a-1&":r"&b&"c"&a+1)
= EDIT.DELETE(2)
b=b-1
mv=mv-1
= END.IF()
= NEXT()
=NEXT()
=SAVE.AS("sub/e")
=CLOSE()

```

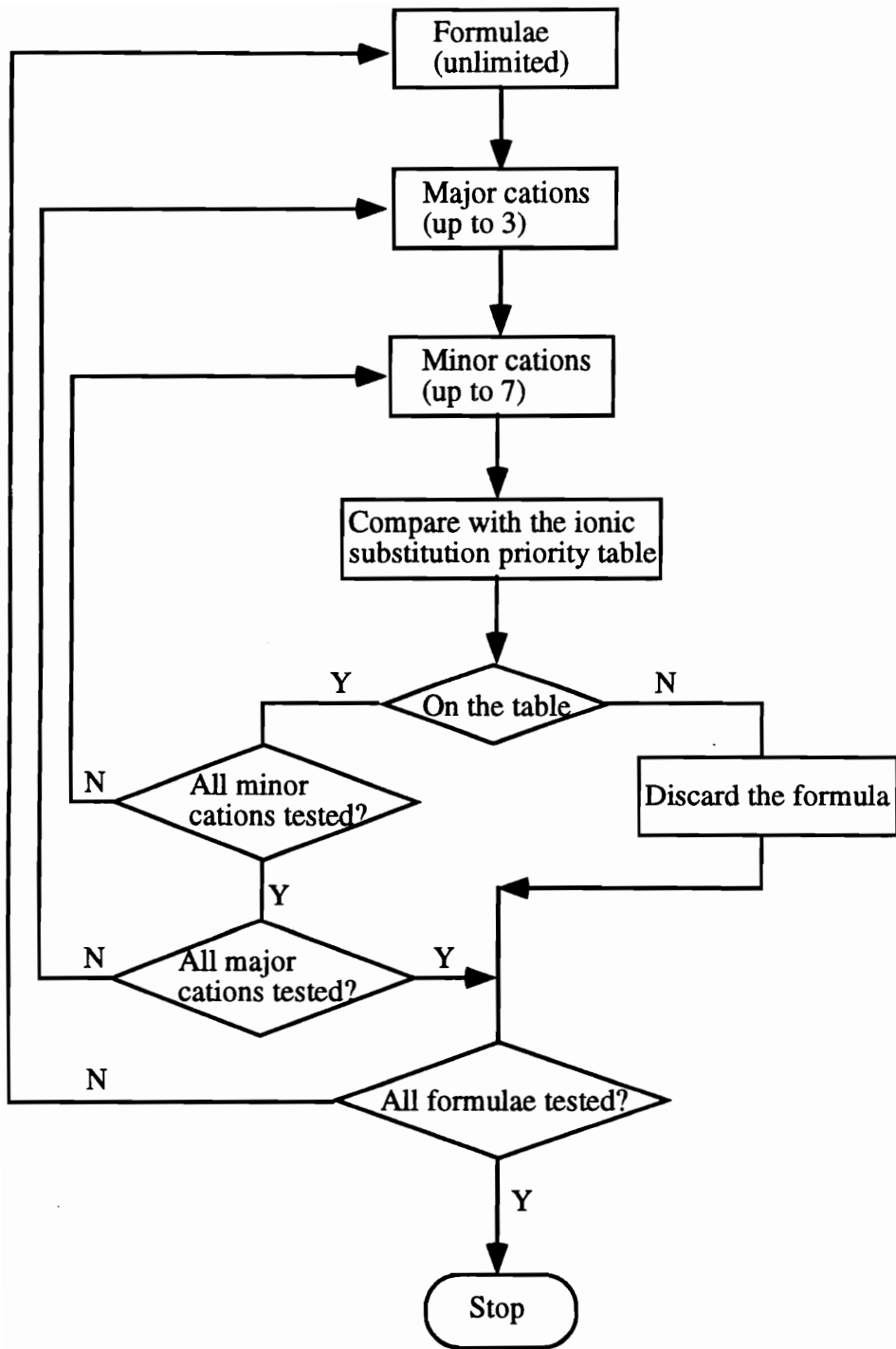
```

=RETURN()
*****Priority list
=DIRECTORY("jl:probe:ionsub1")
=OPEN("sub/e")
*****delete value columns
m=GET.DOCUMENT(10)
n=GET.DOCUMENT(12)
=FOR("a",2,n,3)
=  SELECT("c"&a&":c"&a+1)
=  EDIT.DELETE(1)
    a=a-2
    n=n-2
=NEXT()
*****delete single ion columns
=FOR("a",1,n-1)
=  SELECT("r4c"&a)
=  IF(ISBLANK(ACTIVE.CELL()))
=  SELECT("c"&a)
=  EDIT.DELETE()
    a=a-1
    n=n-1
=  END.IF()
=NEXT()
=SAVE.AS("list")
*****input coordination titles
m=GET.DOCUMENT(10)
n=GET.DOCUMENT(12)
=FOR("a",1,n)
=  SELECT("r3c"&a)
    temp=GET.CELL(5)
    temp1=MID(temp,6,2)
=  SELECT("r2c"&a)
=  FORMULA(temp1)
=NEXT()
=SELECT("r2")
=FORMAT.NUMBER(0)
*****delete parentheses
=FOR("a",1,n)

```

```
= FOR("b",3,m)
=   SELECT("r"&b&"c"&a)
   temp=GET.CELL(5)
   temp1=RIGHT(temp,4)
=   IF(ISBLANK(ACTIVE.CELL()),GOTO(another))
=   FORMULA.REPLACE(temp1,"",2,2,TRUE,TRUE)
= NEXT()
*another
=NEXT()
=CLOSE(TRUE)
=CLOSE(FALSE)
=RETURN()
```

Appendix VI. Excel macro for a short list of chemical formulae



A SHORT LIST OF CHEMICAL FORMULAE

```
=ECHO(FALSE)
time1=NOW()
=OPEN("jl:probe:misc:list")
m1=GET.DOCUMENT(10)
n1=GET.DOCUMENT(12)
=DIRECTORY("jl:probe:formula")
=SET.NAME("fl",FILES())
=FOR("Index",1,COLUMNS(fl))
= SET.NAME("next",INDEX(fl,1,Index))
= OPEN(next)
=DIRECTORY("jl:probe:final")
= SAVE.AS(next&"/")
m2=GET.DOCUMENT(10)
*****replace "NO" with ""
= FOR("a",6,m2)
= SELECT("R"&a)
bn=COUNTA(SELECTION())
= FOR("b",1,bn,2)
= SELECT("R"&a&"C"&b)
x=GET.CELL(5)
x=RIGHT(x,2)
= IF(x="NO")
= FORMULA.REPLACE("NO","",2,1,FALSE,FALSE)
= GOTO(major)
= END.IF()
= NEXT()
= NEXT()
*major
*****look for major cations
= SELECT("R4C6")
water1=GET.CELL(5)
= FOR("a",6,m2)
count0=0
count=0
= SELECT("R"&a)
catn=COUNTA(SELECTION())
catn=catn/2-1
```

```

=      IF(water1 <> 0, catn = catn / 2 - 2)
sn = catn * 2 + 2
=      IF(water1 <> 0, sn = catn * 2 + 4)
cn = 2 * catn - 1
=      FOR("b", 1, cn, 2)
=          IF(catn = 2)
=              SELECT("R4C" & b + 1)
=          ELSE()
=              SELECT("R5C" & b + 1)
=          END.IF()
x = GET.CELL(5)
=      SELECT("R" & a & "C" & b)
ch1 = GET.CELL(5)
y = LEN(ch1)
count0 = count0 + y
=      IF(y = 2, GOTO(site))
ch1x = LEFT(ch1, 2)
=      IF(ch1x = "A6")
=          ch1x = "AL"
=      END.IF()
*****look for minor cations
=      FOR("d", 3, y - 1, 2)
=          cha = MID(ch1, d, 2)
=          *****look for sub. list
=          ACTIVATE("list")
=          FOR("e", 1, n1)
=              SELECT("R2c" & e)
=              z = GET.CELL(5)
=              SELECT("R3c" & e)
=              ch2 = GET.CELL(5)
=              ch2 = LEFT(ch2, 2)
=              IF(AND(ch2 = ch1x, z = x))
=                  FOR("f", 4, m1)
=                      SELECT("R" & f & "c" & e)
=                      IF(ISBLANK(ACTIVE.CELL()), GOTO(delete))
=                          count = count + 1
=                          chb = GET.CELL(5)
=                          chb = LEFT(chb, 2)

```

```

=          IF(chb=cha,GOTO(trace))
=          NEXT()
=          *****delete
=          ACTIVATE(next&"/")
=          SELECT("r"&a)
=          EDIT.DELETE(2)
=          a=a-1
=          m2=m2-1
=          GOTO(formula)
=          END.IF()
=          NEXT()
=          *****trace
=          ACTIVATE(next&"/")
=          NEXT()
=          *****site
=          NEXT()
=          ACTIVATE(next&"/")
=          SELECT("r"&a&"c"&sn+1)
=          FORMULA(count/(count0/2-catn))
=          *****formula
=NEXT()
=          *****formula report
=ACTIVATE(next&"/")
=SAVE()
=          m=GET.DOCUMENT(10)
=          FOR("a",6,m)
=          SELECT("r"&a&"c5")
=          o=GET.CELL(5)
=          sn=GET.CELL(3)
=          IF(o<>"O")
=          SELECT("r"&a&"c7")
=          o=GET.CELL(5)
=          sn=GET.CELL(3)
=          END.IF()
=          IF(water1<>0,sn=sn+2)
=          FOR("b",1,sn,2)
=          SELECT("r"&a&"c"&b)
=          ion=GET.CELL(5)

```

```

        cl=LEN(ion)
=       IF(OR(cl>2,ion="OH"))
=         FORMULA("&ion&")
=       END.IF()
=     NEXT()
add=""
=     FOR("b",1,sn+1)
=       SELECT("r"&a&"c"&b)
=       ion=GET.CELL(5)
=       IF(ion<>1)
=         add=add&ion
=       END.IF()
=     NEXT()
=     SELECT("r"&a&"c1")
=     FORMULA(add)
=     SELECT("r"&a&"c"&sn+2)
=     COPY()
=     SELECT("r"&a&"c2")
=     PASTE()
=     SELECT("r"&a&"c3:r"&a&"c14")
=     CLEAR()
=   NEXT()
=   SELECT("r6c1:r"&m&"c2")
=   SORT(1,"r6c2",1)
=   SELECT("r1:r2")
=   EDIT.DELETE()
=   SELECT("r1c1")
=   FORMULA("These are the possible formulae for "&next&" phase")
=   CLOSE(TRUE)
=   DIRECTORY("jl:probe:formula")
=   SET.NAME("fl",FILES())
=NEXT()
time2=NOW()
time=time2-time1
h=HOUR(time)
m=MINUTE(time)
s=SECOND(time)
time=h&" "&m&" "&s

```

=CLOSE(FALSE)
=RETURN()

VITA

Jun Lu was born in Yinshan, Hubei Province, China on August 13, 1957. Most of his childhood was spent in Anhui and he had his pre-university education in Jinzhai County, Anhui. After graduation from high school, he taught in Yutan Middle School for three years. He earned his Bachelor of Sciences degree in Department of Geology at Hefei Polytechnic University in January, 1982. He then worked in Tongling, Hefei and Beijing for The Geological Bureau of The Ministry of Metallurgical Industry for about nine years. During this period, he also worked in British Columbia, Canada with the provincial Geological Survey as a visiting geologist (1987); in Virginia Tech as a visiting geologist (1989); in Indonesia as a consulting geologist (1990). He came to Virginia Tech as a graduate student in August, 1991. He earned his Master's degree in geology in Department of Geological Sciences, Virginia Polytechnic Institute and State University in June, 1993.

He has a wife, Zhang Li, of twelve years, and a son, Dawei, age 11.